IN VITRO CHARACTERIZATION OF THE ParA FAMILY PROTEIN SOJ FROM *BACILLUS SUBTILIS*

by

Brett McLeod

B.Sc., The University of Western Ontario, 1999

A THESIS SUBMITTED IN PARTIAL FULFILLMENT OF THE REQUIREMENTS FOR THE DEGREE OF

DOCTOR OF PHILOSOPHY

in

The Faculty of Graduate Studies

(Microbiology and Immunology)

THE UNIVERSITY OF BRITISH COLUMBIA
(Vancouver)

July 2008

ABSTRACT

In a response to deteriorating environmental conditions and high population density the common soil bacterium *Bacillus subtilis* undergoes a developmental process characterized by an unusual asymmetric division which results in the formation of two different cell types (the forespore and the mother cell) and ultimately the release of a dormant endospore. This developmental process is under multiple levels of control. Mutation in stage zero genes (*spo0*) block all morphological changes. One stage zero gene *spo0J* and a companion gene in the same operon (*soj*), have been implicated in the negative regulation of sporulation.

Soj and Spo0J are members of ParA and ParB families respectively, implicated in the stable inheritance of low copy number plasmids between daughter cells in bacteria. The role that Soj and Spo0J play in the negative regulation of sporulation is not fully understood. This thesis characterizes the interaction of Soj with nucleotides, DNA, and Spo0J *in vitro* to better understand the activities of Soj in the cell.

I characterized the dimerization and DNA binding of wild type Soj and two Soj point mutants (SojG12V and SojD40A). Wild type Soj was shown to bind adenosine nucleotides, form dimers, and hydrolyze ATP. Multiple lines of evidence demonstrated the nucleotide bound state does not alter the dimerization of Soj but does alter its ability to bind DNA. Multiple Soj-ATP proteins bound DNA to form Soj-DNA complexes as determined by DNaseI protection, electrophoretic mobility shift assays, and electron microscopy. Fixed angle light scattering was used to monitor the binding of Soj to DNA. Time resolved light scattering allowed characterization of multiple stages of Soj DNA binding. Soj was also shown to interact with Spo0J, which resulted in a stimulation of Soj ATPase activity providing evidence that Spo0J can alter Soj activity. The interaction of Soj and Spo0J resulted in the formation of large protein complexes detected by light scattering and by electron microscopy. This data indicated that Spo0J is able to form multimeric structures in response to a Soj interaction. The data were interpreted in a model for changes in the state of Soj and Spo0J.

TABLE OF CONTENTS

LIST OF TABLES.

LIST OF FIGURES.

LIST OF ABBREVIATIONS AND SYMBOLS

ATP	Adenosine 5'-triphosphate
BN	Blue native
bp	Base pair
DAPI	4',6-diamidino-2-phenylindole
dATP	Deoxy adenosine 5'-triphosphate
DNase	deoxyribonuclease
EDTA	Ethylene diamine tetraacetec acid
EMSA	Electrophoretic mobility shift assay
FPLC	Fast Protein Liquid Chromatography
GFP	Green fluorescent protein
GTP	Guanosine 5'-triphosphate
HTH	Helix turn helix
IPTG	Isopropyl-β-D-thiogalactopyranoside
MW	Molecular weight
NTA	Nitrilotriacetic acid
NTP	Nucleotide 5'-triphosphate
OD	Optical density
oriC	Chromosomal origin of replication
ORF	Open reading frame
P-loop	Structural term used to describe Walker A motif
PAGE	Polyacrylamide gel elecrophoresis
PCR	Polymerase chain reaction
PEI	polyethyleneimine
PMT	Photomultiplier tube
PVDF	polyvinylidene fluoride
RNAP	RNA polymerase
spo^+	Sporulation positive
spo^-	Sporulation negative
Spo0A~P	activated phosphorylated form of Spo0A~P
SDS	Sodium dodecyl sulfate
TCA	Trichloroacetic acid

TE	Tris-EDTA
UV	Ultraviolet
YFP	Yellow fluorescent protein

Abbreviations of measurements conform to the International System of Units (SI).

ACKNOWLEDGEMENTS

I would like to thank past members of the Spiegelman Lab for their help and friendship (Martin Richer, lab tech and all around good guy; Steve Seredick, grad student and intellectual mogul; Barb Turner, grad student and great lab manager). I am also grateful to the directed studies who worked on various aspects of Soj with me (Laura Willihnganz, who taught me Quikchange PCR; David Baker, who characterized Soj *in vivo*).

I would like to acknowledge people close to me who have supported me throughout the course of my degree, including (but not limited to) my family and my partner Laura.

I would like to thank the members of my committee; Lindsay Eltis, George Mackie, and Michael Murphy.

I would also like to thank my supervisor George Spiegelman for always being available for discussions regarding anything to do with science and sometimes life in general, and also for being a great editor, and an amazingly supportive teacher/instructor/supervisor.

INTRODUCTION

Bacillus subtilis has been intensively studied in part due to the genetic tools such as transformation that are available and in part due to interest in developmental process of endospore formation. Genetic screens have identified a small set of genes (~10) which control entry into sporulation. Surprisingly, two of these genes (*spo0J and soj*) encode members of protein families usually associated with plasmid partition and stability in Bacteria, *parA* and *parB*. This thesis investigates the *in vitro* characteristics of the protein Soj and Spo0J to better understand how they affect sporulation.

1 Sporulation in *B. subtilis.*

When cells of *Bacillus subtilis* enter stationary phase they express genes to adopt alternative survival strategies, such as the use of alternative metabolic pathways and the scavenging of nutrients from their surroundings (bacterial motility, and competence), to name a few (Claverys *et al.*, 2006; Hamoen *et al.*, 2003; Phillips and Strauch, 2002). When *B. subtilis* cells sense that survival is unlikely they initiate sporulation that results in the formation of a resistant endospore (Errington, 2003; Piggot and Hilbert, 2004). *B. subtilis* endospores have been estimated to be able to remain viable for up to ~2 million years (Nicholson, 2003). The endospore is capable of germination to resume vegetative growth (Moir, 2006; Setlow, 2003). Spore formation in *B. subtilis* is characterized by a series of morphological changes that have been used to divide the sporulation event into eight stages (Fig. 1).

Stage I of sporulation is characterized by the compaction of the bacterial chromosome throughout the length of the cell to form what is called the axial filament. Stage II is characterized by an asymmetric septation of the cytoplasmic membrane but not the cell wall which creates two unequal compartments (Kroos *et al.*, 1999); the smaller is called the forespore compartment, and the larger is termed the mother cell compartment. At each stage, compartment-specific transcription of genes is required to complete development of that stage and to progress to the next stage (Hilbert and Piggot, 2004). In stage III, one chromosome is actively transported through the asymmetric septum into the forespore (Burton *et al.*, 2007; Ptacin *et al.*, 2008). The forespore is then engulfed by the mother cell (Broder and Pogliano, 2006). The fusion of the mother cell membrane around the prespore forms the forespore protoplast which exists as a cell within a cell. In subsequent stages the cortex, a modified form

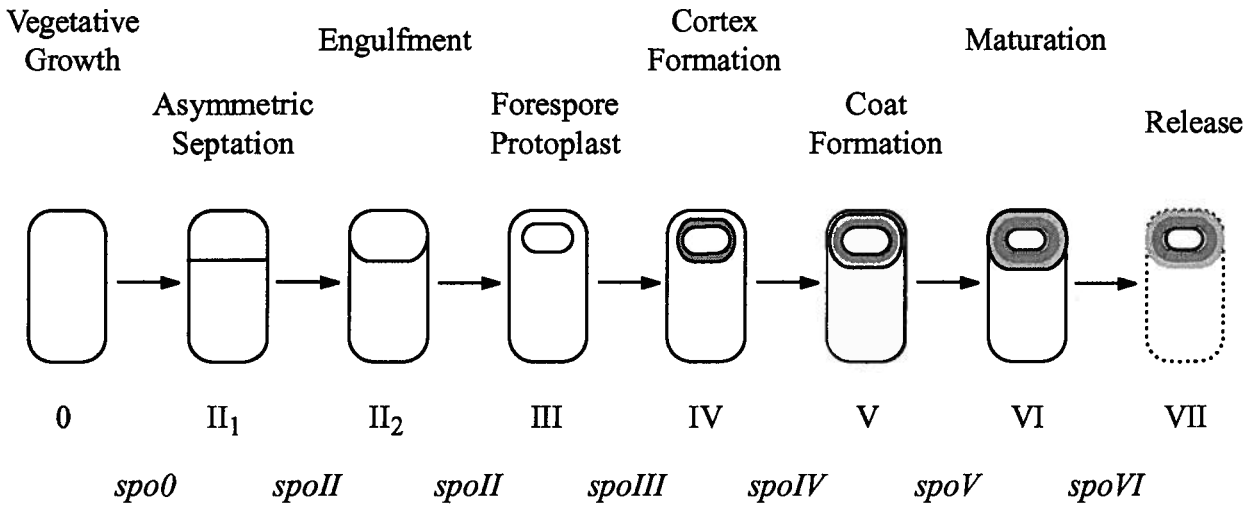

Fig. 1. Morphology of Sporulation in *B. subtilis*. The main sequence of morphological events begins with the vegetative cell and ends with the release of a mature spore. Roman numerals designate the stages of sporulation characterized by electron microscopy. The italicized *spo* designation identifies genes whose mutation stalls sporulation at the stage immediately preceding it. For example, mutation of *spo0A* prevents asymmetric septum formation, while mutation of *spoIIG* prevents engulfment. Stage I represents cells that have replicated their genome and formed axial DNA filaments, but since this is also observed in vegetative cells and no stage I specific mutants have been characterized, the designation has been dropped. Adapted from Errington, 1993, and Seredick, 2006.

of cell wall, is synthesized between the forespore and mother cell membranes (Takamatsu and Watabe, 2002), while the mother cell assembles a proteinacieous coat on the outside surface of the spore. During the deposition of these layers, small acid-soluble proteins are synthesized in large amounts to coat the forespore chromosome conferring resistance to UV radiation (Setlow, 2007), while dipicolinic acid and Ca^{2+} ions are absorbed resulting in dehydration and mineralization of the forespore (Henriques and Moran, 2007). After 6 to 8 hours of development, spore maturation is complete, and the mother cell lyses to release a dormant endospore (Lewis, 2000).

The signals which trigger the initiation of sporulation are not entirely defined. Some of the signals required for the initiation of sporulation are sensed by at least five histidine kinases (KinA to KinE), which transfer a phosphoryl moiety to Spo0F (Jiang *et al.*, 2000). Spo0F transfers the phosphoryl group to Spo0B, which in turn transfers it to Spo0A (referred to as the phosphorelay (Varughese, 2002)). Phosphorylated Spo0A (Spo0A~P) both represses transcription (Greene and Spiegelman, 1996), and activates transcription (Satola *et al.*, 1992) of specific genes, ultimately affecting the expression of over 400 genes (Molle *et al.*, 2003a).

The initiation of sporulation is not favoured until alternate strategies for cell survival have been pursued so *B. subtilis* tightly regulates the initiation of sporulation. Many regulatory and environmental signals directly impact the flow of phosphate to Spo0A. The autophosphorylation of the histidine kinases can be blocked (Wang *et al.*, 1997), as is the case for KinA where a protein, Sda, which responds to DNA damage and replication status, binds to KinA preventing its autophosphorylation causing inhibition of sporulation (Burkholder *et al.*, 2001; Rowland *et al.*, 2004; Ruvolo *et al.*, 2006; Whitten *et al.*, 2007). KinB expression is repressed by CodY whose activity is linked to internal concentrations of GTP and branched chain amino acids (Handke *et al.*, 2008; Molle *et al.*, 2003b; Shivers and Sonenshein, 2004). Spo0F and Spo0A are also the targets of multiple phosphatases (Ohlsen *et al.*, 1994; Perego *et al.*, 1994; Perego, 2001). The Rap phosphatases which reverse phosphorylation of Spo0F are themselves negatively regulated by small pentapeptides that are exported and then re-imported into the cell (Ishikawa *et al.*, 2002; Perego, 1997). The synthesis, import, and export of these pentapeptides are negatively regulated by CodY (Molle *et al.*, 2003b).

Genes that when mutated block progression to stage II have been termed stage zero genes. Most stage zero genes encode proteins that are part of the phosphorelay or affect the flow of phosphate to Spo0A. The mutation of one gene, *spo0J*, has not been shown to affect the phosphorylation level of Spo0A; nonetheless the loss of *spo0J* still causes a 10^4 fold decrease in

sporulation frequency (Ireton *et al.*, 1994). Cells with a Δ*spo0J* mutation do not activate stage II gene expression (Ireton *et al.*, 1994). *Spo0J* is the second gene in a dicistronic operon and encodes a ParB family protein. The first gene in the operon encodes a ParA family protein (Ireton *et al.*, 1994). The disruption of this gene in a Δ*spo0J* background relieves the effect of a Δ*spo0J* mutation, resulting in near wild type sporulation frequencies. Therefore, this gene was named *soj* for suppressor of spo0J (Ireton *et al.*, 1994).

ParA and ParB family proteins were first recognized as proteins that stabilize the vertical transmission of low copy number plasmids (Austin and Abeles, 1983; Austin and Wierzbicki, 1983), so it was striking that members of the ParA family (Soj) and the ParB family (Spo0J) affected the initiation of sporulation in *B. subtilis.*

2 ParA/Soj Belongs to the Mrp/MinD Protein Family.

ParA/Soj proteins are members of the P-loop NTPase fold supergroup (Leipe *et al.*, 2002). P-loop NTPases are one of the most common families of proteins and comprise 10-18% of all gene products (Koonin *et al.*, 2000). The P-loop NTPase fold supergroup is divided into 7 lineages (Leipe *et al.*, 2002). ParA/Soj proteins are grouped with the GTPase group based on sequence and structural data. ParA/Soj proteins are a subfamily within the Mrp/MinD family and MinD/Mrp-Etk superfamily (Leipe *et al.*, 2002). The Mrp/MinD family contains ATPases with various functions, and is divided into subfamilies: Mrp, MinD, NifH, ArsA and ParA/Soj. In some cases, these proteins have been shown to form homodimers and dimerization is believed to be associated with function. In some cases such as those for MinD from *E. coli*, and *T. thermophilus* Soj the proteins have been reported to be dimeric when bound to ATP, and monomeric when bound to ADP.

The Mrp/MinD family has a conserved overall globular structure of 7 central β strands surrounded by 5 α helices. The Mrp/MinD family proteins have what has been referred to as a 'deviant' Walker A motif with a conserved sequence of KGGXGK[S/T][S/T] in the ATP binding site (Koonin, 1993; Lutkenhaus and Sundaramoorthy, 2003). The second lysine is invariant across all Walker motif proteins and is responsible for coordinating ATP binding (Milner-White *et al.*, 1991; Saraste *et al.*, 1990; Walker *et al.*, 1982). This family also has a Walker A' motif, that contains a conserved aspartic acid residue at the C-terminus of the second β strand that has been shown to make a direct or water-mediated hydrogen bond to a Mg^{2+} cofactor in the nucleotide binding pocket (Hayashi *et al.*, 2001; Schindelin *et al.*, 1997; Zhou *et*

al., 2000). The structures of monomeric MinD from *Pyrococcus furiosus* (Hayashi *et al.*, 2001), *P. horikoshii* (Sakai *et al.*, 2001), and *Archaeoglobus fulgidus* (Cordell and Lowe, 2001) are known. Several of *Azotobacter vinlandii* dimeric NifH (Chiu *et al.*, 2001; Jang *et al.*, 2000; Jang *et al.*, 2004; Sarma *et al.*, 2007; Schmid *et al.*, 2002; Sen *et al.*, 2004; Sen *et al.*, 2006; Strop *et al.*, 2001), and ArsA from *Escherichia coli* have also been solved (Zhou *et al.*, 2000, 2001). The structures of monomeric and dimeric Soj from *Thermus thermophilus* are also known (Leonard *et al.*, 2005), as is the structure of the δ protein (ParA) from the *Firmicutes* plasmid pSM19035 (Pratto *et al.*, 2008).

Mrp/MinD proteins have diverse roles in different bacterial species. NifH is the obligate electron donor to the MoFe protein and has multiple roles in the catalytic process of biological nitrogen fixation (Burgess and Lowe, 1996; Howard *et al.*, 1986), as well as in the maturation and assembly of nitrogenase (Allen *et al.*, 1993; Rangaraj *et al.*, 1997). ArsA is the catalytic component of an oxyanion pump that is responsible for resistance to arsenite (As(III)) and antimonite (Sb(III)) (Rosen, 1990). The δ protein has been implicated in plasmid stabilization (Dmowski *et al.*, 2006; Pratto *et al.*, 2008).

2.1 *E. coli* Min proteins.

The Mrp/MinD family protein that has been most characterized is MinD from *E. coli*. MinD together with MinC and MinE is required for accurate placement of the division septum in dividing cells (de Boer *et al.*, 1989; de Boer *et al.*, 1991; Lutkenhaus, 2007). Disruption of any of the 3 *min* protein genes results in the production of minicells that result from formation of a septum near the end or pole of the cell rather than the middle (de Boer *et al.*, 1989). MinD-ATP forms dimers *in vitro*, while MinD-ADP does not readily dimerize (Hu and Lutkenhaus, 2003). MinD-ATP binds liposomes and forms multimeric tube-like structures (50-100 nm diameter) *in vitro* (Hu *et al.*, 2002; Lackner *et al.*, 2003). Fluorescence microscopy of cells expressing MinD-GFP shows that MinD binds to the cytoplasmic side of the inner membrane and forms multimeric structures (Raskin and de Boer, 1999a). Membrane-bound MinD structures bind MinC (Raskin and de Boer, 1999b), and MinC antagonizes the polymerization of FtsZ (Pichoff and Lutkenhaus, 2001). FtsZ is a conserved protein whose polymerization is required for cytokinesis (Margolin, 2005). Destabilization of FtsZ polymers by MinC inhibits cell division. The current model for the interaction of MinCDE is as follows. MinE interacts with MinD, and causes dissociation of MinC from MinD. MinE also stimulates MinD ATPase

activity, and the ATPase stimulation causes MinD to dissociate from the inner membrane (Lutkenhaus, 2007). MinD can exchange ADP for ATP then insert into the membrane. MinC subsequently rebinds MinD (Lutkenhaus, 2007).

MinE forms a ring-like structure that is observed to oscillate back and forth through the mid-cell region. This MinE oscillation drives the oscillation of MinD structures from one pole, to the other with a periodicity of under a minute (Raskin and de Boer, 1999a). The cause of MinE oscillation in the cell is not well understood, but a model which explains these oscillations is based on the attraction of MinE to MinD bound to the membrane (Lutkenhaus, 2007). MinE binds MinD bound to the membrane and promotes MinD membrane dissociation by stimulating its ATPase activity. The dissociated MinD exchanges ADP for ATP and rebinds the membrane at the opposite cell poles. The newly formed MinD polymers attract MinE and cause MinE progression towards new MinD structures. Pole to pole MinD oscillation provides a system in which MinC concentration is highest at cell poles and lowest at midcell. This oscillation of Min E inhibits FtsZ polymerization near cell poles, ensuring that cell division occurs at the midpoint in the cell..

The Min system of *B. subtilis* is similar to that of *E. coli,* except for the absence of a MinE homologue in *B. subtilis* and the presence of a protein termed DivIVA (absent from *E. coli*) (Edwards and Errington, 1997; Lee and Price, 1993). There is a low level of sequence identity between MinC proteins of the two species, and a relatively high level of sequence identity between MinD proteins (40%, Marston *et al.*, 1998). In *B. subtilis,* deletion of either *minC* or *minD* causes a minicell phenotype. In *B. subtilis* MinD-GFP is seen at the cell poles when observed by fluorescence microscopy (Marston and Errington, 1999b). MinC-GFP has a similar polar distribution pattern that is disrupted in *minD* mutants (Marston and Errington, 1999b). MinD-GFP does not concentrate at the poles in the absence of DivIVA (Marston *et al.*, 1998). This indicates that DivIVA is necessary to localize MinD at the poles. A *divIVA* deletion is lethal producing large aseptate filaments; however, this phenotype is suppressed by deletion of *minC*, and the resulting *minC divIVA* double deletion mutant strain has a 'minicell' phenotype (Marston and Errington, 1999a). The Min system in *B. subtilis* is different from *E. coli* in that the proteins do not oscillate, but are similar in that they function to inhibit FtsZ polymerization in polar regions.

3 ParA and ParB Proteins.

ParA and ParB proteins are widely dispersed throughout the Bacteria (Leipe *et al.*, 2002). ParA proteins are ATPases, and ParB proteins bind to specific *parS* DNA sequences (Bignell and Thomas, 2001; Surtees and Funnell, 2003). These genes were first identified on low copy number plasmids (Austin and Abeles, 1983; Austin and Wierzbicki, 1983; Ogura and Hiraga, 1983). Plasmid-encoded ParA and ParB proteins bind to newly replicated plasmids, and actively segregate them to opposite cell quarters in growing cells (Li *et al.*, 2004). The ensuing medial division of the growing cell promotes inheritance of the plasmid by both progeny cells. Disruption of any component of the Par system results in unstable plasmid maintenance and loss of the plasmid from a growing population over several generations (Surtees and Funnell, 2003).

Studies of plasmid and chromosomal ParA and ParB proteins allow several broad generalizations to be made (Ebersbach and Gerdes, 2005). First, the two proteins interact, and the interaction results in a stimulation of ParA ATPase activity. Second, ParB is a site-specific DNA binding protein. Third, ParA and ParB likely act together on DNA that has a *parS* sequence to segregate the DNA after it has been replicated.

Fig. 2 shows a Clustal W sequence alignment of ParA proteins from plasmid P1 (ParA, type Ia), F plasmid (SopA, type Ia), plasmid TP228 (ParF, type Ib), pSM19035 (δ, type Ib), and Soj from *B. subtilis*. These proteins are ones where biochemical and/or structural studies have been carried out. This alignment illustrates that the similarity between these proteins, even between type Ia ParA proteins (P1 and F plasmid), and between type Ib ParA proteins (plasmid TP228 and pSM19035) is primarily found in the ATP binding domains (Walker A, A`, and B motifs). This suggests that other than sharing ATP binding and hydrolysis activities plasmid ParA proteins share few properties with chromosomal Soj/ParA proteins.

Clustal W sequence alignment of selected chromosomal ParA/Soj proteins is shown in Fig. 3. High sequence identity is observed both throughout the motifs required for ATP binding and hydrolysis and the length of their sequences.

4 Plasmid *Par* Loci.

Plasmid *parA* and *parB* genes are usually organized as a single operon (Moller-Jensen *et al.*, 2000). Plasmid *par* loci are grouped based on properties of both ParA and ParB proteins (Ebersbach and Gerdes, 2005; Moller-Jensen *et al.*, 2000). The largest group (type I) has

Fig. 2. Sequence alignment of *B. subtilis* Soj and plasmid encoded ParA proteins. Sequence alignment was generated by Clustal W software v. 2.0.8. Shading indicates protein motifs; Red shading, Walker A motifs; purple shading, Walker A' motifs; green shading, Walker B motifs.

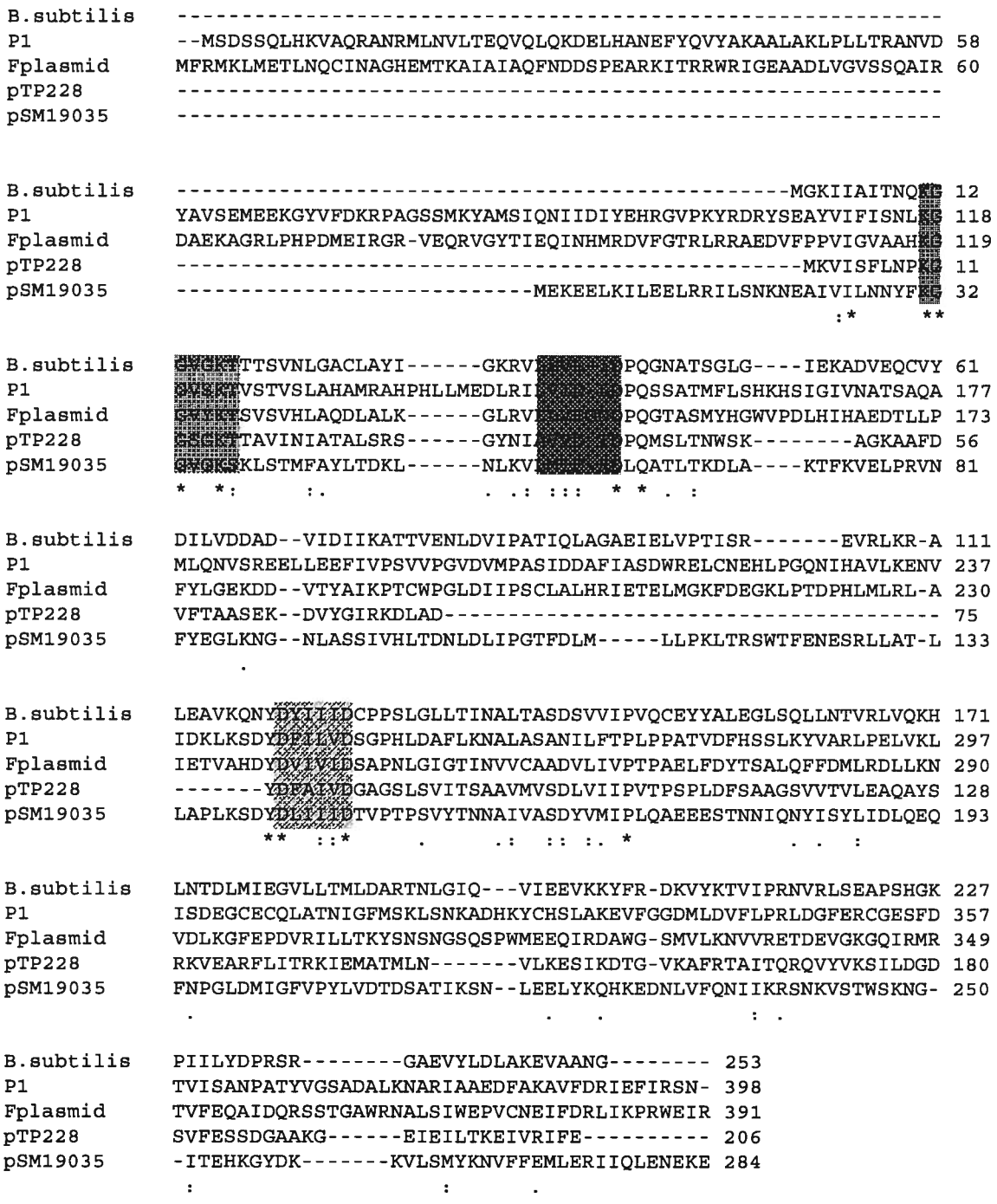
B.subtilis
P1
Fplasmid
pTP228
pSM19035

Fig. 3. Sequence alignment of chromosomal ParA proteins. Sequence alignment was generated by Clustal W software v. 2.0.8. Shading indicates protein motifs; Red shading, Walker A motifs; purple shading, Walker A' motifs; green shading, Walker B motifs; blue shading, residues implicated in Soj DNA binding activity by Hester and Lutkenhaus (2007).

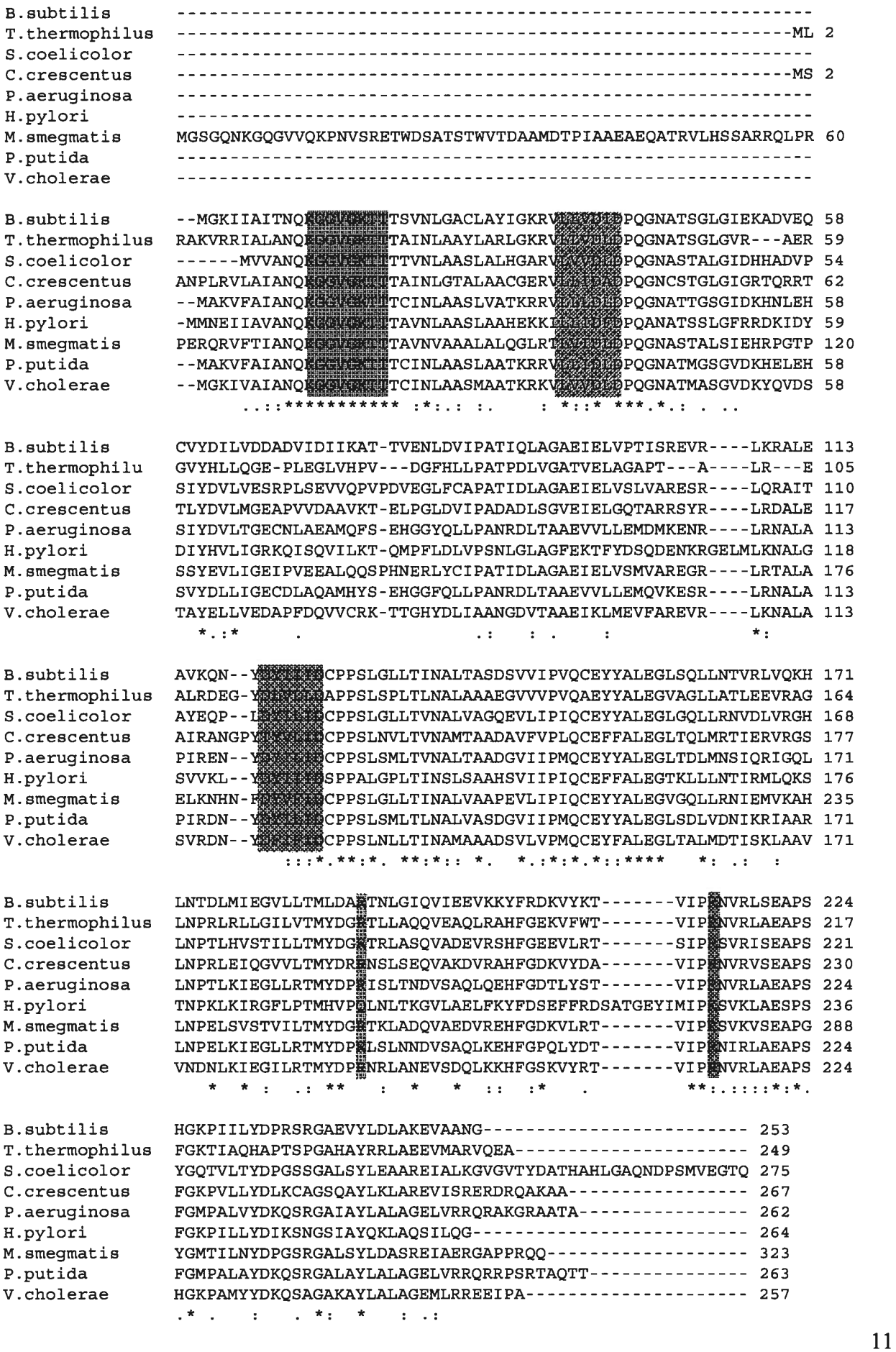
B.subtilis
T.thermophilus
S.coelicolor
C.crescentus
P.aeruginosa
H.pylori
M.smegmatis
P.putida
V.cholerae

Walker A/B (P-loop) ATP binding motifs in the ParA proteins (Koonin, 1993). An Actin/Hsp70 ATP binding motif in ParA characterizes type II *par* loci (Bork *et al.*, 1992). Type I can be further divided based on the type of protein encoded by *parB*. Type Ia loci encode large ParB (>310 amino acid) with helix-turn-helix (HTH) DNA binding motifs, and type Ib loci encode smaller ParB proteins (<140 amino acid) with ribbon helix DNA binding motifs. The general function of most plasmid encoded Par proteins is thought to be promoting equal distribution of plasmids to daughter cells (Ebersbach and Gerdes, 2005; Schumacher, 2008).

4.1 ParA and ParB Proteins from P1 and F Plasmids.

The best studied ParAB system is that from the temperate P1 prophage (type Ia) which can exist as a low copy number plasmid in *E. coli* (Prentki *et al.*, 1977). P1 ParA-ATP dimers interact with ParB multimers bound to *parS* sequences and form the 'partition complex' (Bouet and Funnell, 1999). The partition complex is observed *in vivo* by fluorescence microscopy to localize ParB, ParA and plasmid DNA to specific sites in the cell (Erdmann *et al.*, 1999). ParA-ADP binds specifically to the *par* operon operator (*parOP*) to negatively regulate the expression of the *par* operon by acting directly as a repressor of transcription (Davey and Funnell, 1994; Davis *et al.*, 1992). ParA-ADP autoregulation plays an important role in the proper expression of ParA and ParB proteins and the maintenance of plasmid P1. Overexpression of either, or both, proteins causes a loss of plasmid stability (Funnell, 1988). ParA contributes to the formation of partition complexes *in vivo* (Erdmann *et al.*, 1999; Li *et al.*, 2004). In the absence of ParA, plasmids bound by ParB multimers mislocalize, often failing to form plasmid complexes at the cell centre. Furthermore without ParA, plasmid DNA bound by ParB does not segregate to opposite cell quarters and is inherited by only one progeny cell. This results in plasmid loss (Li *et al.*, 2004). At the partition complex the ATPase activity of ParA-ATP is thought to be needed to eject paired ParB-*parS* complexes away from each other towards opposite cell poles, although the mechanisms of how ParA and ParB move paired plasmids to opposite poles is not well understood (Edgar *et al.*, 2006). *In vitro* ParA-ATP interacts with ParB-*parS* DNA complexes (Bouet and Funnell, 1999). *In vitro* ParA ATPase activity is stimulated in the presence of DNA and further increased in the presence of ParB and *parS* DNA (Davis *et al.*, 1992).

The Par system of the F plasmid of *E. coli* (SopAB, type Ia) functions similarly to the P1 Par system (Surtees and Funnell, 2003). Disruption of SopA, SopB or the *parS* equivalent *sopC*

leads to a random distribution of F-plasmids in *E. coli* (Hirano *et al.*, 1998). SopA-ADP binds to the *sop* promoter and the Sop proteins have been demonstrated to participate in autoregulation of their genes (Hirano *et al.*, 1998). The largest difference between SopA and ParA is that SopA-ATP forms protein filaments in the absence of DNA that vary in size (200-500 nm long, 10-40 nm wide) (Bouet *et al.*, 2007). SopA filamentous structures have been observed *in vivo* but the role they play to support plasmid stabilization is unclear (Hatano *et al.*, 2007).

The autoregulation activities of type Ia ParA proteins such as P1 ParA and SopA is due to a domain (~100 residues) N-terminal to the Walker A motif (Ebersbach and Gerdes, 2005; Moller-Jensen *et al.*, 2000; Surtees and Funnell, 2003). This N-terminal DNA binding motif is absent from type Ib, and all chromosomal ParA proteins, consistent with reports that only type Ia ParA proteins are able to regulate the expression of their own operon (Ebersbach and Gerdes, 2005; Moller-Jensen *et al.*, 2000; Surtees and Funnell, 2003).

4.2 Type II Par System of Plasmid R1.

The Par proteins of the *E. coli* R1 plasmid, ParM (ParA) and ParR (ParB), constitute a type II Par system (Ebersbach and Gerdes, 2005; Moller-Jensen *et al.*, 2000). As mentioned there is little similarity between type II ParA proteins (actin/hsp70 motif) and type I and chromosomal ParA proteins (WalkerAB motif) except that they are all ATPases. However ParR is similar to the ribbon helix type Ib ParB proteins. Functionally there are major differences between the *par* loci of type II and type Ia plasmids (Ebersbach and Gerdes, 2005). ParR (ParB), and not ParM (ParA) is responsible for efficient autoregulation of the R1 *par* genes. ParR is responsible for plasmid pairing *in vitro* and *in vivo*. ParM has been shown to form filaments *in vitro* (Moller-Jensen *et al.*, 2002; van den Ent *et al.*, 2002), and similar filamentous structures have been observed *in vivo* (Moller-Jensen *et al.*, 2003). *In vitro* filamentation of ParM is stimulated by interaction with ATP or non hydrolysable ATP analogues. The long straight filaments can reach lengths up to 1 μm and are structurally similar to filaments formed by F-actin (Orlova *et al.*, 2007). It has been proposed that the insertional polymerization of ParM-ATP monomers at the ParM-ParR interface causes the ParM filaments to grow bidirectionally, thereby pushing the two plasmids apart toward opposite ends of the cell (Garner *et al.*, 2007; Moller-Jensen *et al.*, 2003; Popp *et al.*, 2008).

5 Chromosomal ParA and ParB Proteins.

Chromosomally encoded ParA/Soj and ParB/Spo0J do not fit well in the plasmid-based nomenclature system which is based on the characteristics of plasmid ParA and ParB proteins. Chromosomal ParA/Soj proteins lack the N-terminal HTH DNA binding domain, and therefore are similar to ParA proteins from type Ib Par systems with respect to domain organization (Ebersbach and Gerdes, 2005; Gerdes *et al.*, 2000; Moller-Jensen *et al.*, 2000). Chromosomal ParB/Spo0J more closely resemble ParB proteins from type Ia (HTH DNA binding motif), and are very different from the small ribbon helix domain proteins in type Ib loci (Ebersbach and Gerdes, 2005; Gerdes *et al.*, 2000; Moller-Jensen *et al.*, 2000).

Of the major prokaryotic phyla only *Thermatoga* are completely without any species that encode chromosomal ParA and ParB proteins (Leipe *et al.*, 2002). However within certain phyla chromosomal ParA and ParB proteins are absent from some species, most notably from *E. coli* and its close relatives. Recent studies on the chromosomally encoded Par proteins from species other than *B. subtilis* will be briefly reviewed.

5.1 Par Proteins from *Mycobacterium smegmatis, Pseudomonas aeruginosa, Pseudomonas putida, Vibrio cholerae,* and *Helicobacter pylori.*

Consistent with a role in DNA segregation, *P. putida* or *V. cholerae* chromosomal Par systems can each stabilize a plasmid in the absence of selection in *E. coli* (Godfrin-Estevenon *et al.*, 2002; Yamaichi *et al.*, 2007). In each case plasmid stabilization is dependent on both Par proteins, and having a *parS* sequence on the plasmid. This indicates that ParA and ParB interact with a *parS* plasmid and act independently or with cellular factors present in both *E. coli* to increase plasmid stability. However, in most of these experiments complete plasmid stabilization is not observed. This contrasts with plasmid ParAB systems which maintain plasmids in growing cultures over large numbers of generations. This indicates that chromosomal ParAB proteins are not as effective at plasmid stabilization as their plasmid-encoded counterparts.

V. cholerae is unusual in that it possesses two chromosomes that encode different Par systems, and different *parS* sequences which are responsible for segregation of the chromosome on which they are encoded (Saint-Dic *et al.*, 2006; Yamaichi *et al.*, 2007). The generation of a *V. cholerae* Δ*parB1,* or Δ*parAB1* deletion on the large chromosome has not been successful

despite extensive efforts (Saint-Dic *et al.*, 2006). This indicates that the *par1* locus of the large chromosome might be essential.

An increased frequency of anucleate cells has been reported in *parA* and/or *parB* deletions or overexpression strains in *M. smegmatis*, *P. putida*, and *P. aeruginosa* (Godfrin-Estevenon *et al.*, 2002; Jakimowicz *et al.*, 2007a; Lewis *et al.*, 2002). In these vegetatively growing *par* mutant cultures, anucleate cells constitute a minority (usually <10%) of the population, and for each species neither protein is essential. Therefore, ParA and ParB proteins are not the primary chromosome segregation machinery, and play a dispensable role in maintaining proper chromosome segregation in growing cells.

M. smegmatis and *P. aeruginosa* are reported to grow slower upon deletion or overexpression of Par proteins (Bartosik *et al.*, 2004; Jakimowicz *et al.*, 2007a; Lasocki *et al.*, 2007). In *V. cholerae* the large chromosome is mislocalized in Δ*parA* and Δ*parS* mutants as observed by fluorescence microscopy (Saint-Dic *et al.*, 2006; Yamaichi *et al.*, 2007). For all the organisms in this section, ParB has been shown to bind *parS* (Bartosik *et al.*, 2004; Jakimowicz *et al.*, 2007a; Lee *et al.*, 2006; Yamaichi *et al.*, 2007).

In vitro the presence of ParA from *M. smegmatis* increases the binding of ParB to *parS* indicating a ParA-ParB interaction (Jakimowicz *et al.*, 2007a). Purified *H. pylori* Soj and Spo0J co-immunoprecipitate *in vitro*. Moreover, the inclusion of *H. pylori* Spo0J in reactions with Soj and ATP leads to Soj ATPase stimulation (Lee *et al.*, 2006). An interaction between ParA and ParB from *P. aeruginosa* has been inferred from yeast two hybrid assays (Bartosik *et al.*, 2004). While ParA and ParB from these diverse organisms have similar activities, disruption of their *par* genes results in different DNA segregation and growth phenotypes. Thus the chromosomal Par systems appear to play diverse roles *in vivo*, or have similar roles with diverse effects on each species physiology.

5.2 *Streptomyces coelicolor.*

S. coelicolor sporulates by forming aerial hyphae. In the aerial hyphae multiple chromosomal replications creates a multigenomic compartment which undergoes synchronous septation at evenly spaced sites to form unigenomic prespore compartments. These compartments then develop into mature spores (Chater, 2001; Claessen *et al.*, 2006). Transcription of the *parAB* operon is dramatically upregulated upon sporulation (Jakimowicz *et al.*, 2006; Kim *et al.*, 2000). In *par* gene mutants, hyphal prespore compartment sizes are

disturbed, and a high frequency of anucleate spores are observed (~26%) (Jakimowicz *et al.*, 2007b). ParB binds to 20 *parS* sites near *oriC* (Jakimowicz *et al.*, 2002), and ParB-GFP has been observed by fluorescence microscopy to form DNA-associated foci *in vivo* (Jakimowicz *et al.*, 2005). In the absence of ParA, the ParB-GFP foci are less condensed and mislocalized; in addition FtsZ polymerization (Z-rings) is also mislocalized (Jakimowicz *et al.*, 2007b). *In vivo,* ParA-GFP forms helical structures in hyphal tips with a pitch that corresponds to the length of a prespore compartment (Jakimowicz *et al.*, 2007b). ParAK44A-GFP, (ATPase deficient) still forms helical structures but behaves as a null mutant (anucleate prespore compartments observed). These results indicate that ATPase activity is not important to form ParA structures but it is crucial for proper chromosome segregation during sporulation (Jakimowicz *et al.*, 2007b). *S. coelicolor* ParA ATPase is stimulated *in vitro* by ParB, and the presence of ParA increases *in vitro* DNA binding efficiency of ParB to *parS* sequences (Jakimowicz *et al.*, 2007b). ParA but not ParAK44A interacts with ParB as indicated by *E. coli* two hybrid assays (Jakimowicz *et al.*, 2007b).

An interesting model for the role of ParA and ParB from *S. coelicolor* has been presented (Jakimowicz *et al.*, 2007b). Upon entry into sporulation the *par* operon expression is upregulated. ParB binds *parS*, and ParA forms helical structures in the hyphal tips. The ParA condenses ParB-*parS* structures and act as a 'ruler', ensuring appropriate DNA localization which produces a high frequency of cells with a single chromosome upon septation. This model postulates that ParA positions both ParB-DNA complexes and FtsZ polymerization within hyphal tips.

5.3 *Caulobacter crescentus.*

Caulobacter crescentus is the only reported bacterial species in which both *parA* and *parB* genes are essential (Mohl and Gober, 1997; Mohl *et al.*, 2001). *C. crescentus* is unlike most bacteria in that every cell division is a developmental process which produces two morphologically different cells (Laub *et al.*, 2007). To create mutants, second copies of *parA* and/or *parB* were inserted in the genome under control of an inducible promoter to allow the deletion of the genes (Easter and Gober, 2002; Mohl and Gober, 1997; Mohl *et al.*, 2001). When ParB is depleted cells fail to divide, and instead grow into long filaments. If these cells divide, the placement of the division septa is irregular and results in anucleate minicells (Easter and Gober, 2002; Mohl *et al.*, 2001). Overexpression of ParA results in a phenotype similar to

ParB depletion (Easter and Gober, 2002). The overproduction of both ParA and ParB results in viable cells, but cultures of these cells have a high frequency of anucleate cells (Easter and Gober, 2002). These results indicate ParA and ParB have an essential role and function prior to cell division. *In vitro* ParB binds specific sequences found near the origin of replication (Mohl and Gober, 1997). *In vitro* ParA-ATP, but not ParA-ADP interacts with ParB-DNA complexes and ejects ParB from DNA (Easter and Gober, 2002). ParA-ATP can also interact with ParB and prevent ParB-DNA interactions (Easter and Gober, 2002). The ATPase of ParA is stimulated *in vitro* by ParB by acting as a nucleotide exchange factor (Easter and Gober, 2002). Cells depleted for ParB grow as filaments which have high concentrations of ParA-ADP, so it is thought that in the absence of ParB the increased level of ParA-ADP inhibits cell cycle progression (Easter and Gober, 2002; Figge *et al.*, 2003).

6 *Bacillus subtilis.*

The *soj/spo0J* locus of *B. subtilis* was one of the first chromosomal Par systems to be identified (Ireton *et al.*, 1994). *Spo0J* was recovered in screens to identify genes which blocked sporulation initiation (Mysliwiec *et al.*, 1991). A number of studies have investigated Soj and Spo0J function during vegetative growth as well as during sporulation.

6.1 Role of Soj and Spo0J in Vegetative Growth

The deletion of *spo0J* results in a low levels of anucleate cells during vegetative growth (0.1 % anucleate cells; Ireton *et al.*, 1994; Lee and Grossman, 2006; Ogura *et al.*, 2003). The same low level of anucleate cell phenotype is also present when the whole operon is deleted, but not in cultures of Δ*soj* cells (Ireton *et al.*, 1994; Lee and Grossman, 2006; Ogura *et al.*, 2003). These results are partially consistent with a DNA segregation role for Soj and Spo0J such as that established for plasmid ParA and ParB proteins, but the Soj and Spo0J cannot be the primary determinant of chromosome segregation in vegetative cells. In contrast, consistent with a role in chromosome segregation, Soj and Spo0J significantly stabilize a plasmid with a *parS* sequence in growing *B. subtilis* and *E. coli* cultures in the absence of selection (Hester and Lutkenhaus, 2007; Lin and Grossman, 1998; Yamaichi and Niki, 2000).

In vitro Spo0J binds to DNA with a preference for binding to *parS* sequences (measured to be approximately 40:1, *parS* DNA:non-specific DNA, Lin and Grossman, 1998). Spo0J

spreads on DNA to form Spo0J multimers on DNA *in vivo* and *in vivo*, this spreading was shown to be dependent on *parS in vivo* (Murray *et al.*, 2006). Fluorescence microscopy observation of *B. subtilis* cells that express Spo0J-GFP shows foci distributed near *oriC* (Lin *et al.*, 1997) and Spo0J-GFP foci correspond to the number of replicated chromosomal origins (1:1 ratio of Spo0J-GFP foci to *oriC*; Glaser *et al.*, 1997). Shortly after cell division Spo0J-GFP foci associated with *oriC* are found at one quarter and three quarter positions relative to cell poles. . However, Spo0J does not direct chromosomal segregation because the *oriC* region still localizes correctly at cell quarters in the absence of Spo0J (Webb *et al.*, 1998). In addition, placement of *parS* sequences at sites away from *oriC* is not sufficient to localize that portion of the chromosome to cell quarters (Lee *et al.*, 2003). In Δ*soj* mutants, numerous smaller less intense foci of Spo0J-GFP are observed throughout the cell but still associated with DNA (Marston and Errington, 1999a) but the foci associated with oriC are absent. These data indicate that Soj affects an aspect of Spo0J that is important for its distribution *in vivo*, although it is not clear what role this localization plays.

In *B. subtilis* cells that express Soj-GFP it appears to be located primarily at cell poles or newly formed septa, with some foci within the cytoplasm (Murray and Errington, 2008; Quisel *et al.*, 1999). Disruption of *spo0J* leads to Soj-GFP association along all chromosomal DNA (Autret *et al.*, 2001; Autret and Errington, 2003; Marston and Errington, 1999a; Quisel *et al.*, 1999), a pattern that is strikingly different from the polar localizations observed in wild type cells. Soj-GFP is distributed in the cytosol away from the chromosome in a Δ*minD* strain, but is associated with the nucleoid in a *spo0J/minD* double deletion mutant (Murray and Errington, 2008). These data were interpreted to mean that Soj is directed to cell poles and division septa by MinD, and Spo0J. In the absence of Spo0J, Soj associates with chromosomal DNA.

Effects of mutations in the Soj Walker motif on Soj-GFP distribution have been reported (Autret and Errington, 2003; Murray and Errington, 2008; Quisel *et al.*, 1999). In cells with Δ*soj* and Δ(*soj-spo0J*), ectopically expressed SojK16A and SojD125A GFP fusion proteins are found uniformly throughout the cytosol rather than at the poles, in foci, or distributed on DNA (Murray and Errington, 2008; Quisel *et al.*, 1999). These point mutants affect invariant residues in the Walker A (K16) and Walker B (D125) motifs and would be expected to confer a loss of ATP binding. In Δ*soj* and Δ(*soj-spo0J*) cells SojG12V-GFP is observed at the cell poles and as cytosolic foci (Autret and Errington, 2003; Murray and Errington, 2008; Quisel *et al.*, 1999). SojG12V-GFP is not observed to associate with chromosomal DNA under any condition. In a Δ*soj* background SojD40A-GFP is detected exclusively as bright foci that completely colocalize

with Spo0J-YFP foci on the chromosome, but not at poles or division septa (Murray and Errington, 2008). In Δ(*soj-spo0J*) cells SojD40A-GFP is distributed along all chromosomal DNA in a pattern similar to wild type Soj-GFP in the same background. The expression of SojD40A in a wild type or Δ*spo0J* background results in a low sporulation frequency, but the sporulation frequency is ~100 fold higher than the sporulation frequency when wild type Soj is expressed in a Δ*spo0J* mutant (0.03% vs. 2 x 10^{-4}%) (Murray and Errington, 2008). This indicates that SojD40A is less effective at inhibiting sporulation than is wild type Soj in a Δ*spo0J* background. For the Soj Walker motif mutants (SojK16A, SojK16Q, SojD125A, SojG12V) loss of sporulation inhibition is associated with loss of the ability to form bright foci, or associate with DNA (in Δ*spo0J* strains). This indicates a role for nucleotide binding or hydrolysis in sporulation inhibition by Soj, and supports the idea that when Soj is bound to the chromosome, sporulation in blocked.

In vegetative growth, wild type *B. subtilis* stained with DAPI show a compact chromosomal DNA staining pattern when observed by fluorescence microscopy (Autret *et al.*, 2001; Ogura *et al.*, 2003). Vegetatively growing Δ*spo0J* or cells that overproduce Soj show chromosomes that appear abnormally elongated and diffuse (Autret *et al.*, 2001; Ogura *et al.*, 2003). These observations have been used to suggest an overall decrease in chromosomal DNA structure in mutants lacking Soj or Spo0J that correlates with increased frequencies of anucleate cell in Δ*spo0J*, and Δ(*soj-sp0J*) mutants (Lee and Grossman, 2006), and minicell production in Δ(*soj-spo0J*) mutants (Ogura *et al.*, 2003).

Chromosomal DNA structure in *B. subtilis* is affected by multiple proteins. S*mc* is proposed to compact chromosomal DNA (Britton *et al.*, 1998). Δ*smc* cells have slightly elevated rates of anucleate cells and of cells that place division septa through chromosomal DNA (~5% total) instead of between chromosomes (Lee and Grossman, 2006). In a Δ*smc* background, deletion of either *soj, spo0J*, or both results in 27-30% of the cells being anucleate, and division septa are observed over chromosomes rather than between them (Lee and Grossman, 2006). In a Δ*smc* background the effect of a *soj* or a *spo0J* deletion on the phenotype is equal (Lee and Grossman, 2006). This differs from a wild type background where Δ*spo0J*, but not Δ*soj*, contributes to anucleate cell production (Ireton *et al.*, 1994; Lee and Grossman, 2006; Ogura *et al.*, 2003).

Two studies have reported that disruption of one or both genes of the *soj/spo0J* operon alters the DNA:protein ratio in vegetative *B. subtilis* cultures. One study directly analyzed the protein and DNA content from cultures (Lee and Grossman, 2006), and the other study analyzed

the number of chromosomal origins per cell by flow cytometry (Ogura *et al.*, 2003). Both groups reported that there is overinitiation of chromosomal DNA replication in a Δ*spo0J* mutant. However, Lee *et al.* detected similarily high DNA:protein ratios in Δ*soj* and Δ(*soj-spo0J*) mutants, whereas Ogura *et al.* detected a wild type DNA:protein ratio only in a Δ(*soj-spo0J*) strain. Elevated DNA:protein ratios similar to Δ*spo0J* strains were seen by Ogura *et al.* when Soj was overproduced but when both Soj and Spo0J were overproduced the DNA:protein ratios returned to levels observed in wild type strains. The discrepancy between the two groups provides two different possibilities for the role of Soj in relation to replication. On the one hand, the absence of Soj or Spo0J may lead to increased replication initiation, whereas on the other hand, Soj (in the absence of Spo0J) may function to stimulate replication initiation and this activity is antagonized by Spo0J. While both results indicate a role of the *soj/spo0J* operon in properly timed DNA replication, the contradictory results make the role unclear.

6.2 The Role of Soj (ParA) and Spo0J (ParB) Proteins in *B. subtilis* Sporulation.

As its name suggests disruption of *spo0J* blocks sporulation initiation prior to asymmetric septation (Ireton *et al.*, 1994). This block in sporulation is also characterized by low transcription of *spoIIA*, *spoIIE*, and *spoIIG* operons (Ireton *et al.*, 1994; Quisel and Grossman, 2000). *SpoIIA* and *spoIIG* operons encode forespore and mother cell compartment specific sigma factors, respectively (Clarke and Mandelstam, 1987; Trempy *et al.*, 1985). *SpoIIE* encodes a protein required for properly timed activation of the forespore-specific σ^F encoded by the *spoIIA* operon (Arigoni *et al.*, 1996). Deletion of both *soj* and *spo0J* results in wild type sporulation frequencies, and the restoration of *spoIIA*, *spoIIE*, and *spoIIG* transcription (Ireton *et al.*, 1994; Quisel and Grossman, 2000). Disruption of *soj* alone does not produce an effect on sporulation efficiency (Ireton *et al.*, 1994).

The available evidence indicates that Spo0A phosphorylation (Spo0A~P) is not affected by deletion of *spo0J*. Repression of the *abrB* gene in stationary phase and during sporulation requires Spo0A~P, and increased transcription of the *spo0A* gene upon entry into sporulation is also dependent on Spo0A~P levels. In Δ*spo0J* strains (spo$^-$), both *abrB* repression and *spo0A* transcription are similar to wild type *B. subtilis* (Cervin *et al.*, 1998).

Immunoprecipitation of DNA chemically crosslinked to Soj *in vivo* found that Soj was associated with *spoIIA*, *spoIIE*, and *spoIIG* (Quisel *et al.*, 1999). The amount of specific stage II DNA crosslinked to Soj increased in the absence of Spo0J. This result supports the idea that Soj

bound to the chromosome represses transcription which blocks sporulation, and Spo0J modulates Soj chromosome association.

The correlation between a chromosomal DNA distribution of Soj and sporulation inhibition is supported by analysis of *divIB* mutants (Real *et al.*, 2005). DivIB (a homologue of FtsQ in Gram-negative bacteria) is a bitopic membrane protein which interacts with multiple components of the division apparatus, and promotes its stability (Daniel *et al.*, 2006). When DivIB levels are reduced by ~30% (*divIB80* mutation) sporulation is inhibited, Spo0J-GFP is found in scattered small foci (very similar to Δ*soj* mutants), and Soj-GFP is chromosomally distributed (as described for Δ*spo0J* mutants). The sporulation inhibition in cells with reduced DivIB levels is rescued by deletion of the *soj/spo0J* operon and more specifically by deletion of *soj* (Real *et al.*, 2005). Thus like deletion of *spo0J*, lowering DivIB concentrations in the cell results in the distribution of Soj on DNA and sporulation inhibition.

Murray and Errington recently found (personal communication; in press, 2008) that in a Δ*spo0J* background, DnaA-dependent replication initiation increased. The same trend was observed for SojD40A in a wild type or Δ*spo0J* background. In a Δ(*soj-spo0J*) background replication initiation was also slightly elevated. When mutant Soj proteins (SojG12V, SojK16A) that do not localize to the chromosome were expressed replication initiation was less stimulated than when wild type Soj was expressed. These data indicate that Soj might either inhibit DnaA-dependent replication initiation, or stimulate it depending on Soj localization in the cell. Thus when Soj is bound to the chromosome it is not able to inhibit the activity of DnaA and the chromosome is replicated, but when Soj is antagonized by Spo0J or mutated so that it no longer binds DNA, it inhibits replication initiation by DnaA. In support of this model, Soj-DnaA interactions were detected *in vivo*. The study suggests that Soj localization to the chromosome results in over initiation which in turn activates a DNA replication checkpoint (Sda), Sda then inhibits sporulation possibly by inhibiting KinA. In support of this model the spo$^-$ phenotype of a Δ*spo0J* mutant was rescued by an additional *sda* mutation (a *spo0J sda* double deletion mutant was spo$^+$), indicating that Sda might be responsible for the sporulation inhibition observed in Δ*spo0J* strains). This model indicates that a key question regarding Soj and Spo0J is what affects the DNA binding properties of Soj.

7 Structure of ParA/Soj Proteins.

7.1 *T. thermophilus*

While Soj (ParA) and Spo0J (ParB) from *Thermus thermophilus* have been studied *in vitro*, nothing is known about how Soj and Spo0J affect *T. thermophilus* physiology. Spo0J from this organism is a site-specific DNA binding protein, which constitutively forms dimers (Leonard *et al.*, 2004). The two HTH DNA binding motifs of the Spo0J dimer align in a manner that suggests it binds to successive major grooves in the DNA helix (Leonard *et al.*, 2004). The crystal structure of *T. thermophilus* Soj-ADP is monomeric (Leonard *et al.*, 2005, Fig. 5A) and Soj dimers are formed only in the presence of ATP (Leonard *et al.*, 2005). A point mutant of Soj (SojD44A) was reported to be required for the determination of a Soj ATP dimer structure (Leonard *et al.*, 2005, Fig. 4A). Soj-ATP binds DNA with little sequence specificity, and can form multimeric Soj structures on DNA. The ATPase activity of Soj is stimulated by Spo0J *in vitro* (Leonard *et al.*, 2005).

Soj from *B. subtilis* is similar to Soj from *T. thermophilus* at the level of amino acid sequence and motif organization (Figs. 3, 4B). BlastP alignment of *B. subtilis* vs. *T. thermophilus* sequences, and the inverse alignment indicate 50% identity and 65% similarity between the two. For this reason the structure of *B. subtilis* and *T. thermophilus* Soj are likely very similar. The sequence identity is the strongest close to the ATP binding pocket. Strikingly Soj from either *T. thermophilus* or *B. subtilis* does not have a classic DNA binding motif. Recently Hester and Lutkenhaus (2007) used the structure of *T. thermophilus* Soj to identify residues that when mutated in *B. subtilis* Soj resulted in loss of DNA binding *in vivo* and *in vitro*, indicating that these residues are in a motif which is responsible for DNA binding .While Soj from *T. thermophilus* has not been well characterized *in vivo*, I used the structure of this protein as a model for studies of *B. subtilis* Soj due to their sequence similarity.

7.2 Plasmid pSM19035 δ Protein.

Recently a structural and functional characterization of the dimeric δ protein (ParA) from the *Streptococcus pyogenes* plasmid pSM19035 was published (Pratto *et al.*, 2008). The structure of the δ protein differs from that of *T. thermophilus* Soj. The δ protein made a 'U-like' dimer where the nucleotide binding pockets were solvent-exposed. *In vitro* the δ protein

Fig. 4. Motifs of *B. subtilis* and *T. thermophilus* Soj. (A) The structure of Soj from *T. thermophilus*. The Soj dimer structure was solved by x-ray crystallography of SojD44A bound to ATP (Leonard *et al.*, 2005). The Soj monomer structure was solved by x-ray crystallography of wild type Soj bound to ADP. For each structure nucleotides and Mg^{2+} are coloured orange, α-helices are coloured yellow, β-sheets are coloured turquoise, and motifs are coloured as follows; Walker A motifs (red), Walker A' motifs (puruple), Walker B motifs (green), and residues involved in DNA binding by *B. subtilis* Soj (blue). The residues equivalent to positions G12 and D40 in *B. subtilis* Soj are indicated as space filled residues in the *T. thermophilus* Soj structures. Structure images were generated using Rasmol. (B) Linear representation of Soj motifs. The sequences, and positions of the Walker A motifs (red), Walker A' motifs (purple), Walker B motifs (green), and residues involved in DNA binding by B. subtilis Soj (blue) are indicated for Soj from both *B. subtilis* and *T. thermophilus*.

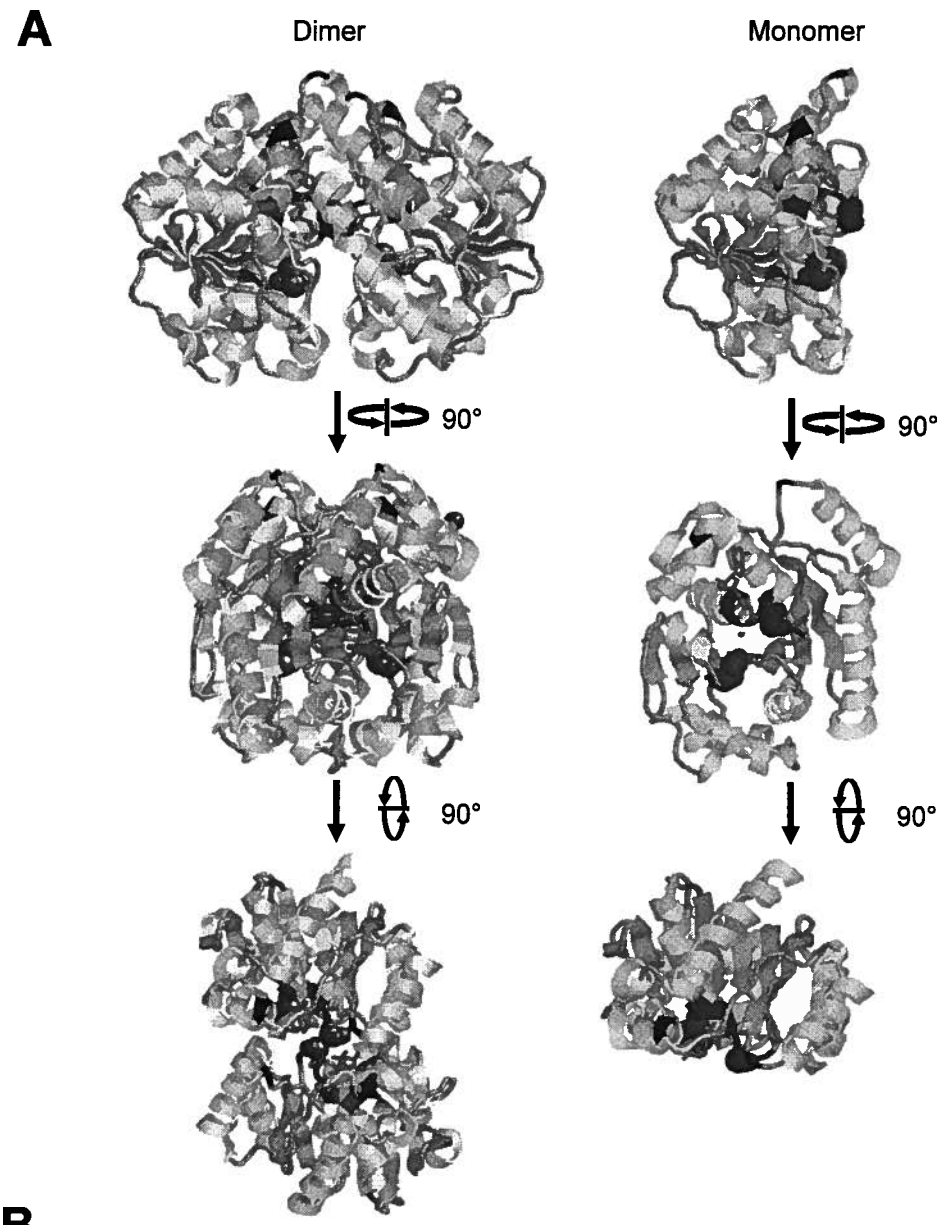
A
Dimer
Monomer
90°
90°
90°
90°

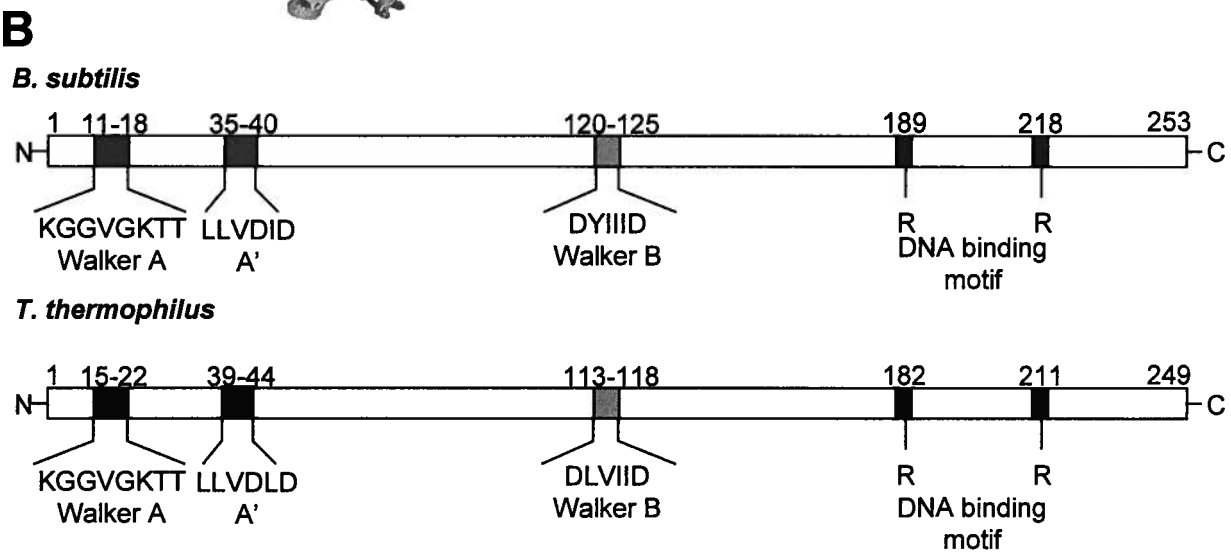
B
B. subtilis
1
11-18
35-40
120-125
189
218
253
N
C
KGGVGKTT
Walker A
LLVDID
A'
DYIIID
Walker B
R
R
DNA binding
motif
T. thermophilus
1
15-22
39-44
113-118
182
211
249
N
C
KGGVGKTT
Walker A
LLVDLD
A'
DLVIID
Walker B
R
R
DNA binding
motif

is primarily dimeric in the presence of either ATP or ADP, and also in the absence of nucleotide. When the invariant lysine of the Walker A motif was mutated so the protein no longer bound or hydrolyzed ATP, the protein was still observed to dimerize *in vitro*. The formation of the dimer in all conditions was stabilized by intermonomer interaction of a large hydrophobic patch, and by several intermonomer salt bridges. The δ protein along with ω protein (ParB) were required for stabilization of the plasmid pSM19035. In *B. subtilis* cells harbouring pSM19035 observed by fluorescence microscopy the δ protein fused to GFP was observed to make dynamic structures that made spirals and associated with cellular DNA.

BlastP alignment of *B. subtilis* Soj vs. δ protein sequences, as well as the inverse alignment, indicated 28% identity and 49% similarity between the two. The sequence identity was the strongest for the Walker motif sequences, and residues which are close to the ATP binding pocket in the δ protein structure (Fig. 3). While the structure of the δ protein is interesting, it does not share high sequence similarity with Soj from *B. subtilis*, and this structural information was not used the work described below.

8 Experimental Aim.

Previously the functions of Soj and Spo0J in *B. subtilis* have been inferred through the behavior of Soj and Spo0J *in vivo*, and by their contribution to sporulation initiation. These experiments have indicated that Soj prevents sporulation initiation, and is antagonized by Spo0J. The role of ATP binding and hydrolysis has been suggested to be important to Soj function on the basis of mutants, but biochemical characterization of these activities had not been carried out. In addition, the association of Soj with DNA, observed by microscopy, correlates with inhibition of sporulation, and with a decrease in sporulation-specific gene transcription, but there had been no investigation of this property in vitro,

To study the role of ATP and ATP hydrolysis, I started this work by examining the ATPase activity of *B. subtilis* Soj. The *in vitro* characterization of Soj and two Soj point mutants predicted to affect the ATPase activity (SojG12V and SojD40A) was included to link their in vitro activities to the effect on sporulation. Experiments were carried out to investigate how adenine nucleotides affect association with DNA and Spo0J *in vitro*. The experiments in the thesis indicated that Soj forms multiple complexes with DNA and that this property is dependent on ATP binding. The experiments contribute to a more complete characterization of the role of Soj in *B. subtilis* physiology.

MATERIALS AND METHODS

1 Standard Techniques.

Standard molecular biology techniques (precipitation of DNA, extraction of protein from nucleic acids, digestion of DNA with restriction endonucleases, ligation of DNA restriction fragments, SDS-PAGE of proteins, polyacrylamide and agarose electrophoresis of DNA) were performed as described (Sambrook *et al.*, 1989). The sources of enzymes were as follows; Restriction endonucleases, DNA ligase, and DNase I (Invitrogen), Pfu turbo DNA polymerase (Stratagene), Pfu DNA polymerase (Fermentas). All chemicals were reagent grade. Oligonucleotide primers were purchased from Alpha DNA (Montreal, QC).

2 Manipulation of DNA and Oligonucleotides.

Plasmid DNA and other DNAs used in this thesis are listed in Table 1. Primers and plasmid templates used to generate site-directed mutant plasmids are listed in Table 2. All DNA fragments used in this thesis and the primers and templates used to prepare them are listed in Table 3. For all molar DNA concentrations throughout this thesis, the values are given per base pair of DNA (assuming 650 Da/bp DNA) unless stated otherwise.

2.1 Site-Directed Mutagenesis.

Plasmids generated by QuikChange PCR reactions in this thesis are listed in Table 2. PCRs were composed of the indicated primer pairs (125 ng, ~0.28 μM final each), 250 μM dNTPs, 1 unit Pfu Turbo DNA polymerase (Stratagene) in 1x *Pfu* Turbo reaction buffer in a 50 μl reaction. The reactions were subject to 18 cycles of 30 s at 95°C, 1 min at 55°C, and 4 min at 68°C. The reaction products were treated with 10 units of DpnI for 1 hour. The DNA was ethanol precipitated, resuspended in 20 μl of water, and used to transform *E. coli* DH5α. Mutations in plasmids recovered from transformants were verified by DNA sequencing (Nucleic acids and protein services (NAPS), UBC).

Table 1. Plasmids Used in this Thesis

Plasmid[a]	Description	Reference or Source
pET20Soj	pET20b-based Soj over-expression plasmid.	(Cervin, et al., 1998)
pET20SojG12V	pET20b-based SojG12V over-expression plasmid generated by site directed mutagenesis PCR.	This work
pET20SojD40A	pET20b-based SojD40A over-expression plasmid generated by site directed mutagenesis PCR.	This work
pET16spo0J	pET16b-based Spo0J over-expression plasmid. Used to generate pETspo0JQC.	(Glaser, et al., 1997)
pET16spo0JQC	pET16b-based Spo0J over-expression plasmid generated by site directed mutagenesis to remove a NdeI site.	This work
pET20spo0J	pET20b-based Spo0J overexpression plasmid.	This work
pUC19		Invitrogen
pUC*IIGtrpA*	240 bp *spoIIG* promoter fragment in pUC19*trpA*.	(Satola, et al., 1991)
pUC*IIGBglIItrpA*	pUC*IIGtrpA* with g→t at position -22 of the *spoIIG* promoter.	Gift, V. Mendoza
pUC*IIG18*	pUC*IIGtrpA* with 18 bp spacer, generated from pUC*IIGBglIItrpA*	This work
pUC*A2trpA*	200 bp A2 promoter fragment in pUC19*trpA*.	(Dobinson, et al., 1985)
pJM5134	*abrB* promoter fragment containing plasmid.	(Greene, et al., 1996)
Φ29	Bacteriophage φ29 genomic DNA	Lab stock

a. all plasmids contained ampicillin resistance markers (amp^r).

Table 2. Primers and Templates Used to Generate Site-Directed Mutant Plasmids by PCRs.

Plasmid	Primer	Primer Sequence	Template
pET20sojG12V	sojG12V-F	gaaccaaaaagtcggggtcggcaaaaca	pET20soj
	sojG12V-R	gccgaccccgacttttttggttcgtaat	
pET20sojD40A	sojD40A-F	gtagatattgctccgcagggaaatgcg	pET20soj
	sojD40A-R	tccctgcggagcaatatctaccagcag	
pET16spo0JQC	0JQC-F	gggagtcatacgcctgagcctcttcaag	pET16spo0J
	0JQC-R	gaggctcaggcgtatgactccctttg	

Table 3. Primers and Templates to Generate PCR DNA Fragments Used in this Thesis.

DNA	Primer	Primer Sequence	Template
2 kb	2k-R	gacctcgagttagctagtgcgttcatga	φ29 genomic DNA
	2k-F	ctgaagcttgttaggcacacaagacaacg	
1 kb	1k-F	gtcgaattcgctagaattgtttgcggctg	φ29 genomic DNA
	1k-R	cagctcgagttatagagccgctaccgct	
0.5 kb	500-F	gcgtcacatatgccattaacgccaaat	*B. subtilis* JH642 genomic DNA
	500-R	gctgcactcgagttccttttcctcaaa	
0.3 kb	300-F	cgagtctagcggcactg	φ29 genomic DNA
	300-R	gataggatagttaaagtc	
0.1 kb	100-F	catcgtggaacaaatgag	φ29 genomic DNA
	100-R	cttaactgcattgtgtaactactc	
24 bp	24-F	gagtagttacacaatgcagttaag	no PCR (annealed)
	100-R	cttaactgcattgtgtaactactc	
Spo0J insert	0J20-F	gcgtcacatatggctaaaggccttgga	pET16spo0JQC
	0J20-R	gctgcactcgagtgattctcgttcaga	

2.2 Oligonucleotide Labeling.

Primer 100-R (100 pmol) was incubated with 3.5 µl [γ^{32}P]-ATP (8.3 µM, ~6000 Ci mmol^{-1}, GE Healthcare) and 5 units of polynucleotide kinase (Roche) in 10 µl of 1x Kinase Buffer (Roche) at 37°C for 3 hrs. The primer was separated from unincorporated [γ^{32}P]-ATP and ADP by use of a nucleotide removal kit (Qiagen). The primers eluted from nucleotide removal columns were ethanol precipitated on crushed dry ice and resuspended in 60 µl of Tris HCl-EDTA (TE) pH 8.

2.3 Preparation of Labeled DNA Fragments for EMSAs.

Radiolabeled primer 100-R was used to create 100 bp PCR products for use in electrophorectic mobility shift assays (EMSAs). Reactions contained labeled primer 100-R and primer 100-F (0.15 µM each), 1 ng µl^{-1} bacteriophage φ29 genomic DNA, 250 µM dNTPs, and 1 unit *Pfu* DNA polymerase in 50 µl of 1 x *Pfu* reaction buffer. The reactions were subjected to 30 cycles of 95°C for 30s, 55°C for 1 min, and 68°C for 1 min in a Biometra T Gradient thermocycler (Montreal Biotech). Labeled PCR products were purified using a PCR cleanup kit (Qiagen). Labeled 24 bp DNA was generated by annealing 5 µl of radiolabeled primer 100-R (8.3 pmol) and 5 µl of unlabeled primer 24-F (9 pmol) in 30 µl of 2 x SSC buffer. The reaction was heated to 95°C for 2 min in a Biometra T Gradient thermocycler (Montreal Biotech), and the temperature was decreased by 5°C every minute until the temperature reached 50°C.

2.4 Preparation of Internally Labeled DNA Fragments for DNase Protection Assays.

Internally [α^{32}P]-dATP labeled 1 kb DNA fragments were generated by PCR. Reactions were cycled for 16 cycles of 95°C for 30s, 55°C for 1 min, and 68°C for 1 min. Reactions contained primer 1k-F and primer 1k-R (0.15 µM each), 1 ng µl^{-1} bacteriophage φ29 genomic DNA, and 1 unit *Pfu* DNA polymerase in 50 µl of 1 x *Pfu* reaction buffer. Concentration of each dNTP was 200 µM, except for dATP, which was [α^{32}P]dATP (50µM, ~20 Ci mmol^{-1}, GE Healthcare). Unlabelled dATP was added to PCR tubes at a final concentration of 200 µM for 14 additional cycles. The 1 kb PCR products were subjected to 4.5% PAGE through a 4.5% native gel in 1x Tris-acetate (Sambrook *et al.*, 1989), the position of the 1 kb PCR product in the gel was resolved by autoradiography and the band was excised from the gel. The 1 kb products

were electroluted from the gel slice into dialysis tubing (12-14 kDa MW cutoff, SpectraPor). The DNA was collected, ethanol precipitated, and resuspended in 50 µl of TE pH 8.

2.5 Preparation of DNA Fragments for Light Scattering Assays.

The different length DNA fragments used in light scattering experiments were generated by PCR using primers and templates listed in Table 1. PCRs were composed of the indicated primers (0.15 µM each), 1 ng μl^{-1} DNA template, 250 µM dNTPs and 1 unit *Pfu* DNA polymerase in 50 µl of 1 x *Pfu* reaction buffer. The reactions were subjected to 30 cycles of 95°C for 30s, 55°C for 1 min, and 68°C for 1 min. The products were purified using a PCR purification kit (Qiagen). PCR products were quantified by calculating the concentration from the OD_{260} values after being diluted 50 fold. All PCR products used in light scattering assays were also quantified by densitometry to compare the intensity of bands of interest to those of serially diluted DNA ladders of known concentrations following agarose gel electrophoresis and staining of the gel with ethidium bromide.

2.6 Construction of pET20spo0J.

pET16spo0J (a gift from M. Perego) was subject to QuikChange site-directed mutagenesis to generate pET16spo0JQC, containing a silent mutation that removed an internal NdeI site from the Spo0J coding region (see section 1.2). To reclone the mutated *spo0J*, the *spo0J* coding region, flanked by NdeI and XhoI restriction endonuclease sites at the 5` and 3` end respectively, was generated by PCR amplification. The PCR was composed of primer 0J-F and 0J-R (7.5 pmol each), 1 ng μl^{-1} pET16spo0JQC, 250 µM dNTPs and 1 unit Pfu DNA polymerase in 50 µl of 1 x Pfu reaction buffer. The reactions were subjected to 30 cycles of 95°C for 30s, 55°C for 1 min, and 68°C for 1 min in a Biometra T Gradient thermocycler (Montreal Biotech). The PCR products were purified using a PCR cleanup kit (Qiagen), and were treated with NdeI and XhoI. The NdeI/XhoI treated PCR fragments were gel purified (Qiagen) and ligated into gel purified pET20b treated with NdeI and XhoI. The ligation products were used to transform *E. coli* DH5α. Plasmids purified from tranformants were screened for the appropriate size insert by agarose elecrophoresis of NdeI and XhoI treated plasmids. Candidate plasmid preparations with the appropriate sized insertion were sequenced (NAPS, UBC).

2.7 Generation of pUC*IIG18*.

The *spoIIG18* promoter was created from plasmid pUCIIG*Bgl*II*trpA*. pUCIIG*Bgl*II*trpA* is a derivative of pUCIIG*trpA,* in which the G at position –22 of the promoter was changed to T, introducing a unique *Bgl*II site. pUCIIG*Bgl*II*trpA* was treated with *Bgl*II, ethanol precipitated and resuspended in TE, pH 8. Mung bean nuclease (3.3 units, Invitrogen) was added to 8 μg of the *Bgl*II treated DNA in mung bean nuclease buffer in a final volume of 30 μl, incubated at 50°C for 1 hour and stopped by the addition of 1μl of 10% (w/v) sodium dodecyl sulfate (SDS). The reaction was phenol extracted, and the DNA was precipitated by the addition of ethanol. The DNA precipitate was collected, dried and redissolved in 10 mM Tris-HCl, pH 8 and re-circularized by ligation. The ligation reaction was extracted with phenol, and the DNA was precipitated by addition of ethanol, collected by centrifugation, and resuspended in React 2 buffer (Invitrogen) and treated with *Bgl*II prior to transformation of *E. coli* DH5α. To identify clones with shortened promoters, transformants were selected by slot lysis (Sambrook *et al.*, 1989) and sequenced to confirm deletions (NAPS, UBC).

3 Protein Purification.

3.1 Soj.

Plasmid pET20Soj, containing the Soj coding sequence ligated into the NdeI and XhoI sites of pET20b (C-terminal hexahistidine tagged overexpression plasmid) was a gift from J. Hoch. A fresh *E. coli* BL21 (*pLysS*) pET20Soj transformant colony was used to inoculate 1 litre of Luria-Bertani broth supplemented with 100 μg ml^{-1} ampicillin and 35 μg ml^{-1} chloramphenicol. Cultures were grown with vigorous shaking at 37°C until an OD_{600} of 0.8 was reached. Isopropyl-β-D-thiogalactopyranoside (IPTG) was added to a final concentration of 0.5 mM. Cultures were grown at 37°C for 3 hours. The cells were harvested by centrifugation (12k x g, 15 min) and cell pellets from 1 litre of culture were stored at -70°C.

All purification steps were carried out at 0-4°C. The cell pellet from 1 litre was resuspended in 10 ml of lysis buffer (20mM HEPES (pH 8), 10mM magnesium acetate (Mg acetate), 80 mM potassium acetate (K acetate), 1.9 M NaCl, 1 mM ADP, complete protease cocktail tablet (Roche), 1 mM β-mercaptoethanol) with 20 mM imidazole. Cells were lysed by addition of lysozyme to a final concentration of 1 mg ml^{-1} and sonication on ice (Ultrasonic

Table 4. Bacterial Strains Used in this Thesis

E. coli Strain	Genotype	Source
DH5α	[*hsdR17* (r_K^- m_K^+) *supE44 thi-1 rexA1 gyrA* (*Nal*^{r}) *relA1* Δ(*lacZYA-argF*) *U169*]	Invitrogen
BL21(DE3) pLysS	F^- *ompT hsdS*$_B$ ($r_B^-m_B^-$) *gal dcm* (DE3) pLysS (Cam^R)	Invitrogen
BL21 Star (DE3)	F^- *ompT hsdS*$_B$ ($r_B^-m_B^-$) *gal dcm rne1*31 (DE3)	Invitrogen

processor XL2020, 15 x 20 s at power level 3.5, Misonix Inc.). The lysate was cleared by centrifugation (25k x g, 20 min) and the supernatant was stirred on ice with Ni-NTA agarose (2.5 ml, Qiagen) pre equilibrated with lysis buffer for 45 minutes and loaded into a 10 ml column. The column was washed with 30 ml of lysis buffer with 20 mM imidazole, 30 ml of lysis buffer with 60 mM imidazole, and then was equilibrated with 30 ml elution buffer (20 mM HEPES, 10 mM Mg acetate, 80 mM K acetate, 300 mM NaCl, 100 μM ADP, 1 mM β-mercaptoethanol, 0.5 mM phenylmethylsulfonyl fluoride) with 20 mM imidazole. Protein was eluted with elution buffer, with 300 mM imidazole. Fractions (~0.3 ml) were immediately aliquoted, snap frozen on crushed dry ice and stored at -70°C.

3.2 Soj Mutants.

Over expression vectors were made by site directed mutagenesis of pET20Soj (section 2.1). Induction of mutant Soj overexpression and purification of Soj mutants was like wild type except cell pellets from 0.5 litre of induced cells were used in the lysis reaction and the final wash buffer and elution buffer contained 1 M NaCl.

3.3 Spo0J.

E. coli BL21 Star was transformed with pET20spo0J. A single transformant colony was used to inoculate 1 L of Luria-Bertani broth supplemented with 100 μg ml^{-1} ampicillin. Cultures were grown at 37°C until an OD_{600} of 0.6 was reached, IPTG was added to a final concentration of 1 mM. Cultures were grown at 37°C for 3 h, and the cells were harvested by centrifugation (12k x g, 15 min) and pellets from 0.5 L of culture were stored at -70°C.

Cell pellets from 0.5 L were resuspended in 10 ml of Spo0J lysis buffer (20 mM HEPES, 10 mM MgAc, 80 mM KAc, 1.9 M NaCl, Complete protease cocktail tablet (Roche), 1 mM β-mercaptoethanol) with 20 mM imidazole. Cells were lysed by addition of lysozyme to a final concentration of 1 mg ml^{-1} and sonication on ice (Ultrasonic processor XL2020, 15 x 20 s at power level 3.5, Misonix Inc.). The lysate was cleared by centrifugation (25k x g, 20 min) and the supernatant was stirred on ice with Ni-NTA agarose (2.5ml, Qiagen) pre equilibrated with lysis buffer for 45 minutes and loaded into a 10 ml column. The column was washed with 30 ml of Spo0J lysis buffer with 20mM imidazole, followed by a wash of 30 ml of Spo0J lysis buffer with 65mM imidazole, then equilibrated with 30 ml Spo0J elution buffer (20mM HEPES,

10mM MgAc, 80 KAc, 300 mM NaCl,) and 20mM imidazole. Protein was eluted with Spo0J elution buffer with 250mM imidazole. Fractions (~0.3 ml) were immediately aliquoted and snap frozen on crushed dry ice and stored at -70°C.

Because the imidazole and NaCl were not dialyzed from Soj and Spo0J protein preparations, in assays that compared the effect of protein concentration input of these salts was kept constant. This was achieved by diluting the protein in elution buffer and/or adding additional dilution buffer to the reactions.

3.4 Protein Quantification.

Protein concentrations were determined by the Bradford assay kit (Bio-Rad) standardized to BSA. Purified proteins used in this thesis were judged to be over 95 % pure by Coomassie brilliant blue stained 12% SDS-PAGE gels of recombinant purified protein samples.

4 Protein-Nucleotide UV Crosslinking.

The protein was incubated with α^{32}P-labeled nucleotide at 37°C in 20 µl of transcription buffer (10 mM HEPES pH 8, 10 mM Mg acetate, 80 mM K acetate) with 100 mM NaCl (protein, nucleotide concentrations, and specific activities are indicated in figure legends). The samples were transferred to a 96 well plate on ice and irradiated for the indicated time in a GS Gene Linker UV chamber (Bio-Rad). The reaction was transferred to a microfuge tube, and 20 µl of 1 mM unlabeled nucleotide was added. The well was washed with 100 µl of water which was added to the microfuge tube. Proteins were precipitated by addition of trichloroacetic acid (TCA) to 10% and incubation on ice for 40 minutes. The precipitate was collected by centrifugation for 40 minutes at 4°C. The pellet was washed with 10% TCA, followed by an acetone wash and the sample was then dissolved in 40 µl of SDS-PAGE loading buffer and separated by electrophoresis through a 12% SDS polyacrylamide gel. The gel was stained with Coomassie Brilliant Blue, dried, and exposed to a phosphorimager intensifying screen.

5 ATPase Assays.

ATPase assays were performed in 30 µl of ATPase buffer (20 mM HEPES pH 8, 10 mM Mg acetate, 80 mM K acetate) with 100 mM NaCl. The indicated concentrations of Soj were mixed with α^{32}P-ATP (12.4-0.62 Ci mmol^{-1}) and incubated at 37°C. At the indicated time points 2 µl of the reaction were removed and stopped by addition of EDTA to 20mM, and SDS to 0.05%. Samples were spotted on dry PEI cellulose thin layer chromatography (TLC) plates (Sigma-Aldrich) which were developed in 1 M formic acid and 0.5 M LiCl. TLC plates were dried, exposed to a phosphorimager intensifying screen, scanned, and exposed pixels were quantified using Imagequant software v.5.2 (GE Healthcare). ADP production was calculated by dividing the volume of exposed pixels in the phosphorimage spot corresponding to ADP by the sum of the volume of exposed pixels in the spots corresponding to ATP and ADP. All values were corrected by subtracting background α^{32}P-ADP levels of control reactions with no protein addition, Spo0J alone, and DNA alone for each time point where appropriate to reflect Soj ATPase activity. GTPase activity was assayed as described for ATPase activity assays except α^{32}P-GTP was added to the reactions to the indicated final concentrations (specific activities are indicated in figure legends).

6 Soj Size Exclusion Chromatography Assays.

The indicated protein (~ 60 µg, ~80 µM) was incubated in the presence of ATP or ADP (1 mM) in a 25 µl reaction at room temperature for 5 min in ATPase Buffer supplemented with 150 mM NaCl. The reaction was applied to a Superdex200 3.2/30 column on an ÄTKA purifier FPLC system (GE Healthcare) equilibrated with ATPase buffer supplemented with 150 mM NaCl, 10 % glycerol, and 100 µM of the indicated nucleotide at a flow rate of 70 µl min^{-1}. Protein elution from the column was detected by monitoring the absorption of the eluate at 230 and 280 nm and the absorption was plotted as a function of elution volume by Unicorn 5.11 FPLC system software. Absorption peaks at 230 nm corresponding to protein elution were analyzed with Unicorn software.

7 Blue Native PAGE Assays.

Blue native PAGE (BN PAGE) of purified proteins was performed essentially as described (Wittig *et al.*, 2006) except the level of Coomassie dye was greatly reduced. The indicated protein (2 μM) was incubated with the indicated nucleotide (1 mM) in ATPase Buffer with 100 mM NaCl in a 20 μl reaction for 5 min at 37°C. Two μl of 10 x BN PAGE loading buffer (10 x ATPase buffer with 2 x 10^{-3}% (w/v) Coomassie blue G-250) were added to the reactions and the reactions were applied to a 6-20% acrylamide gel, made in a 1 x gel buffer composed of 75 mM imidazole, and 1.5 M 6-aminohexanoic acid-HCl, pH 7. The cathode buffer (50 mM tricine, 7.5 mM imidazole, 2 x 10^{-4} % Coomassie blue G-250, pH 7), anode buffer (25 mM imidazole-HCl, pH 7), and gel were supplemented with the indicated nucleotide and Mg acetate (100 μM, and 4 mM respectively). For no nucleotide BN PAGE assays, the conditions were the same as above, except nucleotides and Mg acetate were omitted, and EDTA (1 mM) was added to reaction buffers, gel buffers, cathode, and anode buffers. Following electrophoresis (50 min, 130 V), 12 cm gels were silver stained with a BioRad silver stain kit (BioRad), and digital images of gels were generated by scanning the stained gels using an Epson 2450 Photo scanner. Digital gel images were analyzed with Imagequant software v5.2.

8 Electrophoretic Mobility Shift Assays (EMSAs).

For EMSAs using polyacrylamide gels, the indicated concentrations of Soj were incubated for 1 min with the indicated nucleotide (1mM) prior to the addition of ^{32}P end labeled DNA (40k Cerenkov counts per reaction) in 10 μl of ATPase buffer supplemented with 100 mM NaCl, 0.1 mg ml^{-1} BSA, and 0.5% glycerol. Reactions were incubated for 5 minutes at 37°C and 5 μl aliquots were loaded onto running 7.5 or 5.5 % acrylamide gels (23:1, acrylamide: bisacrylamide), made with 0.5x tris borate buffer (Sambrook *et al.*, 1989). Both gel and reservoir buffer were supplemented with 5 mM Mg acetate, and 100 μM of the indicated nucleotide. Samples were separated on a 12 cm gel at 120 V for 45 min at room temperature, the gels were dried, and phosphorimages of gels were generated using a Phosphorimager SI (GE Healthcare).

For EMSAs using agarose gels, the indicated concentrations of Soj were added to reactions with the indicated nucleotide (1 mM, same conditions as EMSAs using acrylamide gels) for 1 min prior to the addition of pUC19 DNA (1.5 ng μl^{-1} final concentration). The 40 μl

reactions were incubated for 5 minutes prior to electrophoresis through 12 cm, 0.5% agarose gels for 50 min at 90V, where both gel and buffer (0.5X Tris borate) were supplemented with 5 mM Mg acetate, and 100 μM of the indicated nucleotide. Gels were stained with ethidium bromide, rinsed briefly, and images were captured using an AlphaImager Gel documentation system (AlphaInnotech).

9 Sedimentation Assays.

To investigate Soj-DNA interactions, Soj was incubated in 40 μl of ATPase buffer with 100 mM NaCl, at 37°C, with 1mM of the indicated adenosine nucleotide for 1 min prior to the addition of linearized pUC19 DNA (4 ng μl^{-1} final concentration) where indicated. Reactions were further incubated for 5 minutes before centrifugation in an Eppendorf 5415C microfuge (16k x g) for 20 min. Supernatants were removed and pellet fractions were resuspended in 40 μl of ATPase buffer. Where protein sedimentation was investigated, 1X SDS-PAGE loading buffer was added to the fractions, and they were heated in a boiling water bath and subjected to 12% SDS-PAGE. The gels were stained with Coomassie Brilliant Blue. Where DNA sedimentation was investigated fractions were treated with Pronase (0.4 mg ml^{-1} final concentration, Roche) prior to electrophoresis through 0.8% agarose in 1X Tris Acetate (Sambrook *et al.*, 1989). Gels were stained with ethidium bromide and analyzed using a gel documentation system (Alphaimager EC, Alpha Innotech Inc.).

To investigate Soj-Spo0J interactions, Soj was incubated in 40 μl of ATPase Buffer with 100 mM NaCl, at 37°C, with 1mM of the indicated adenosine nucleotide for 1 min prior to the addition of Spo0J. Reactions were incubated for 5 min and treated as described for Soj-DNA sedimentation reactions to resolve protein sedimentation. Protein and DNA band density was determined from digital gel images using ImageJ (Abramoff *et al.*, 2004) or Imagequant v5.2 software.

10 DNase Protection Assays.

DNase I protection assay reactions were performed in 20 μl of ATPase buffer supplemented with 100 mM NaCl, and 100 μg ml^{-1} BSA (New England Biolabs) at 37°C. Soj was preincubated with either 1mM ATP or ADP for 1 min prior to the addition of internally labeled 1 kb DNA and incubation for 5 min. DNase I (4.8 units, Invitrogen) was added to the

reaction and after 1 min the reaction was terminated by addition of SDS and Pronase (0.1%, and 400 ug ml^{-1} final concentrations, respectively) and vigorous vortexing. Ten µl of DNase reactions were electrophoresed through 20 cm, 6% polyacrylamide (23:1, acrylamide: bisacrylamide) gels in 1X Tris acetate (Sambrook *et al.*, 1989). The gels were dried and a phosphorimage of the gel was generated using a Phosphorimager SI (GE Healthcare). Phosphorimage analysis used Imagequant v5.2 (GE Healthcare). Electrophoretic mobilities of 0.1 kb and 0.3 kb standards generated by PCR with ^{32}P end-labeled primers, and undigested 1kb DNA used for DNase assay were used to interpolate the size of partial DNase I protected species.

11 *In Vitro* Transcription Assays.

Transcription assays were carried out in a 20 µl final volume of Transcription buffer (10 mM HEPES pH 8, 10 mM Mg acetate, 80 mM K acetate) with 0.1 mg ml^{-1} BSA (Sigma, fraction V). Linearized plasmids containing promoter template DNA (6 nM DNA molecules) were incubated with the C-terminal domain of Spo0A which constitutively activates RNAP transcription from the *spoIIG* promoter (Spo0AC, 1 µM, gift of Steve Seredick), when indicated, RNAP (25 nM, gift of Steve Seredick), ATP (0.6 mM), and [α-^{32}P]-GTP (7.7 µM, 23 Ci $mmol^{-1}$) and the indicated concentrations of Soj for two minutes at 37°C. Complexes were then challenged with heparin plus UTP and CTP and allowed to elongate for 5 minutes at 37°C. Final concentrations were: heparin, 15 µg ml^{-1}; UTP, 0.6 mM; CTP, 0.6 mM. After elongation, transcription reactions were stopped by the addition of 10 µl of 8 M urea, 0.1% xylene cyanol, 0.1% bromophenol blue in 0.5× TBE. Transcripts were separated on an 8% polyacrylamide gel containing 7 M urea in 0.5× TBE and exposed to a phosphorimager intensifying screen (Molecular Dynamics, GE Healthcare). Phosphorimages of the gels were generated using a Phosphorimager SI (GE Healthcare). Phosphorimage analysis used Imagequant v5.2 (GE Healthcare).

12 Light Scattering Assays.

Light scattering assays were performed in a Cary Eclipse fluorescence spectrophotometer (Varian Inc., excitation and emission wavelengths 350 nm, slit widths 5 nm)

in the Laboratory of Molecular Biophysics Shared Spectroscopy and Kinetics Hub at UBC. Reactions were performed in ATPase buffer supplemented with indicated concentrations of nucleotides at 30°C and a final reaction volume of 1.5 ml in a stirred cuvette (4.5 ml, UV/vis plastic, 10 mm light path). Soj or mutant Soj protein was added at 1 min, the indicated concentrations of DNA were added at 2 min, and reactions were monitored for up to 10 min. In light scattering assays to detect Soj-Spo0J interactions Spo0J was added at 2 min in lieu of DNA. Data points were collected at 0.2 s intervals. The photomultiplier tube (PMT) voltage varied among experiments and is noted in figure legends. Changes in the PMT voltage result in scale differences for light scattering intensities (in arbitrary units) but light scattering intensity was reproducible for many different experiments and Soj preparations.

13 Transmission Electron Microscopy.

13.1 Resolution of Soj DNA Structures.

Soj sedimentation reactions in the presence of 4 μM Soj, 1 mM ATP and 2 ng μl^{-1} linearized pUC19 were performed as described for Soj DNA sedimentation assays. Following centrifugation supernatant was removed and the pellet fraction was resuspended in 10 μl of ATPase buffer without nucleotide, and 5 μl was placed on a glow discharged (Balzers carbon evaporator and glow discharge apparatus, Bal-Tec) carbon coated 400 mesh copper grid (Structure Probe incorporated). After 1 min 5 μl of 0.5% uranyl acetate was placed on grid for a further minute before wicking the majority of the reaction off the grid with filter paper, and the remaining material on grid was allowed to dry. Grids were examined with a Hitachi H7600 transmission electron microscope (80 kV filament voltage) at the UBC BioImaging Facility. 150 000 times direct magnification micrographs were captured using a side mount AMT Advantage CCD camera. Micrographs were analyzed using ImageJ software (Abramoff *et al.*, 2004).

13.2 Resolution of Soj-Spo0J structures.

Soj and Spo0J (1 μM each) were incubated for 5 min at 37°C in ATPase buffer with 100 mM NaCl and 100 μM ATP. Five μl of the reaction was placed on a glow discharged carbon coated 400 mesh copper grid (Structure Probe incorporated) for one minute. The majority of the

sample was removed by wicking with filter paper briefly; the grid was washed with 5 µl of distilled water before wicking dry. Samples on the grid were stained, the grids were examined and electron micrographs were captured as described for the resolution of Soj DNA structures.

13.3 Resolution of pUC19 DNA.

pCU19 DNA linearized by incubation with HindIII was ethanol precipitated and resuspended in sterile distilled water to a final concentration of 1 ng μl^{-1}. Five µl of the DNA solution was placed on a glow discharged carbon coated grid (same specifications as above), and was stained and washed as described for the resolution of Soj-Spo0J structures. Grids were examined and electron micrographs were captured as described for the resolution of Soj DNA structures.

RESULTS

1 Phylogenetic Analysis of ParA/Soj and MinD Proteins.

Phylogenetic analysis of plasmid and chromosomal ParA protein, and MinD protein sequence alignments was carried out using PAUP phylogenetic software v.4.0. An unrooted phylogram tree and an unrooted radial tree are shown in Fig. 5. No extensive analysis of these data was carried out but in general the patterns indicate that chromosomal ParA/Soj proteins group together, and are distinct from plasmid ParA proteins and MinD proteins). The separate grouping of plasmid and chromosomal ParA/Soj proteins suggests these proteins have functions dissimilar to those of plasmid ParA proteins. As a result the paradigms of plasmid encoded ParA family proteins might not be good guides for Soj activity and function.

2 Experimental Rationale.

To better understand the activities of Soj two mutants were also selected for characterization in addition to examining wild-type protein. The properties of the mutants are described in the Introduction. Briefly, SojG12V cannot repress sporulation in a Δ(*soj-spo0J*) mutant background, and a SojG12V-GFP fusion does not have the same chromosomal distribution as wild type Soj-GFP in Δ(*soj-spo0J*) cells (Murray and Errington, personal communication; Quisel *et al.*, 1999). SojD40A was examined because it was predicted to increase the stability of dimer formation and to be ATPase-deficient but still inhibit sporulation initiation.

3 Soj Mutant Overexpression Plasmids.

Both SojG12V and SojD40A expression plasmids were created by site-specific mutagenesis using pET20bsoj as a template. This plasmid encodes wild type Soj with an C-terminal hexahistidine tag fusion. The primers used are listed in Table 1, and the conditions used to generate the mutant protein overexpression plasmids are described in the Materials and Methods.

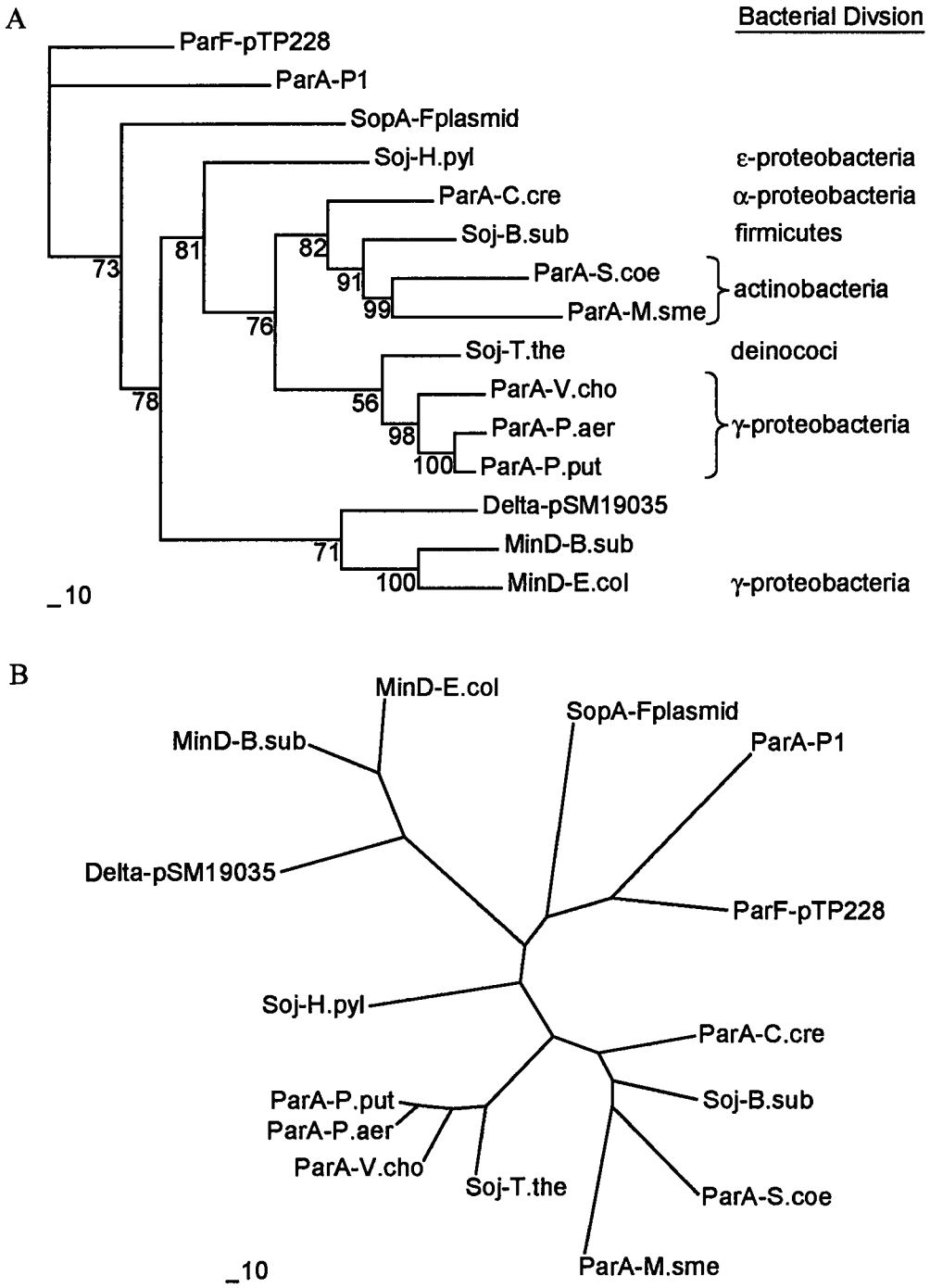

Fig. 5. Phylogenetic analysis of ParA/Soj, and MinD proteins. Protein sequences were analysed by PAUP phylogenetic software package v. 4.0 to generate an unrooted phylogram tree (A), and an unrooted radial tree (B) based on the neighbour-joining method. Bootstrap values are shown for each branch in panel A and are based on 100 replicates. The proteins and species or plasmids are indicated. Species abbreviations are as follows; B.sub, *Bacillus subtilis*; E.col, *Escherichia coli*; H.pyl, *Helicobacter pylori*; C.cre, *Caulobacter crescentus*; P.put, *Pseudomonas putida*; P.aer, *Pseudomonas aeruginosa*; V.cho, *Vibrio cholerae*; T.the, *Thermus thermophilus*, M.sme, *Mycobacterium smegmatis*; S.coe, *Streptomyces coelicolor*. Species phylogentic divisions are indicated. Scale bar indicates 10 units of phylogenetic distance as calculated by PAUP phylogenetic software.

4 Protein Purification.

Purified Recombinant Soj and Spo0J used in these experiments were both expressed and purified as C-terminal hexahistidine fusion proteins.

4.1 Soj Purification.

The goal of my thesis was to investigate Soj activities *in vitro* to better understand interactions of Soj with nucleotide cofactors, DNA, and Spo0J. To achieve this goal a Soj purification protocol which maximized yield while ensuring high purity and conservation of Soj activities was required.

The hexahistidine extension of purified recombinant Soj was assumed to not affect Soj activities *in vitro* because expression of C-terminal hexahistidine Soj protein is capable of blocking sporulation in a Δ*spo0J B. subtilis* strain, which indicates that the protein is active *in vivo* (Cervin *et al.*, 1998). Also in *B. subtilis* strains Soj-GFP hybrid proteins with GFP translationally fused to the C-terminus of Soj are capable of negative regulation of sporulation in a Δ*spo0J* strain (Quisel *et al.*, 1999).

Early experiments using an overnight culture to inoculate flasks for Soj production with gave inconsistent yields. After multiple trials I found that when Soj was over expressed by induction of a 1 litre culture inoculated with cells from a single freshly transformed *E. coli* BL21 (pLysS) pET20bsoj colony, the protein yield was far more consistent. The cultures were induced at an OD_{600} ~0.8 by addition of IPTG and shaken for 3 h. Growth was observed to halt shortly after IPTG addition, and microscopic examination revealed filamentous *E. coli* cells. The induced cells overproduced Soj despite the arrested growth, as observed by SDS-PAGE analysis of cell lysates (Fig. 6).

Initial attempts of Soj purification followed a standard protocol for purification of a hexa-histidine tagged proteins using Ni-NTA agarose (Cervin *et al.*, 1998). ATPase assays (described in Introduction section 5) indicated that Soj purified by this protocol had almost no activity which demonstrated that a significant fraction of purified Soj was not active (not shown). During my studies a report was published that indicated that isolation of active recombinant *C. crescentus* ParA purified from *E. coli* required the presence of ATP or ADP throughout the purification protocol. In light of those results, purification protocols were

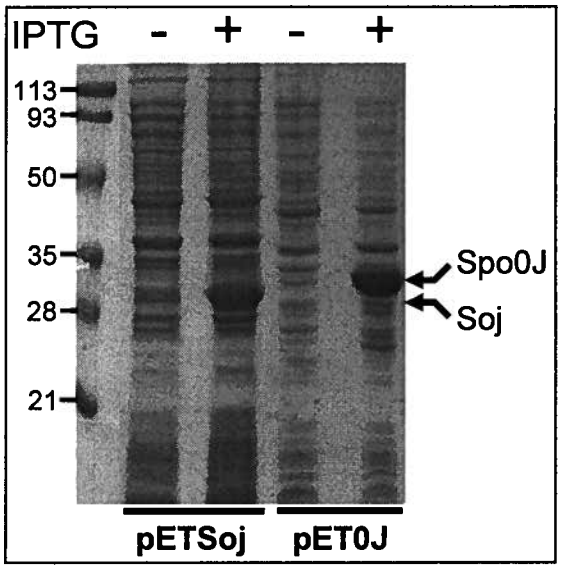

Fig. 6. Induction of Soj and Spo0J overexpression. One litre of LB containing ampicillin (100 μg ml^{-1}) and chloramphenicol (35 μg ml^{-1}) was seeded with a fresh *E. coli* BL21(pLysS) pET20soj transformant. One litre of LB with ampicillin (100 μg ml^{-1}) was seeded with a fresh *E. coli* BL21 Star pET20spo0J transformant. Cultures were grown at 37°C with vigorous shaking. Protein expression was induced by addition of IPTG to 0.5 mM (BL21 pET20soj) or 1 mM (BL21 Star pET20spo0J) at an OD_{600} of 0.8 for 3 h. One ml samples of cultures before IPTG addition (-), or after 3 h of IPTG addition (+) were removed, centrifuged, resuspended in 50 μl SDS loading buffer, and boiled for 5 min. Five μl of the indicated lysate was subjected to SDS PAGE and staining with Coomassie blue. Protein bands corresponding to overexpressed recombinant hexahistidine Soj and Spo0J are indicated. The molecular weight of low-range standards (Bio-Rad) are indicated in kDa.

modified to include ATP or ADP in all purification buffers. This modification resulted in Soj which was ~95% pure as estimated by Imagequant densitometry of images of Soj samples subjected to SDS-PAGE and stained with Coomassie blue (Fig. 7A) and had significant ATPase activity (see Section 3).

Control experiments done while examining DNA binding with early preparations of Soj, showed the presence of DNA in protein purified using buffers that had NaCl concentrations below 1 M in both the cell lysis and Ni-NTA column steps. This is shown in Fig. 7. Agarose gel electrophoresis of 3 μg of purified Soj and ethidium bromide staining of the gel detected fluorescing material (Fig. 7B). The incubation of Soj with DNase I, but not RNase A or Pronase prior to electrophoresis removed the fluorescing material, indicating that the contamination was DNA of varied length with an average size of approximately 500 bp (Fig. 7B). I estimated approximately 120 ng of DNA was co-purified per μg Soj, by comparing the staining intensity of the DNA in the pronase condition to the 0.5 kb MW ladder in Fig. 7B.

To eliminate the DNA contamination, I tried increasing the ionic strength in the lysis buffer, Ni-NTA agarose binding buffer and column wash buffers. As seen in Fig. 7C when Soj was purified using a high ionic strength buffer (1.9 M NaCl) for the lysis, Ni-NTA binding, and wash steps, the DNA contamination, assessed by agarose gel electrophoresis and staining with ethidium bromide of 9 μg of purified Soj, was greatly reduced (Fig. 7C). Presumably, this DNA contamination represented DNA bound to Soj.

Since high ionic strength in the Soj preparations might affect subsequent assays, after loading Soj onto the Ni-NTA agarose, packing the loaded resin into a column and washing the column with buffer containing 1.9 M NaCl, the column was washed with buffer containing 300 mM NaCl. Soj was then eluted using a buffer containing 300 mM NaCl, 100 μM ADP, and 300 mM imidazole. In numerous trials of different conditions I found that Soj precipitated and ATPase activity decreased more than two-fold when the purified Soj protein was subject to dialysis to remove either imidazole or nucleotide. As a result Soj eluted from the Ni-NTA agarose column in 300 mM NaCl and 100 μM ADP was immediately aliquoted and snap frozen. Long term storage (more than ~30 days) at either -20 or-70 °C also led to a 60-70 % reduction of ATPase activity, even though Soj degradation as assayed by SDS-PAGE was not observed. This loss of ATPase activity during storage occurred regardless of storage conditions. Approximately 2 mg of recombinant Soj were purified per litre of induced *E. coli* culture.

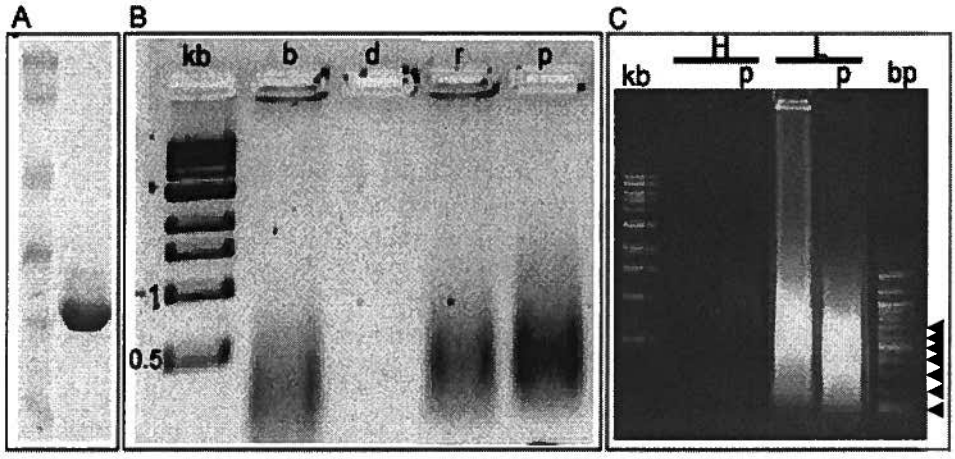

Fig. 7. Analysis of purified hexahistidine tagged Soj. (A) SDS-PAGE (12% polyacrylamide) of Soj (4.6 μg) purified under high ionic strength conditions stained with Coomassie brilliant blue, Soj was judged to be over 95% pure by Imagequant v5.2 software densitometry. Low-range molecular weight standards are shown on the left (from bottom; 21, 28, 35, 50, 93, 113 kDa, Bio-Rad Laboratories). (B) Agarose gel electrophoresis of Soj purified using low ionic strength lysis and wash buffers. After elution from a Ni-NTA column, Soj was pretreated with: buffer (b), DNase I (d), RNase A (r), or Pronase (p) prior to electrophoresis through 0.8% agarose along with a sample of 1 kb DNA ladder (kb, New England Biolabs). The gel was stained with ethidium bromide. (C) Effect of ionic strength on DNA in Soj preparations. Soj was purified by Ni-NTA chromatography using high (H; 1.9 M NaCl), or low (L; 0.3 M NaCl) salt in lysis and column wash buffers. After elution a sample was separated by electrophoresis through agarose. P indicates pronase treatment prior to electrophoresis. 1 kb (kb) and 100 bp (bp) ladders were included (New England Biolabs). Arrow heads on the right indicate DNA molecular weight standards (from bottom, 100-700bp, increasing by 100 bp).

4.2 Spo0J Purification.

Spo0J was over expressed by IPTG induction of a culture of *E. coli* BL21 star transformed with pET20-0J (Fig. 6). The Spo0J purification protocol followed a published purification protocol (Cervin *et al.*, 1998), with a modification in which the cell lysate was bound to Ni-NTA agarose, and washed with 1.5 M NaCl to remove a significant ATPase activity. Spo0J was eluted at lower ionic strength in order to not affect subsequent applications. Spo0J overproduction did not halt cell growth as did Soj overproduction, and there was no evidence of DNA contamination. Approximately 5 mg of Spo0J was purified per litre of induced *E. coli* culture, and could be stored at -70 °C for prolonged periods of time (~6 months).

5 ATP Binding and Hydrolysis by Soj.

Phylogenetically Soj is a member of a large Walker AB motif containing NTPase superfamily (Leipe *et al.*, 2002). Therefore it was expected that purified Soj would bind, exchange, and hydrolyze ATP. The importance of Soj ATP binding and hydrolysis activities has been suggested by the altered localization and loss of sporulation inhibition observed for *B. subtilis* strains expressing mutant Soj proteins predicted to have altered ATP binding and hydrolysis compared to wild type Soj. The *in vitro* characterization of the ATP binding and hydrolysis activities of Soj was central to my thesis for two reasons. First, it would establish that purified Soj protein preparations contained active Soj protein. Second, it was possible that the nucleotide bound state of Soj would alter its properties. The ability to monitor ATP binding and hydrolysis could be a tool to better understand the function of Soj.

Binding of nucleotide triphosphates by Soj was investigated by UV cross linking assays. Soj was added to reactions containing α-^{32}P labeled NTPs and the reactions were incubated prior to irradiation with UV light which covalently links bound α^{32}P-NTP to Soj. Following UV irradiation the protein in the sample was precipitated by addition of TCA. The precipitate was collected by centrifugation, washed with acetone, resuspended in SDS-loading buffer and the protein was subjected to SDS-PAGE. Proteins covalently linked to the ^{32}P nucleotide by UV irradiation were detected on a phosphorimage of the gel. As seen in Fig. 8A, ATP was readily linked to Soj. To investigate the NTP binding specificity of Soj, the purified protein was incubated with α^{32}P labeled ATP, dATP, or GTP (Fig. 8A). A lower intensity band was observed when Soj was incubated with labeled dATP instead of ATP prior to crosslinking.

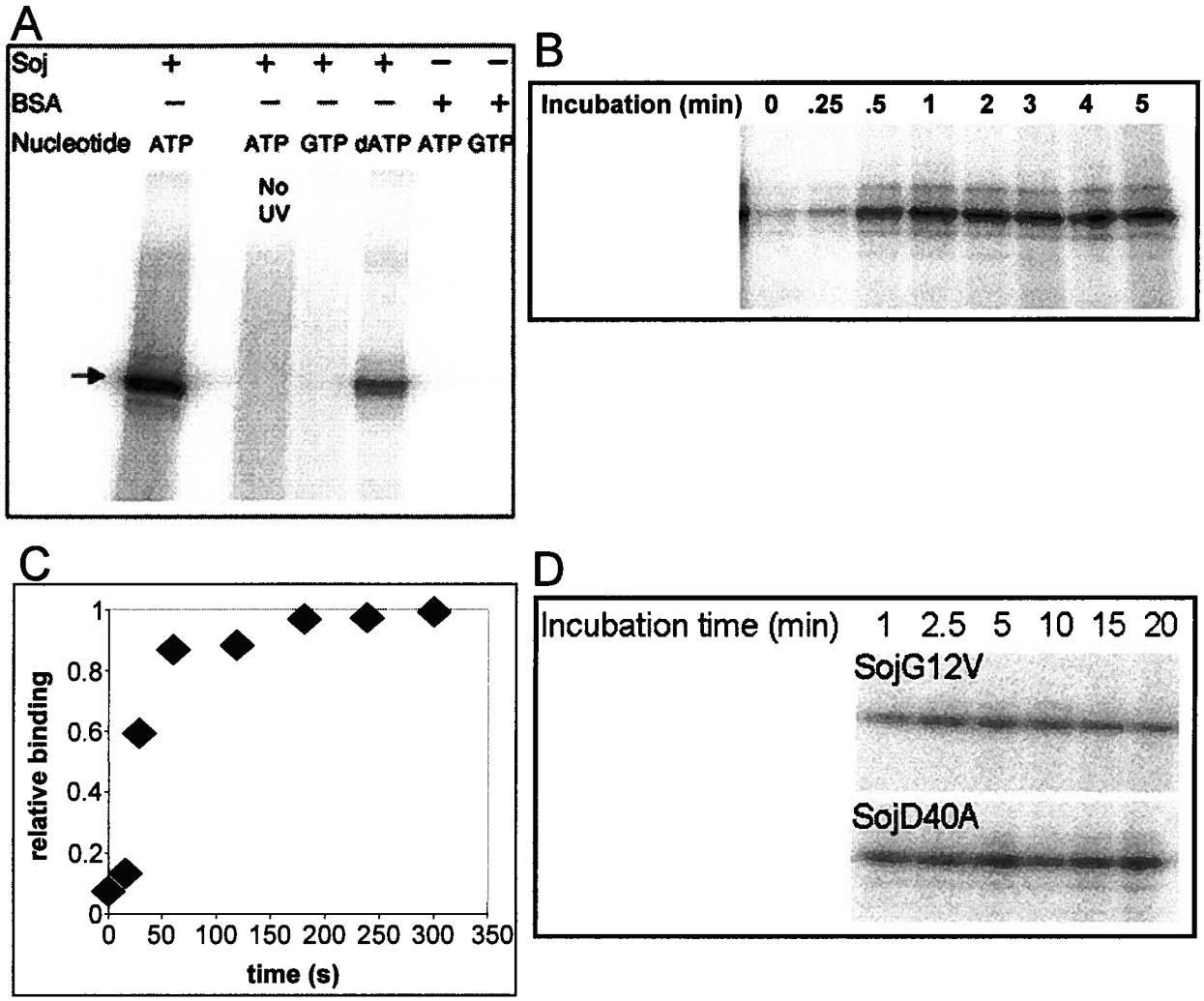

Fig. 8. Nucleotide binding by Soj assayed by UV cross linking. (A) Nucleotide binding specificity of Soj. α^{32}-P-labeled nucleotides (50 μM, 24.8 Ci mmol^{-1}) were incubated with 12.5 μM Soj or 0.1 mg ml^{-1} of bovine serum albumin (BSA) for 5 min in 20 μl of ATPase buffer with 100 mM NaCl. Samples were irradiated with UV for 5 min on ice, followed by trichloroacetic acid precipitation and solubilization in SDS-PAGE loading buffer. Samples were subjected to 12% SDS-PAGE. The gel was dried and a phosphorimage was generated as described in Materials and Methods (section 4). (B) Time course of Soj ATP binding detected by UV cross linking assays. Reactions of Soj (5 μM), and α^{32}P-ATP (200 μM, 6.2 Ci mmol^{-1}) were incubated at 37°C for the indicated time, and then irradiated with UV for 2 min on ice. Samples were treated and a phosphorimage was generated as described for panel A. (C) Phosphorimage densitometry of the major cross-linked bands from panel B were determined using Imagequant v5.2. Data were normalized to the density of the band in 5 min incubation and plotted as a function of incubation time. (D) SojG12V and SojD40A ATP binding assayed by UV cross-linking. The indicated Soj mutant (5 μM) was incubated with α^{32}P-ATP (500 μM, 2.5 Ci mmol^{-1}) for the indicated time at 37°C in 20 μl reactions, and irradiated with UV for 3 min on ice. Reactions were then treated as described in panel A.

When Soj was incubated with labeled GTP prior to crosslinking no band was observed. To test the validity of this assay Soj was incubated with α^{32}P-ATP but was not UV irradiated, and BSA, a protein with no nucleotide binding activity, was incubated with α^{32}P-ATP prior to UV irradiation. In the latter two cases, no signals corresponding to protein covalently linked to α^{32}P-ATP were observed, which indicated that the UV cross-linking assay was an indication of nucleotide binding, and that Soj specifically bound ATP (and dATP to a lesser extent), but not GTP.

ATP binding by Soj as a function of both time and temperature was assayed by UV cross-linking. To test the rate of ATP binding, Soj was added to reactions which contained α^{32}P-ATP and the reactions were allowed to incubate at 37 °C for various times before UV irradiation on ice (Fig. 8B). Soj binding of ATP increased rapidly reaching 90% of maximum at approximately 90 s (Fig. 8C). When either SojG12V or SojD40A were included in cross linking reactions with ^{32}P-ATP a maximum crosslinking signal was reached by 1 min (Fig. 8D) indicating both mutants could bind ATP. While these assays show that the mutant Soj proteins bind ATP, is it possible that the kinetics of binding were different in the first minute of the assay. This point was not considered of great importance, since it was clear that a 1 min incubation with ATP would give maximum binding. A more detailed examination of SojG12V and SojD40A ATP binding activities at earlier time points such as those in Figs. 8B and 8C would be required to determine the ATP binding constants and ATP binding rates for these proteins.

The amount of ATP crosslinked to Soj was calculated by comparing the densitometries of Soj bands to those of known amounts of α^{32}P-ATP. The amount of ATP crosslinked to Soj was determined using the specific activity of α^{32}P-ATP in the crosslinking reactions. At maximum binding of Soj to ATP, ~0.05 % of Soj was crosslinked to ATP. The low level may reflect the fact that UV irradiation is an inefficient method of crosslinking. On the other hand possibly the Soj that was purified was primarily inactive. I was not able devise a second ATP binding assay which could determine a specific Soj activity. It seems unlikely that the Soj purified was only 0.05% active since the ATPase level (see below) was within the range seen for other MinD family members. An independent ATP binding assay would have greatly improved my analysis of Soj by indicating how much Soj was active from a specific Soj purification. UV-crosslinking efficiencies for other Walker A motif ATPases have not been reported, to my knowledge, so it is possible that the values observed in Fig. 8 are reasonable.

Because of the low crosslinking efficiency, I considered the possibility that a contaminant which binds ATP and migrates in an SDS-PAGE gel is responsible for the crosslinking observed in Fig. 8. Crosslinking assays with a Soj mutant which is predicted to not bind ATP (such as SojK16A, a Walker A motif invariant lysine mutant) was not done. If such an experiment resulted in greatly reduce UV-crosslinking it would confirm the UV-crosslinking of ATP to wild type Soj and not a contaminant in Fig. 8.

Minor bands were observed in the UV cross-linking assays that migrated differently than Soj, and were not present in conditions without UV crosslinking. I investigated the identity of the anomalous protein bands. Soj was subjected to SDS-PAGE. The area of an SDS-PAGE gel stained with Coomassie brilliant blue which contained the larger species was excised from the gel, subject to in gel proteolysis, and analyzed by mass spectroscopy at the University of Victoria. The only detectable peptides were derived from Soj. A directed studies student separated samples of purified Soj by SDS-PAGE, transferred the proteins to a PVDF membrane, and probed the membrane with α-Soj antibodies (a gift from M. Perego, data not shown). Both the upper and lower bands cross reacted with the α-Soj antibodies indicating that the bands contained Soj or Soj breakdown products. The lower band may have been a degradation product of Soj, and the higher band appeared to be Soj with anomalous electrophoretic mobility. The higher band constituted only a very small fraction of purified Soj and the cause of this anomaly is unknown. Later Soj preparations used buffers supplemented with dissolved protease inhibitor cocktail tablets (Roche), and fewer Soj degradation products were observed.

Soj hydrolysis of ATP to ADP was investigated by following the production of ADP. The purified protein (3 μM) was incubated with α^{32}P-ATP. Aliquots of the reactions were removed and the ATPase was stopped by the addition of SDS (0.2 % final concentration) and EDTA (50 mM final concentration). Four μl of the quenched aliquot were spotted on a PEI cellulose plate which was then developed to separate α^{32}P-ATP and α^{32}P-ADP. Phosphorimage intensities of the spots corresponding to both ^{32}P- ATP and ^{32}P-ADP were used to calculate the percentage of ADP in the reaction or total moles of ADP produced.

The production of ADP by Soj was linear for the first 60 min of the assay (Fig. 9). Incubation of SojG12V with α^{32}P-ATP also resulted in the production of α^{32}P-ADP and at a similar rate as seen with wild type Soj. SojD40A showed a reduced ADP production compared to both Soj and SojG12V. The reduced ATP hydrolysis by SojD40A was a catalytic defect of the protein, since the mutation did not affect its ATP binding as shown in Fig. 8D. This was the expected result as the mutated residue has been shown in the *T. thermophilus* structure of Soj to

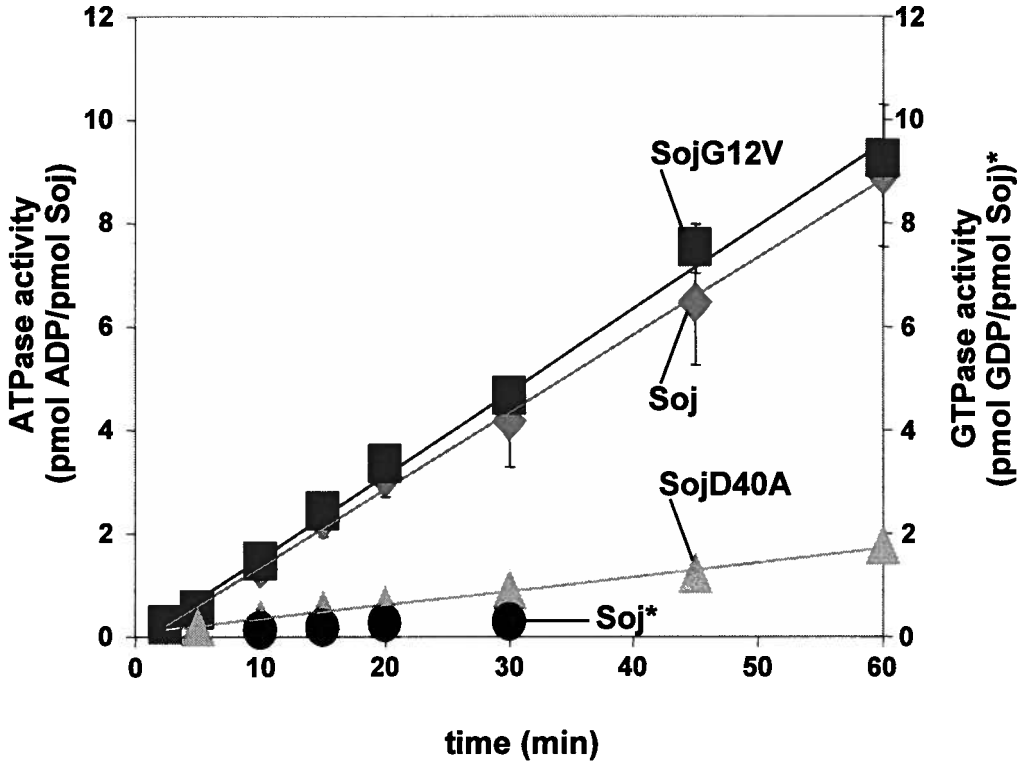

Fig. 9. ATPase activities of Soj, SojG12V, and SojD40A. The indicated protein (4 μM) was incubated with 250 μM [α-^{32}P]ATP (1.33 Ci mmol^{-1}) in 30 μl of ATPase Buffer containing 100 mM NaCl. Aliquots of reactions were removed at the indicated times, stopped as described in Materials and Methods (section 5), and subjected to thin layer chromatography. The amount of ATP hydrolyzed was calculated from the densitometry of ATP and ADP spots as described in Materials and Methods (section 5). The data points labeled Soj* correspond to GDP production from GTPase reactions (same conditions as ATPase reactions except for the absence of α^{32}P-ATP and the presence of α^{32}P-GTP (250 μM, 1.33 Ci mmol^{-1})). Each time point is the average value of 3 independent reactions; error bars represent standard deviations for each time point. Linear trend lines were fitted by Microsoft Excel. Values were corrected for trace ADP or GDP presence detected in reactions containing no protein for each time point.

coordinate the binding of a Mg^{2+} ion cofactor required for ATP hydrolysis but does not affect ATP binding by the Walker A motif of Soj. Since SojD40A was purified the same way as Soj and SojG12V, it was expected that any contaminants would be present equally in all of the recombinant proteins. Therefore, this result also provided evidence that ADP production was mediated by Soj and not by a contaminating ATPase. The result that SojG12V was a functional ATPase and produced similar levels of ADP as wild type was surprising as the equivalent mutation in related ATPases has been shown to severely reduce ATPase activity (addressed in the Introduction and Discussion). As an additional control, the ability of Soj to hydrolyze GTP was assayed (indicated as Soj* in Fig. 9). No significant GDP production was observed, consistent with nucleotide cross linking experiments that detected no GTP binding. The latter result supported the idea that there was not a contaminating purine nucleotidase activity in purified Soj samples.

I also noted that the presence of ADP rather than ATP during purification was more effective at stabilizing the solubility of Soj after elution, resulting in higher yields of soluble Soj (data not shown). Therefore, Soj was purified in the presence of 100 μM ADP. The inclusion of ADP in Soj purification protocols resulted in the presence of small concentrations of ADP (≤ 10 μM) in all experiments. The presence of ADP in Soj ATPase assays had a negative effect on Soj ATPase activity, especially at lower ATP concentrations (data not shown). These results suggested that ADP was a ligand for Soj and that the presence of ADP in kinetic assays could cause product inhibition giving inaccurate data. To address this problem the Soj purification protocol was changed for protein to be used in kinetic analyses. Prior to Soj elution the Ni-NTA agarose column was equilibrated with ten column volumes of purification buffer with reduced ADP concentration, or without nucleotide. This modification did have an impact on ATPase (Fig. 10), but the effect was observed to be small but reproducible. Despite the small decrease in ATPase activity, Soj used in the initial velocity kinetic assays was prepared with a 'no nucleotide' wash to eliminate the worry about product inhibition.

To determine the initial velocity of Soj ATPase, purified Soj was incubated with the indicated concentration of α^{32}P-ATP and the production of ADP was measured over time. An example of ADP production plotted versus time at 10 μM ATP is shown in Fig. 11A. The slope of the best fit line was used to calculate the initial velocity (v, pmol/nmol Soj/min) of Soj ATPase. The initial velocity of Soj ATPase was calculated for a range of ATP concentrations

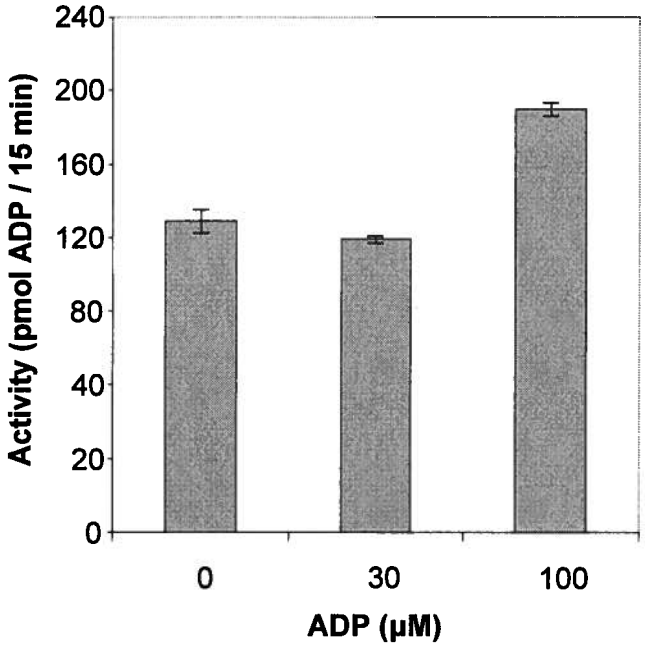

Fig. 10. ATP hydrolysis by Soj eluted in different ADP concentration conditions. Soj was purified as described in Materials and Methods (section 3.1) except the Ni-NTA column was equilibrated with buffer containing the indicated concentration of ADP, and the protein was eluted from the column in elution buffer with the indicated ADP concentration. Soj (3 μM) was incubated with 50 μM α^{32}P-ATP for 15 min at 37°C in ATPase buffer with 100 mM NaCl; each reaction was repeated in triplicate. Reactions were stopped and ADP was detected and quantified as described in Materials and Methods (section 5). Values were corrected for trace radioactive ADP present in reactions containing no protein.

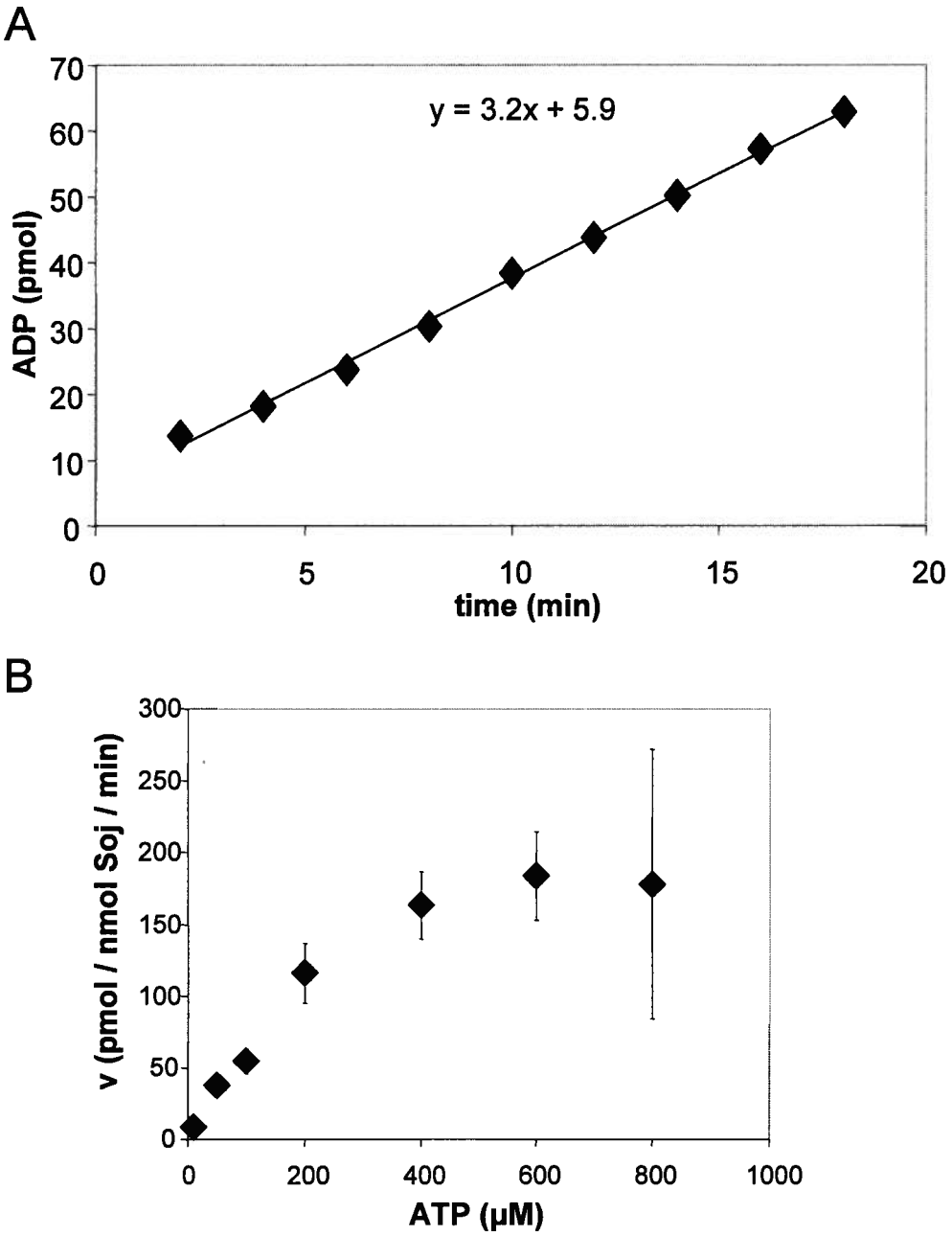

Fig. 11. Soj ATPase kinetics. (A) An example of the determination of the initial rate of ATP hydrolysis for kinetic analysis. Soj (3 μM) was incubated with α^{32}P-ATP (10 μM, 24.8 Ci mmol^{-1}) in a 40 μl of ATPase buffer containing 100 mM NaCl, at 37°C. At the indicated times aliquots were removed and stopped. ADP was detected and quantified as described in Materials and Methods (section 5). The ADP production was plotted as a function of time and the rate was calculated from a trend line slope fitted by Microsoft Excel assuming linearity. (B) The rate of ATP hydrolysis was determined from curves such as shown in panel A. The rate was divided by the quantity of Soj to give the initial velocity (v, pmol ADP/ nmol Soj / min) The initial ATPase velocity of Soj was determined at the indicated ATP concentrations. The initial velocity was plotted as a function of ATP concentration. Each point represents the average initial velocity calculated from at least 3 independent reactions; error bars representing standard deviations are indicated.

and the initial velocity of Soj ATPase activity as function of ATP concentration is plotted in Fig. 11B.

Visual examination of Fig. 11B. (initial velocity versus ATP) indicated a V_{max} of 175-180 pmol ATP consumed / nmol of Soj / min and an apparent K_m of 175±62 μM ATP. At V_{max}, the turnover number (k_{cat}) was calculated to be 3±1 $x10^{-3}$ s^{-1}. Due to the large standard deviations of K_m and k_{cat} values the calculation of k_{cat}/K_m ranged between 8.4-35.4 M s^{-1}. The range of k_{cat}/K_m values indicated that Soj is not an efficient ATPase. These values are similar to other ParA/MinD proteins that also have low ATPase activity (Davis *et al.*, 1992; de Boer *et al.*, 1989).

6 Characterization of Soj Multimerization.

6.1 Size Exclusion Chromatography of Soj.

As discussed in the Introduction, the ParA/MinD protein family members undergo nucleotide-dependent dimerization and in some instances can form higher order complexes. Size exclusion chromatography was used to monitor the formation of Soj multimers in the presence of either ATP or ADP. For these experiments Soj (~ 60 μg, ~80 μM) was incubated with 1 mM of the indicated nucleotide for 5 min at room temperature in a 25 μl volume and loaded onto an analytical Superdex200 column equilibrated with buffer containing 0.1 mM of the same nucleotide at room temperature. The elution profile was monitored by absorption at 230 nm and was plotted versus the elution volume. The elution volumes for a set of molecular weight standards (Fig. 12, Table 5), was also determined. The elution profiles of wild type and mutant Soj had higher peak intensities when detected by absorbance at 230 nm compared to 280 nm. Peptide bonds, tryptophan residues and tyrosine residues all absorb at 230 nm. Both absorption spectra at 230 nm and 280 nm were monitored simultaneously and showed the same elution patterns. Only Soj elution profiles monitored by absorption at 230 nm are shown. Soj showed absorption peaks at ~1.78-1.81 ml and 2.15-2.17 ml corresponding to the molecular weights of 58 kDa (possible Soj dimers) and 29 kDa (possible Soj monomers) respectively (Fig. 13). In the presence of ATP, the peak centred at 1.78 ml showed a shoulder that was not seen in the presence of ADP suggesting the presence of a Soj species larger than that of a dimer (possibly a tetramer, ~105 kDa), or a fraction of the protein with an altered shape.

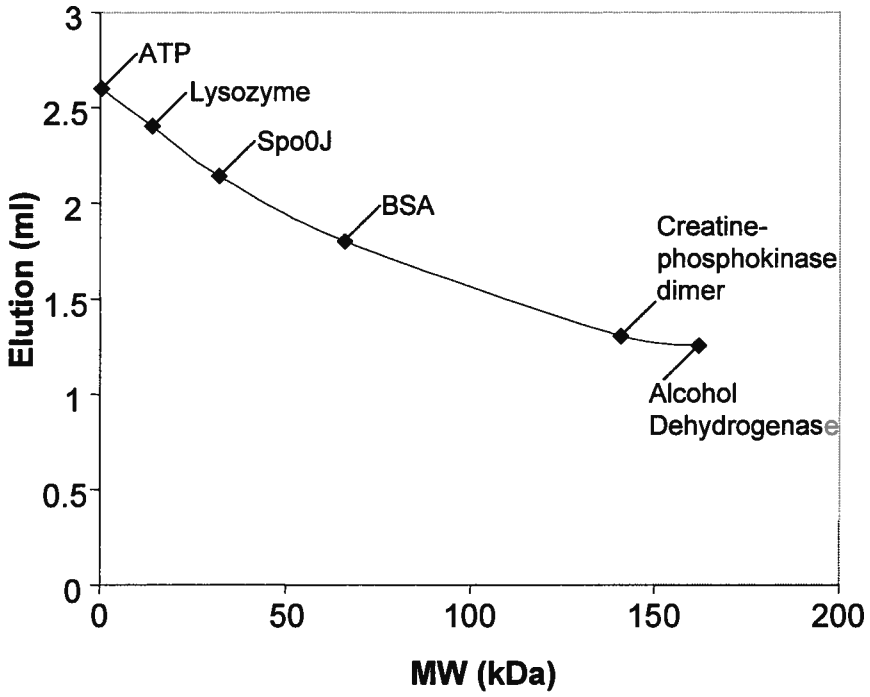

Fig. 12. Elution of molecular weight standards used to estimate size of Soj dimers. The elution volume of molecular weight standards (listed in Table 5) from a Superdex 200 3.2/30 size exclusion chromatography column attached to an ÄTKA purifier FPLC system was plotted as a function of molecular weight.

Table 5. Molecular Weight Standards Elution Volumes Used for Size Estimation of Soj Multimers.

Standard	MW (kDa)	Elution (ml)
Creatine Phosphokinase dimer	162	1.25
Alcohol Dehydrogenase	141	1.30
BSA	66	1.80
Spo0J	32	2.10
Lysozyme	14	2.40
ATP	0.551	2.60

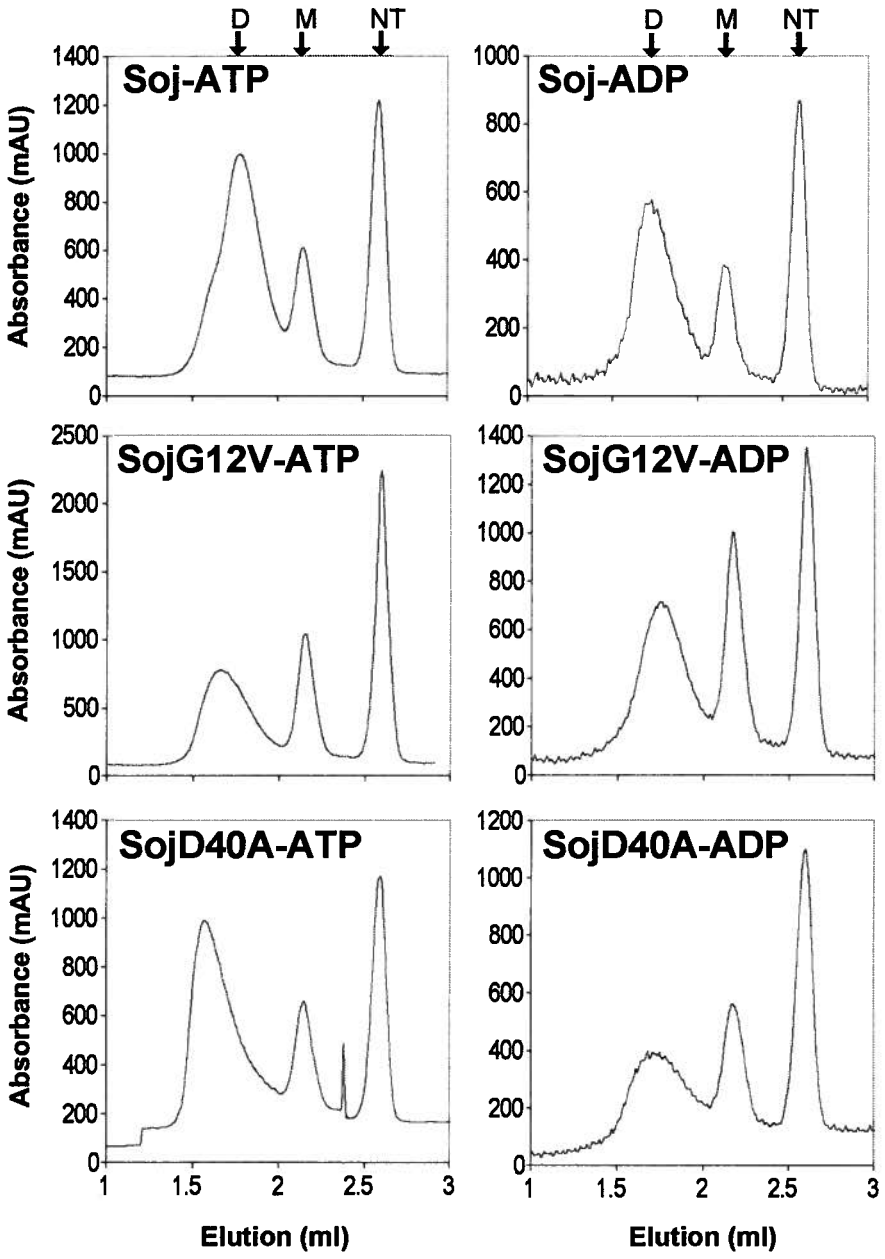

Fig. 13. Analysis of purified Soj and Soj mutants by FPLC size exclusion chromatography. The indicated protein (~60 μg, 80 μM) was incubated in the presence of ATP or ADP (1 mM) in 25 μl of Soj elution buffer at room temperature for 5 min as described in the Materials and Methods (section 6). The mixture was applied to a Superdex 200 3.2/30 column attached to an ÄTKA purifier FPLC system equilibrated in ATPase Buffer with 100 mM NaCl, 10 % glycerol, and 100 μM of the indicated nucleotide. The A_{230} of the elution was monitored and plotted as a function of the elution volume. Vertical arrows indicate the elution position of peaks that correspond to Soj dimers (D), Soj monomers (M), and nucleotides (NT).

The elution of SojG12V in the presence of either ATP or ADP showed absorption peaks centred at 2.15-2.17 ml and 1.68-1.75 ml which correspond to the elution volume expected from proteins with masses equal to Soj monomers and dimers respectively. The elution of SojD40A in the presence of ATP or ADP showed an absorption peak centred at 2.15-2.17 ml corresponding to the elution volume expected for a protein equal in size to a Soj monomer. However, SojD40A eluted differently in the presence of ATP or ADP. In the presence of ATP, the first absorbance peak was centred at 1.57 ml, whereas in the presence of ADP the first absorbance peak detected was centred at 1.74 ml. The SojD40A peak at 1.57 ml corresponded to the elution volume of the shoulder of the peak in the elution profile of wild type Soj in the presence of ATP, suggesting the presence of Soj protein complexes with higher molecular weight in the presence of ATP (possibly a tetramer, ~105 kDa), or a significant change in shape. For both Soj and SojD40A in the presence of ATP, the presence of a peak eluting at a lower elution volume indicating a shape change in Soj dimers or the elution of a tetramer was not due to loading error as the elution of monomeric Soj and ATP remained constant throughout these assays.

FPLC system software was used to determine the area of the peaks corresponding to Soj monomers, dimers and ATP or ADP. Peak elution volumes, areas, and areas relative to the area of the peak corresponding to Soj dimers are shown in Table 6. No clear trend in the ratio of the peaks between ATP and ADP conditions was observed for Soj or SojG12V which indicated that ATP and ADP did not differentially affect the dimerization of Soj from *B. subtilis*.

For all three Soj proteins regardless of which nucleotide was present no absorbance peaks were observed in the void volume of the column eluate (0.6 ml). This indicates that under the conditions of this chromatography, larger multimers of Soj were not detected. However I routinely found that the back pressure in the FLPC column increased in successive runs, implying that Soj might be forming large complexes that come out of solution (see below). In agreement with that possibility, I noted incomplete recovery of Soj A_{230} units in the eluates.

6.2 Blue Native PAGE Analysis of Soj.

It was reasoned that observed Soj dimerization from size exclusion chromatography could be influenced by the high concentrations of Soj (~ 60 μg, ~80 μM) loaded on the column. Therefore, blue native PAGE (BN-PAGE) was used as an independent technique to assay for Soj multimerization with the advantage of small sample volumes (20 μl) with low Soj

Table 6. FPLC Absorption Peak Integration[a].

Nucleotide	Protein	Peak[b]	Elution (ml)	Area (mAU*ml)	Relative Area[c]
ATP	Soj	D	1.78	262	1
		M	2.15	67	0.26
		NT	2.59	115	
	SojG12V	D	1.66	222	1
		M	2.15	118	0.53
		NT	2.60	196	
	SojD40A	D	1.57	234	1
		M	2.15	71	0.30
		NT	2.59	103	
ADP	Soj	D	1.73	159	1
		M	2.15	50	0.31
		NT	2.60	89	
	SojG12V	D	1.75	208	1
		M	2.17	126	0.60
		NT	2.60	137	
	SojD40A	D	1.68	136	1
		M	2.17	82	0.60
		NT	2.60	122	

a. Integration of the peaks from elution profiles in Fig. 13 was performed with Unicorn FPLC software.
b. Peaks identified corresponding to Soj dimer (D), Soj monomer (M), or nucleotide (NT).
c. The relative area of indicated peak relative to the area of the dimer peak in the same chromatograph.

concentrations (2 μM). BN-PAGE includes Coomassie brilliant blue in the loading and anode (top) buffers which confers negative charge to proteins in their native state which mediates protein mobility through a gradient gel. This technique has been reported to allow resolution of high molecular weight complexes (Switzer *et al.*, 1979). To assay for the effect of ATP or ADP on higher order Soj interactions, reactions of Soj were incubated with ATP, ADP, or buffer without nucleotide at 37°C, and were loaded onto blue native gels. When Soj was subjected to BN-PAGE with nucleotides the gels and buffers were supplemented with the indicated nucleotide and Mg acetate. When Soj was subjected to BN-PAGE without nucleotides, nucleotides, and Mg acetate were omitted from reactions, gels, and running buffers, and EDTA was added to each at final concentration of 1 mM.

When Soj was subject to BN-PAGE multiple bands were resolved. The apparent molecular weights of these bands corresponded to multiple Soj complexes (Fig. 14A). The electrophoretic mobilities of molecular weight standards subject to BN-PAGE were calculated by Imagequant software analysis and were plotted as a function of their molecular weight (Fig. 14B). The curves from Fig. 14B were used to estimate the molecular weight of Soj bands which ranged from ~30-900 kDa (summarized in Table 7). The purity of Soj analyzed by SDS-PAGE ensured that resolved bands were only composed of Soj protein and were not contaminants. The high molecular weight Soj species (>175 kDa) were not seen when Soj was incubated in the absence of nucleotide. Instead smaller molecular weight Soj species (~30-110 kDa) were resolved. Similar banding patterns observed for wild type Soj, SojG12V, and SojD40A in BN-PAGE assays in the different nucleotide conditions. One notable exception was the different banding pattern observed with SojD40A in the absence of nucleotide; a single sharp band of higher molecular weight was observed but the pattern was not similar to SojD40A in the presence of either ATP or ADP. These results indicate that Soj may form multiple high molecular weight complexes some of which require ATP or ADP binding.

It is unclear how to interpret the BN-PAGE pattern. The key question is whether the Soj multimers were artifacts caused by the electrophoresis conditions (e.g. non-specific aggregation). One piece of evidence against non-specific aggregation is that differences in apparent molecular mass between the complexes detected is not random. For example, aside from the monomer and dimer bands, adjacent band differed by more than the mass of a single Soj monomer. In fact, adjacent bands above 170kDa (the size of Soj hexamers) increased by a mass that suggested addition of hexamers. A second piece of evidence suggesting the higher

Fig. 14. Blue native PAGE of Soj and Soj point mutants in the presence of ATP, ADP, or in the absence of nucleotide. (A) Soj (wt), SojG12V (G12V), or SojD40A (D40A) were incubated at a final concentration of 2 μM with ATP or ADP (1 mM), or EDTA (1 mM) at 37°C in 20 μl of ATPase buffer with 100 mM NaCl for 5 min. Incubations containing ATP or ADP were subjected to BN PAGE on a 6-20% gel with the gel, anode, and cathode buffers supplemented with the indicated nucleotide (100 μM), and Mg acetate (4 mM). "No nucleotide" conditions were the same except that nucleotide and Mg acetate were omitted from, and EDTA was included in the gel, anode, and cathode buffers. After electrophoresis as described in Materials and Methods (section 7) the acrylamide gels were stained using the BioRad silver stain kit and a digital image of the gel was generated with an Epson 2450 Photo scanner. A Native protein molecular weight ladder (L, Native Mark, Invitrogen) was included on each BN PAGE. Arrows indicate molecular weight ladder bands (from bottom, 20, 66, 146, 242, 480, 720, 1048, 1236 kDa). (B) Estimation of the size of Soj complexes from BN PAGE. The mobility of the native protein molecular weight standards, determined by Imagequant analysis of the digital images of the gels from panel A, is plotted as a function of protein size. The mobility of wild type Soj complexes in each condition (determined by Imagequant) is shown by vertical arrows on the molecular weight axis.

A

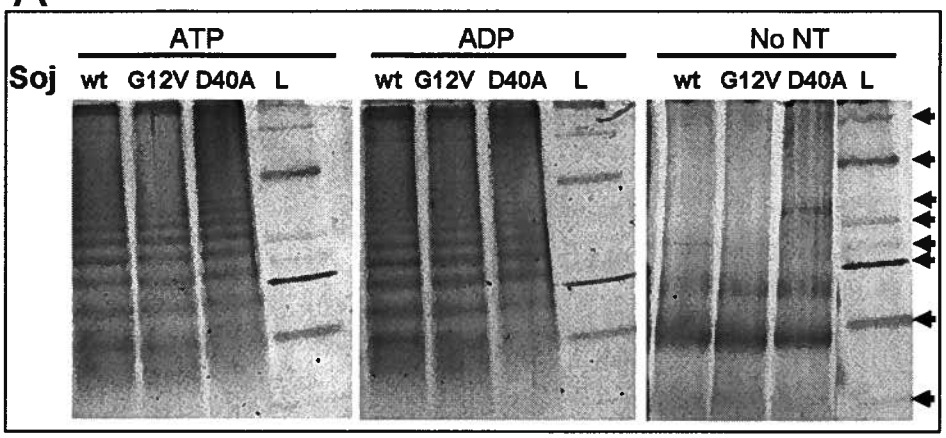
ATP
ADP
No NT
Soj
wt G12V D40A L
wt G12V D40A L
wt G12V D40A L

B

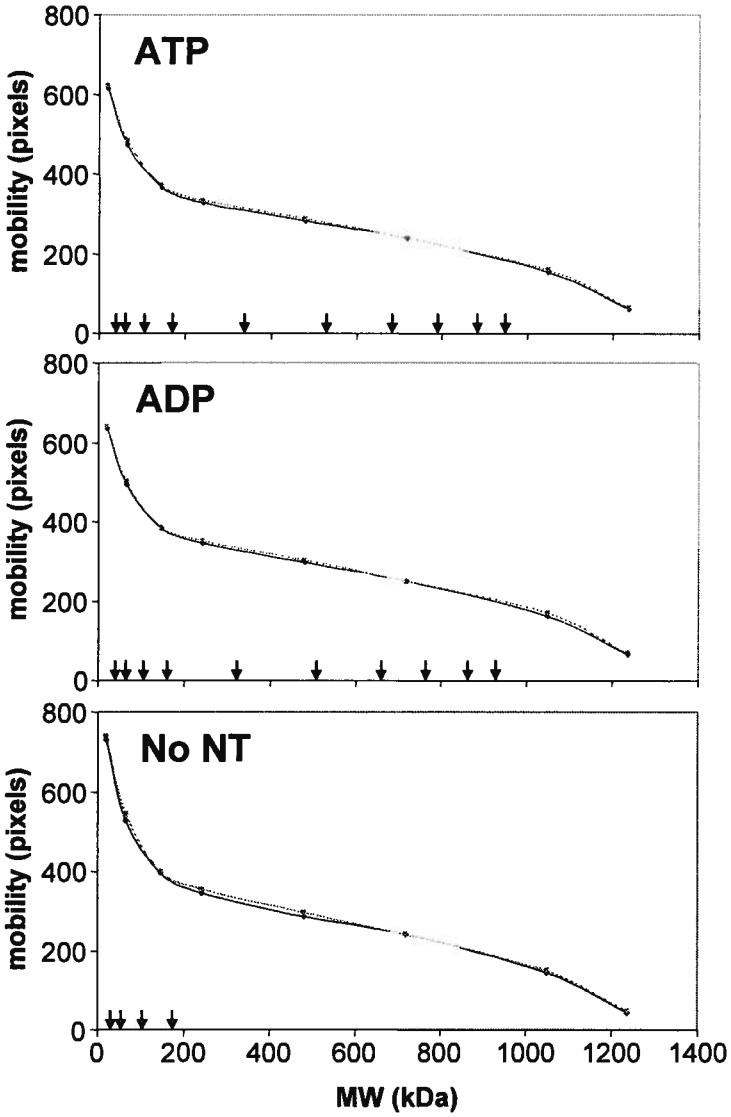
ATP
ADP
No NT
mobility (pixels)
0
200
400
600
800
0 200 400 600 800 1000 1200 1400
MW (kDa)

Table 7. Soj Complex Size Estimation from BN-PAGE

Nucleotide Condition	Molecular Weight Estimate (kDa)[a]	Oligomeric State Estimate[b]
ATP	38	1 (29)
	59	2 (58)
	105	4 (116)
	175	6 (174)
	360	12 (348)
	530	18 (522)
	685	24 (696)
	787	27 (783)
	885	30 (870)
ADP	39	1 (29)
	60	2 (58)
	105	4 (116)
	167	6 (174)
	352	12 (348)
	510	18 (522)
	660	23 (667)
	771	27 (783)
	865	30 (870)
No Nucleotide	25	1 (29)
	50	2 (58)
	105	4 (116)

a. Molecular weight estimate values are the average of two molecular weight estimates from independent BN-PAGE assays.
b. Molecular weight of the Soj complex resolved by BN-PAGE was divided by the molecular weight of recombinant his-tagged Soj (29 kDa), and rounded to the closest whole number. The expected molecular weight (in kDa) for the indicated oligomeric Soj species is shown in parentheses.

molecular weight species are specific is that Soj multimers larger than a tetramer were not observed in the absence of nucleotide. These BN-PAGE results are difficult to interpret without further experimental investigation. The relevance of higher order multimers resolved by BN-PAGE that were not also observed by size exclusion will not be addressed in the thesis Discussion or in the general model given for Soj interaction with nucleotides, DNA, and Spo0J. These results have been included because they were reproducible and striking and to indicate that Soj multimerization is an aspect of this research that warrants more investigation.

7 Soj DNA Binding.

When this work was started, the possibility that Soj would bind to DNA was predicted from multiple lines of evidence from genetic and microscopic techniques. *In vivo*, inhibition of sporulation by Soj is characterized by low transcription of stage II sporulation genes suggesting transcriptional repression. In Δ*spo0J B. subtilis* strains that express a Soj-GFP fusion protein, the GFP signal is observed to localize evenly with chromosomal DNA. As mentioned in Section 2.1 Soj purified under conditions of low ionic strength contained large amounts of contaminating DNA. It seemed likely that a Soj DNA binding activity would be detectable *in vitro*. Recently a group investigating the DNA binding activity of *B. subtilis* Soj identified surface-exposed residues that, when mutated, abrogated DNA binding by Soj (Hester and Lutkenhaus, 2007). A structural model of Soj bound to DNA based on the structure of *T. thermophilus* Soj was presented. This model suggests a DNA binding surface on the Soj dimer where the residues implicated in the DNA binding activity of Soj are situated. Although the authors did not report experimental evidence, approximately 20 bp of DNA are closely associated with the proteins, predicting that Soj would have a 20 bp DNase I footprint.

7.1 Soj DNA Complexes Resolved by EMSAs.

To characterize the putative DNA binding activity of Soj gel electrophoretic mobility shift assays (EMSAs) were performed using ^{32}P-labeled 24 bp or 100 bp DNA. Initial experiments indicated that Soj exhibited no sequence preference for DNA binding. Therefore, DNAs were amplified from the genome of φ29, a *B. subtilis* bacteriophage. These DNA sequences were previously used to assay for Spo0J DNA binding and could be easily generated in large quantities by PCR as described in the Materials and Methods. For the EMSA reactions,

Fig. 15. Nucleotide dependence of Soj binding to DNA. (A) Soj-ATP dependent shift of DNA elecrophoretic mobility. Soj, SojG12V, or SojD40A at the indicated concentration was preincubated with ATP (1 mM) in ATPase buffer with 100 mM NaCl, prior to the addition of either 100 bp (~0.2 ng μl^{-1}, ~0.3 μM final bp concentration) or 24 bp (~10 pg μl^{-1}, ~8.4 nM final bp concentration) ^{32}P-labeled DNA fragments in a 10 μl final reaction volume. After 5 min at 37°C, half the reaction was loaded onto a running acrylamide gel. Both the gel and running buffers were supplemented with 5 mM Mg acetate and 100 μM ATP. Reactions containing 100 bp or 24 bp fragments of DNA were separated by electrophoresis through 5.5% and 7.5% acrylamide gels respectively (10 V cm^{-1}, 45 min). Gels were dried and bands were detected using a Phosphorimager SI as described in Materials and Methods (section 8). Horizontal arrows indicate wells of the gel. (B) Electrophoretic mobility shift of plasmid DNA in the presence of Soj and ATP. The indicated concentrations of Soj were preincubated with ATP or ADP (1 mM) where indicated prior to the addition of linear pUC19 DNA (1.5 ng μl^{-1}, 2.3 μM bp final concentration). The reactions were loaded onto running 0.5% agarose gels and electrophoresed for 50 min at 7.5 V cm^{-1}. Following electrophoresis the gel was stained with ethidium bromide and a digital image was generated as described in the Materials and Methods. (C) Hill plot of Soj binding the 100 bp DNA fragment. The fraction of 100 bp DNA bound by Soj in EMSAs in panel A at each Soj concentration relative to binding observed with 8 μM Soj and 100 bp DNA was determined by Imagequant densitometry. Relative binding values were used to construct a Hill plot. The Hill coefficient (slope of the best fit curve at the x-axis, n_H) calculated from the linear best fit curve using Microsoft Excel is shown.

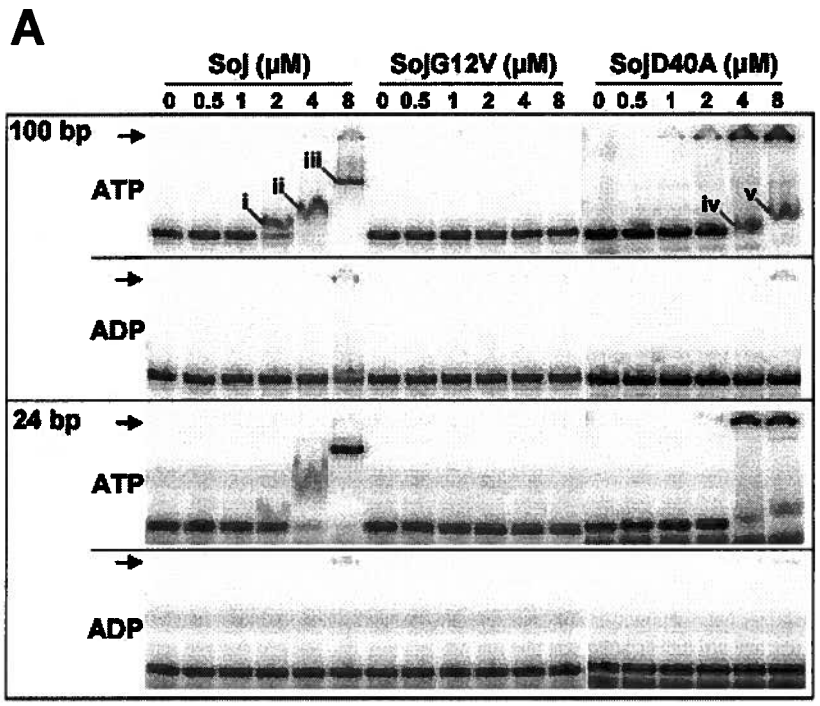
A
Soj (μM)
SojG12V (μM)
SojD40A (μM)
0 0.5 1 2 4 8 0 0.5 1 2 4 8 0 0.5 1 2 4 8
100 bp
ATP
i
ii
iii
iv
v
ADP
24 bp
ATP
ADP

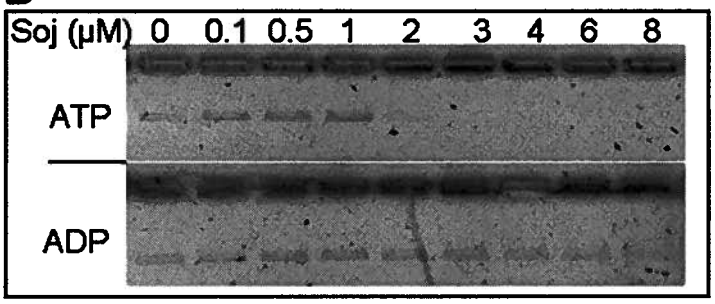
B
Soj (μM) 0 0.1 0.5 1 2 3 4 6 8
ATP
ADP

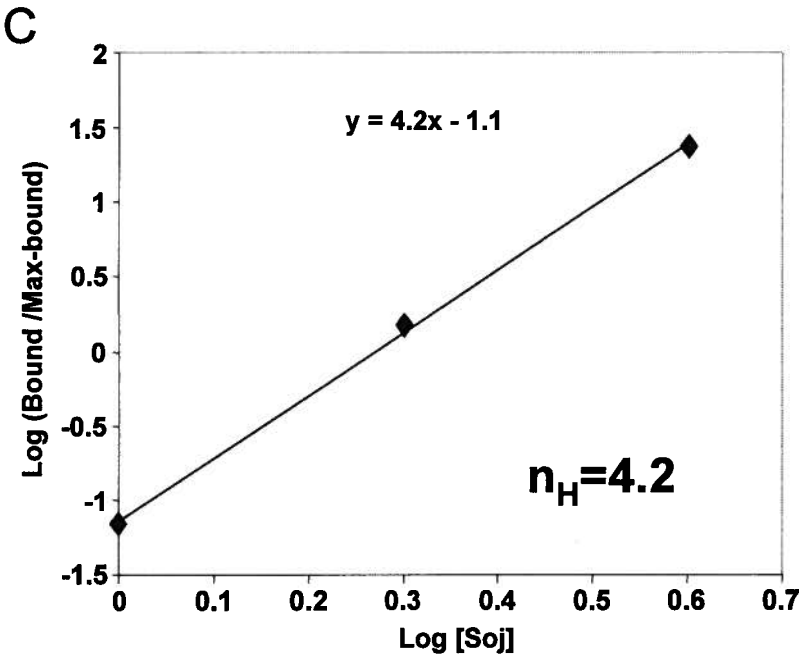
C
y = 4.2x - 1.1
n_H=4.2
Log (Bound /Max-bound)
Log [Soj]
2
1.5
1
0.5
0
-0.5
-1
-1.5
0
0.1
0.2
0.3
0.4
0.5
0.6
0.7

Soj was incubated with ATP or ADP (1 mM) for 1 min at 37°C before addition of DNA (24 bp, 8.4 nM final bp concentration; 100 bp, 0.3 μM final bp concentration) in a final volume of 20 μl. After an additional 5 min, 10 μl of the reactions were loaded onto a running gel where the gel buffer and running buffers were supplemented with the indicated nucleotide, and Mg acetate (100 μM and 4 mM respectively). At a concentration of ~2 μM, in the presence of ATP, Soj was able to bind and alter the mobility of both DNA species tested (Fig. 15A). When higher concentrations of Soj were incubated with labeled DNA prior to electrophoresis further changes in DNA mobility wereobserved. At 4 μM Soj the mobility of all 100 bp DNA was altered, and at 8 μM all 24 bp DNA had altered mobility. The observed patterns of DNA mobility shifts mediated by Soj-ATP for both 24 bp and 100 bp DNA were unusual. A single altered DNA mobility complex, which would indicate the presence of only a single protein-DNA species was not observed. Instead, EMSAs using wild type Soj and the 24 bp DNA produced two different Soj-DNA species with distinct electrophoretic mobilities. Since Hester and Lutkenhaus (2007) suggest that the DNA binding site involves both subunits of the Soj dimer, it is possible that these two species with lower mobility represent DNA binding by a Soj dimer, and Soj tetramer. The binding of a Soj dimer to the 24 bp DNA would be consistent with the ~20 bp footprint in the structural model of Soj DNA binding. The structure of a Soj tetramer bound to a 24 bp DNA fragment is not easily predicted from the structure of the dimer, but as shown below there is evidence that Soj dimers might interact.

For EMSAs using the 100 bp DNA fragment, three discrete complexes of Soj-DNA complexes with different electrophoretic mobility, and Soj-DNA trapped in the well were observed (Fig. 15A, bands labeled i, ii, iii, and the origin are indicated). The relative mobilities (mob_r) of observed bands were calculated by dividing the mobility of the species by the mobility of unbound DNA. The bands i (mob_r 0.87, 1 μM Soj lane), ii (mob_r 0.75, 2 μM Soj lane), and iii (mob_r 0.43, 8 μM Soj lane) observed over increasing Soj concentrations suggest the binding of multiple Soj proteins (presumably mostly dimers) to a single molecule of DNA, respectively. Soj-DNA trapped in the well could represent higher order Soj-DNA multimers of sufficient size to prevent electrophoresis into the gel. The observation of a single Soj-DNA electrophoretic species at a particular Soj concentration instead of a mixture of two or three Soj-DNA electrophoretic species was unexpected. Possible explanations for the appearance and disappearance of single electrophoretic species between Soj inputs are given in the Discussion.

Soj induced DNA mobility shifts were not observed in the presence of ADP. SojG12V was not able to alter the mobility of either DNA species under any condition indicating that

SojG12V is deficient in binding DNA. SojD40A was also observed to alter DNA electrophoresis, but only in the presence of ATP, indicating that ATP binding but not ATPase activity is required for DNA binding.

In the case of SojD40A EMSAs with 100 bp fragments of DNA, bands with similar mobilities to bands i and ii seen with wild type Soj were observed (band iv (mob_r 0.92, 4 μM SojD40A lane), band v (mob_r 0.77, 8 μM SojD40A lane)). However, a band with a similar relative mobility to band iii was not observed. Instead SojD40A-DNA complexes were detected in the wells. This finding might indicate that SojD40A could more readily form Soj-DNA complexes that cannot enter the gel than is wild type Soj.

I tested Soj binding to linearized pUC19 DNA using agarose gels to separate bound and free plasmid (Fig. 15B). Agarose EMSA reactions were performed as described for the 24 bp, and 100 bp EMSA reactions, except pUC19 DNA linearized by HindIII treatment was added to the reaction (1.5 ng μl^{-1}, 2.3 μM final bp concentration). The reactions were loaded on a 0.5% agarose gel where the gel and running buffers were supplemented with the indicated nucleotide and Mg acetate (100 μM, and 4 mM respectively). At 2 μM Soj, the intensity of the band corresponding to unbound plasmid DNA decreased however discrete bands of plasmid DNA with altered mobilities were not observed; rather, the plasmid DNA became trapped in the wells of the agarose gels. In the presence of ADP plasmid became trapped in the wells only when 8 μM Soj was added. Even with the lower molecular weight DNAs, addition of 8 μM Soj led to some trapping of the DNA in the wells, so possible this is due to a non-specific effect. The presence of ATP and magnesium in the reaction, gels, and running buffers were required to support Soj-dependent mobility shift of DNA probes (data not shown), further supporting the importance of ATP in Soj DNA binding activity.

The disappearance of free 100 bp DNA or linearized plasmid DNA in the EMSAs seemed to occur over a very narrow Soj concentration range. As a simple measure for DNA binding by Soj, I measured the amount of unbound 100 bp DNA at each Soj input using band densitometry using Imagequant v5.2 software. I constructed a Hill plot using the data for the binding to the 100 bp DNA, using the intensity value of unbound DNA from the highest Soj concentration to represent maximum binding. While based on only three data points and the assumption of a linear relationship at the x-axis intercept the apparent Hill coefficient for Soj binding to 100 bp DNA was approximately 4 (Fig. 15C) indicating that Soj binding to DNA was cooperative.

7.2 Soj-DNA Sedimentation.

The possibility that Soj binding to DNA resulted in the formation of large Soj-DNA complexes was investigated by sedimentation assays using low speed centrifugation. These experiments used a plasmid DNA to provide many Soj binding sites which could allow oligomeric protein structures to form. To carry out the sedimentation assay, Soj was preincubated with either ATP or ADP for 1 min. pUC19 DNA was then added (4 ng μl^{-1}, 6.2 μM bp concentration final) and after an additional 5 min, the reaction was centrifuged at 16k x g for 20 min in an Eppendorf 5414C microfuge. Aliquots from the supernatant and resuspended pellet were subjected to SDS-polyacrylamide gel electrophoresis (PAGE, Fig. 16A). The digital image was analyzed by band densitometry using Imagequant v5.2 software. A small amount (12%) of Soj was found in the pellet fraction when the reaction contained only Soj and ATP. In contrast, inclusion of DNA with Soj and ATP resulted in a 4-fold increase in sedimented Soj compared to reactions of Soj incubated with ATP alone (Fig. 16A, compare lanes 2 and 4). When the reaction buffer did not contain magnesium, even in the presence of ATP and DNA, Soj sedimentation was reduced to background level (Fig. 16A-B). Since magnesium is reported to be required as a cofactor for nucleotide binding by Walker box motifs such as found on Soj, this result indicated that a bound nucleotide is required to form a structure that could be pelleted. When the sedimentation assays contained ADP instead of ATP the fraction of Soj in the pellet was lower, although still appreciable. In retrospect I noticed that it looks like the total amount of Soj in the plus ADP condition in Fig. 16A is lower that in the other lanes, although all had the same protein input. One possibility is that there was a loading error of the Soj+ADP+DNA supernatant (but not the pellet of the same condition) onto the SDS-PAGE gel, which would have artificially increased the fraction of total protein observed in the pellet.

I also investigated the fate of the DNA in the sedimentation assays, by analyzing the pellet and supernatant fractions by agarose gel electrophoresis. Using a digital image of the gel, the amount of DNA in each fraction was analyzed by Imagequant software (Fig. 16B). DNA sedimentation was observed only in the presence of Soj, ATP, and Mg acetate. Fig. 16C shows that as the concentration of Soj in the sedimentation assays increased, the amount of DNA sedimented also increased, with a concomitant loss of DNA from supernatant fractions (Fig. 16C and D). DNA sedimentation was detected at ~2 μM Soj, and at 6 μM essentially all DNA was found in the pellet fraction. DNA sedimentation was not a linear function of Soj input since at low concentrations of Soj (<1 μM) only traces of DNA were detected in the pellet fraction.

Fig. 16. Sedimentation of Soj-DNA complexes in the presence of ATP. (A) Soj sedimentation in the presence of adenosine nucleotide and DNA. Soj (4 μM) was incubated for 1 min with indicated nucleotide (NT) prior to the addition of linearized pUC19 DNA (4 ng μl^{-1}, 6.2 μM bp final concentration). Supernatant (s) and pellet (p) fractions were separated by centrifugation for 20 min at 16k x g at room temperature. Fractions were treated as described in the Materials and Methods (section 9), separated by SDS-PAGE and stained with Coomassie Brilliant Blue. Numbers in parentheses indicate the band density of the pellet fraction divided by the sum of densities of supernatant and pellet fraction bands as determined by ImageJ software. (B) DNA sedimentation in the presence of Soj and ATP. Sedimentation assay conditions were identical to those in part A, except Soj was included at 5 μM, nucleotides were included at 1 mM (T indicates ATP; D, indicates ADP), and DNA was included at 4 ng μl^{-1} where indicated. Supernatant and pellet fractions were treated as described in the Materials and Methods (section 9). Fractions were separated by agarose gel electrophoresis and the gel was stained with ethidium bromide. Negative image shown. (C) DNA sedimentation as a function of Soj concentration. Sedimentation assays were identical to those in panel A except they contained the indicated concentration of Soj and 1 mM ATP. Supernatant and pellet fractions were treated as described in the Materials and Methods (section 9). Fractions were separated by agarose gel electrophoresis and the gel was stained with ethidium bromide. Negative image shown. Numbers in parentheses indicate the band density, determined by Image J, of the pellet fraction divided by the sum of supernatant and pellet fraction band densities. (D) The supernatant (♦) and pellet (■) band density values from C were plotted as a function of Soj input. Densities were normalized relative to the value of the pellet fraction with 6 μM Soj. (E) Hill plot of Soj-ATP mediated DNA sedimentation values from panel D. Relative sedimentation values observed for each Soj concentration from panel D were used to construct a Hill plot. The slope of the linear best fit curve at the x-axis (Hill coefficient, n_H) calculated from the indicated equation using Microsoft Excel is shown.

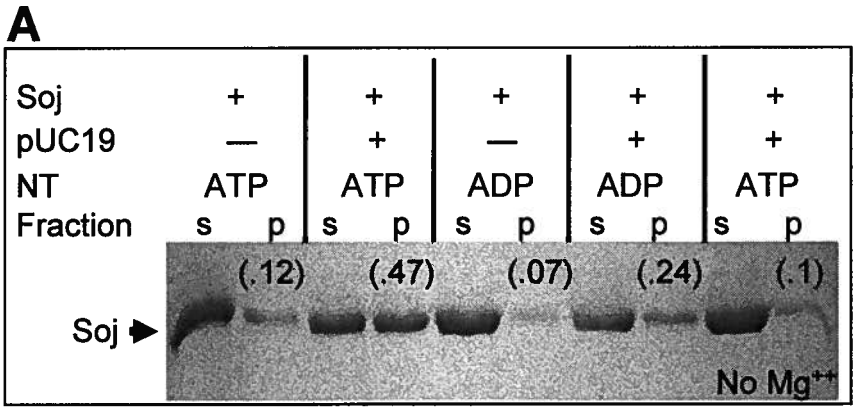
A
Soj
pUC19
NT
Fraction
ATP
ADP
s p
(.12) (.47) (.07) (.24) (.1)
Soj
No Mg++

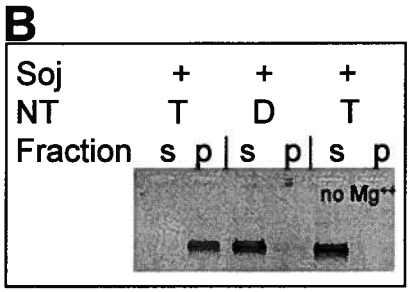
B
Soj
NT
Fraction
T D T
s p s p s p
no Mg++

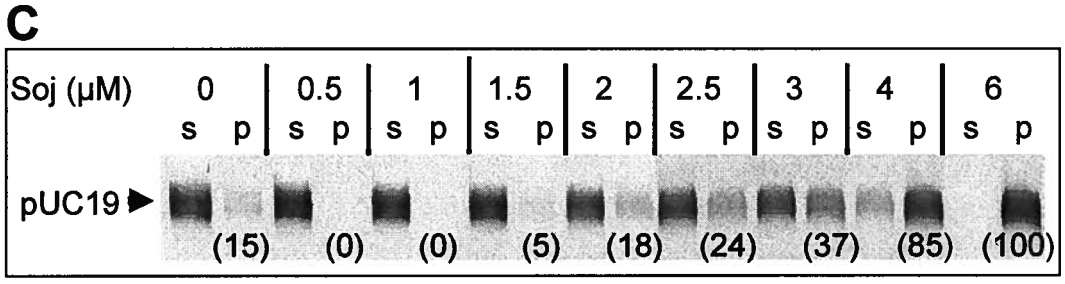
C
Soj (μM)
0 0.5 1 1.5 2 2.5 3 4 6
s p
pUC19
(15) (0) (0) (5) (18) (24) (37) (85) (100)

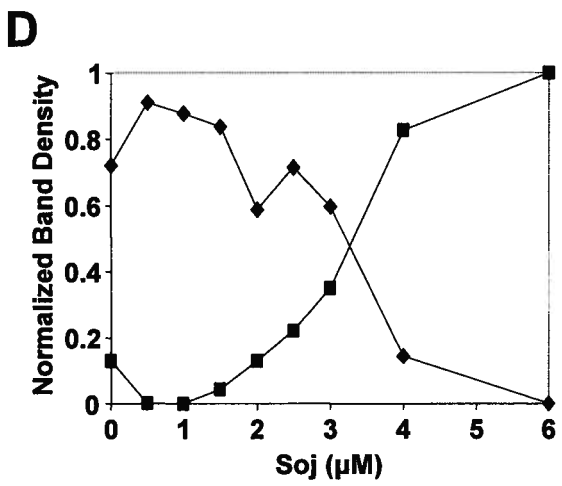
D
Normalized Band Density
Soj (μM)
0 0.2 0.4 0.6 0.8 1
0 1 2 3 4 5 6

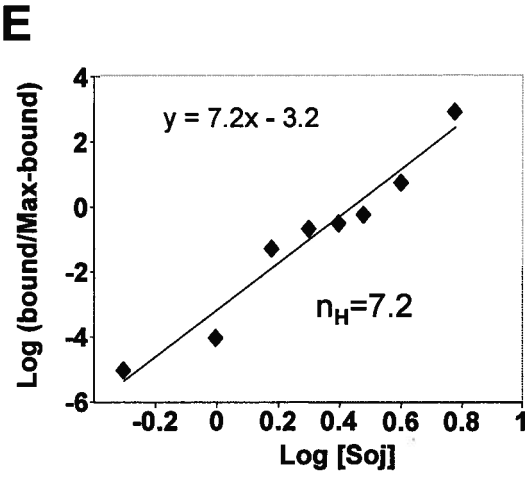
E
Log (bound/Max-bound)
Log [Soj]
y = 7.2x - 3.2
nH=7.2
4 2 0 -2 -4 -6
-0.2 0 0.2 0.4 0.6 0.8 1

The fraction of pelleted DNA as a function of Soj concentration was used to construct a Hill plot, using sedimentation observed at 6 μM Soj as a maximum. Assuming the Hill plot is linear, the best fit line of the data had a slope at the x-axis approximately 7 (Fig. 16E). This would indicate a very high degree of cooperativity in forming these sedimentable Soj-DNA complexes.

7.3 Soj Protection of DNA from DNase I Digestion.

It was reasoned that the cooperative binding observed in EMSAs and DNA sedimentation reflected protein-protein interactions between adjacent Soj dimers as they bind to DNA. The general model for the binding would be represented by a 'spreading' process on DNA. To investigate this, I employed a DNase footprint assay. Since I expected that the initial Soj binding event on a DNA would be random, instead of using an end-labeled DNA, I used an internally labeled 1 kb PCR product to test DNase protection. Primers 1kb(+)-F and 1kb(+)-R were used with bacteriophage φ29 genomic DNA as a template, and α^{32}P-dATP was included to internally label the PCR products. The accurate resolution of DNase products in the assays required that the labeled 1 kb DNA did not contain smaller molecular weight DNA species that would interfere with experimental analysis, so the products of the PCR reaction were subjected to PAGE through a 4.5% non-denaturing gel. The position of the 1 kb PCR product in the gel was determined by autoradiography and the band was excised from the gel. The 1 kb product was electroluted from the gel slice into dialysis tubing, and the electroluted DNA was collected and ethanol precipitated as described in the Materials and Methods.

To test DNase I protection, labeled DNA (~0.38 μM final bp concentration) was added to reactions with Soj and nucleotide. After 5 min, DNase I was added for a minute before the reaction was stopped. The products were separated by electrophoresis and phosphorimages were generated from dried gels to determine the size of the protected DNA fragments. I first tested dilutions of DNase to establish the amount I needed to add so that there would be no full length product in the absence of Soj (Fig. 17A). In the absence of Soj, DNase I treatment (1/50) reduced the 1 kb internally labeled DNA fragment to a distribution of small DNA fragments with a median size less than 0.1 kb (Fig. 17 A and B). Preincubation of the DNA with 4 μM Soj in the presence of ATP partially protected the DNA fragments from digestion by DNase (Fig. 17A, 1/50 DNase dilution). When ADP was substituted for ATP, DNase I protection was lost

Fig. 17. DNase protection of DNA by Soj-ATP. (A) Calibration of DNaseI. Soj (4 μM) was incubated with 1mM ATP (T) or ADP (D) for 1 min prior to the addition of an internally ^{32}P-dATP labelled 1 kb PCR product (~0.25 ng μl^{-1}, ~0.38 μM bp concentration final). The reactions were incubated for 5 min. DNase I was added to the reaction for 1 min at the indicated dilution, where indicated, and the reaction was stopped. Reaction products were separated by electrophoresis and a phosphorimage of the dried gel was generated. Arrows indicate the mobility and size of molecular weight standards from lane 1 (0.3 kb, and 0.1 kb) and 1 kb labeled PCR product. (B) Protection at varying Soj concentrations. Soj was preincubated with 1 mM ATP for 1 min prior to the addition of an internally ^{32}P-dATP labelled 1 kb PCR product. Reactions were treated with a 1/50 dilution of DNase I for 1 min before the reaction was stopped. Reaction products were separated by electrophoresis and a phosphorimage of the dried gel was generated. Lane 1, 0.3 kb and 0.1 kb standards. Lanes 2-10, reactions contain indicated Soj concentrations. Arrows indicate the mobility of molecular weight standards and 1 kb labeled PCR product. (C) Densitometry profiles of lanes 2-10 from panel B. Densitometry profiles were generated by Imagequant software v5.2 and lanes 2, 7-10 are indicated. The hash mark on the horizontal axis at the top indicates a density of 1500 arbitrary units. The densitometry scan of lane 2 reached a maximum at 10 000 a.u. (D) Protection of 1 kb DNA from DNaseI digestion as a function of Soj concentration. The fraction of 1 kb completely protected DNA from DNaseI digestion (determined by densitometry using Imagequant v5.2) relative to the densitometry of 1kb DNA without DNaseI treatment (panel A, lane 2) was plotted as a function of Soj concentration. (E) Hill plot of appearance of fully protected 1 kb DNA. Relative protection values (P) observed for each Soj concentration from panel D were used to construct a Hill plot. The slope of the best fit curve at the x-axis (Hill coefficient, n_H) calculated from the indicated equation, using Microsoft Excel is shown.

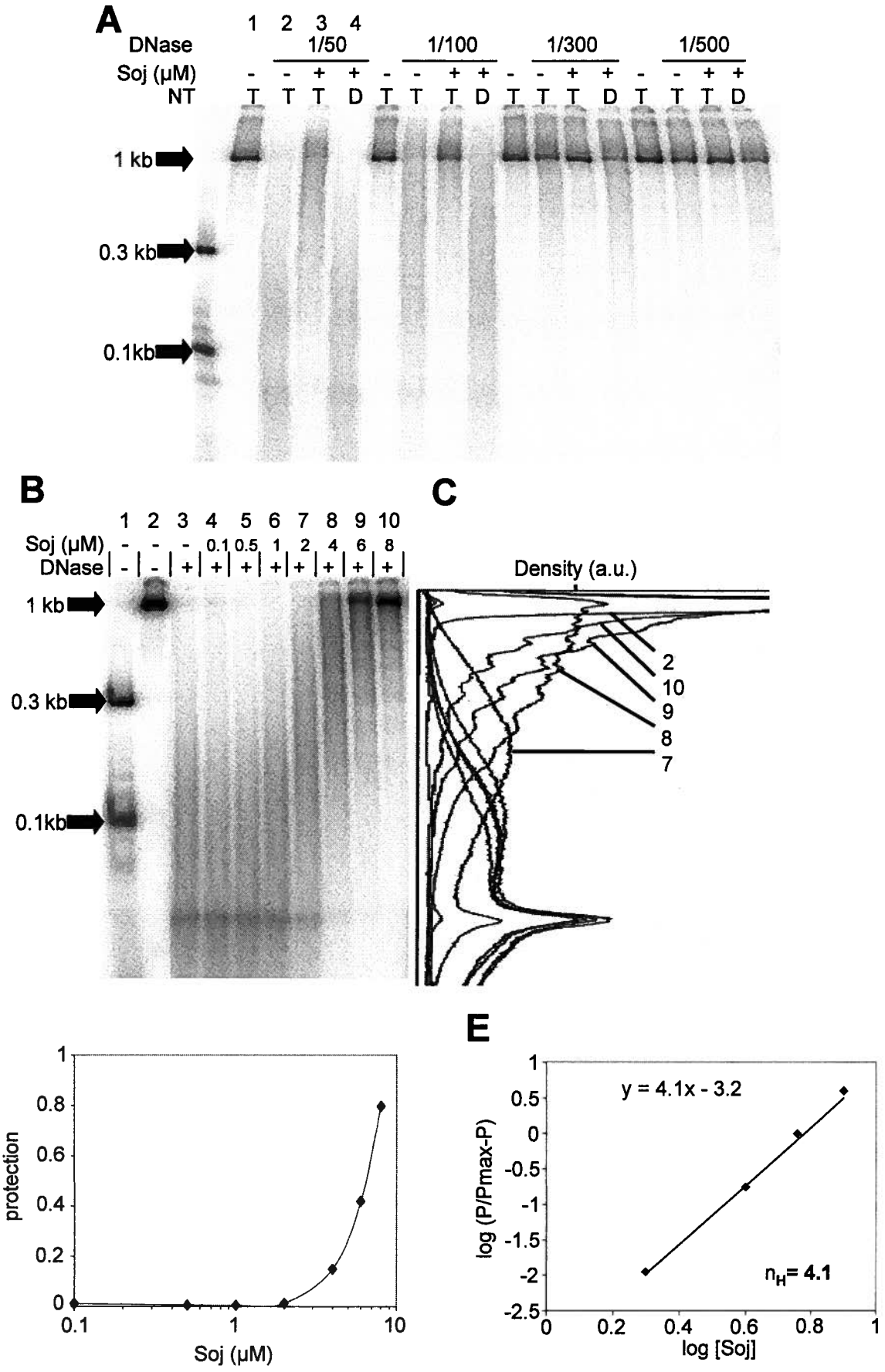
A
1 2 3 4
DNase
1/50
1/100
1/300
1/500
Soj (μM)
NT
T T T D T T T D T T T D T T T D
1 kb
0.3 kb
0.1kb
B
1 2 3 4 5 6 7 8 9 10
Soj (μM) - - - 0.1 0.5 1 2 4 6 8
DNase - - + + + + + + + +
1 kb
0.3 kb
0.1kb
C
Density (a.u.)
2
10
9
8
7
D
fraction of full DNA protection
1
0.8
0.6
0.4
0.2
0
0.1
1
10
Soj (μM)
E
y = 4.1x - 3.2
log (P/Pmax-P)
1
0.5
0
-0.5
-1
-1.5
-2
-2.5
0
0.2
0.4
0.6
0.8
1
log [Soj]
n_H= 4.1

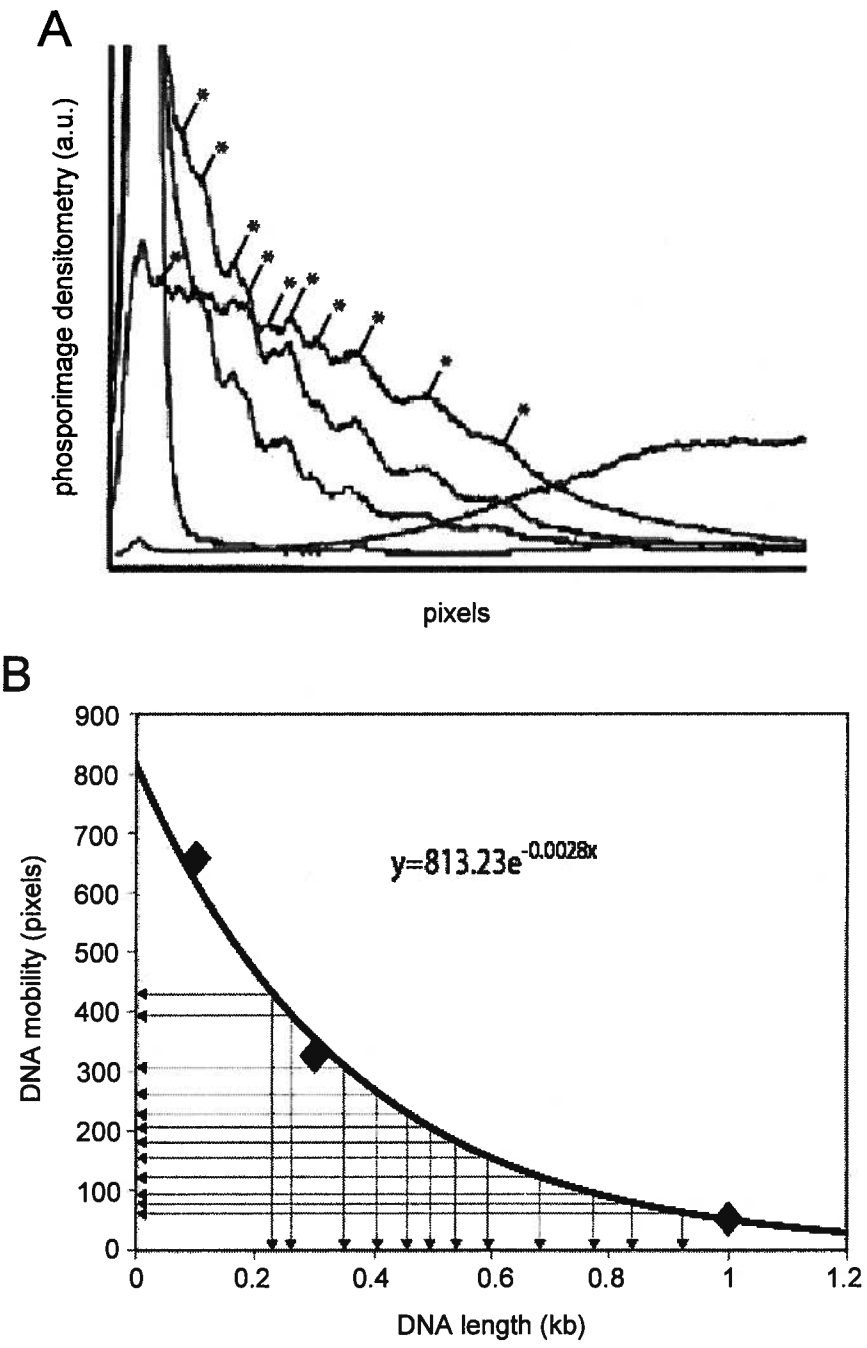

Fig. 18. Estimation of DNA sizes protected from DNaseI digestion by Soj. (A) Densitometry profiles of lanes 2-10 from Fig. 13B. Discreet length DNA species appeared over a range of Soj inputs as a series of small peaks (*) on the densitometry profiles. (B) Size estimation of the DNAs. The electrophoretic mobility of 1 kb, 0.3 kb, and 0.1 kb molecular weight standards from Fig. 15B were used to estimate a mobility curve. A best fit curve equation was calculated ($y=813.23e^{-0.0028x}$) and was used to estimate the sizes of DNA bands detected as peaks in densitometry profiles in panel A (perpendicular jointed arrows).

and the pattern was similar to that generated by DNase I treatment without Soj (Fig. 17A, compare lanes 3 and 4).

I then tested the protection of DNA from DNase I digestion (at 1/50 dilution) using a range of Soj concentrations (Fig. 17B). There was a dramatic shift in the pattern of protected DNA fragments between Soj concentrations of 1 μM and 4 μM. The densitometry profiles of protected fragments at greater than 2 μM Soj showed multiple small peaks most obvious in the 4, 6 and 8 μM Soj conditions. These peaks corresponded to visually observable bands on the phosphorimage (Fig. 17 B and C, Fig. 18A). The size of DNA fragments being protected changed over a small range of Soj concentrations, which indicated cooperativity of Soj DNAbinding. The appearance of 1 kb DNA, which represented full DNase protection, was observed at 4 μM Soj where 15% of DNA was fully protected. The fraction of full length DNA protected from DNase by Soj binding increased sharply over a narrow range of Soj concentration (Fig. 17D), and appeared to be cooperative. Imagequant was used to calculate the amount of full length DNA protected at the various Soj concentrations, and those data were used to produce a Hill plot (Fig. 17E). Assuming that the Hill plot is linear at the x-axis, it had an intercept slope of approximately 4 which supported cooperative binding Soj along the length of DNA. The DNase protection profiles were analyzed assuming that the small peaks observed represented specific DNA species. The sizes of these protected DNA species were estimated by comparing their electrophoretic mobilities to the electrophoretic mobilities of 1 kb, 0.3 kb, and 0.1 kb DNA (Fig. 18B). The mean differences in size between adjacent DNA species detected in multiple Soj input conditions and replicate experiments were ~47 or ~90 bp. The approximate 20 bp DNA footprint of a Soj dimer on DNA proposed by Hester and Lutkenhaus suggest the ~45 bp gradations between protected DNA species could reflect the expected size of DNA occupied by the binding of a Soj tetramer. However, the a 47 bp difference in the length of protected DNA could also result from the simultaneous binding of two Soj dimers to both ends of a cluster of Soj proteins.

7.4 Soj Inhibition of Transcription *in Vitro.*

The sporulation negative phenotype observed in Δ*spo0J* cells is characterized by low transcription of essential stage II sporulation genes (*spoIIA, spoIIE, spoIIG,*(Ireton *et al.*, 1994; Quisel and Grossman, 2000)). The deletion of *soj* in a Δ*spo0J* background rescues the sporulation negative phenotype of a Δ*spo0J* strain, and could indicate that Soj could directly

inhibit sporulation by acting as a repressor of transcription (Cervin *et al.*, 1998; Ireton *et al.*, 1994; Quisel *et al.*, 1999; Quisel and Grossman, 2000). It has been noted that transcription of the *spoIIA*, *spoIIE*, and *spoIIG* operons is activated by the phosphorylated form of Spo0A (Spo0A~P) (Ireton *et al.*, 1994; Quisel and Grossman, 2000). Non-specific binding of Soj to DNA to act as a direct repressor of all transcription is not compatible with the operon-specific transcription inhibition observed *in vivo*, but Soj could inhibit sporulation by selectively repressing transcription activated by Spo0A~P. To investigate this possibility, transcription repression by Soj was examined by single round transcription assays *in vitro*. Soj, ATP+α^{32}P-GTP, and a DNA fragment with the indicated promoter (P) were incubated for two minutes prior to the addition of purified *B. subtilis* RNAP. Spo0AC (the constitutively active C-terminal DNA binding domain of Spo0A) was added when transcription from P*spoIIG* was assayed. The reactions were incubated for another two minutes to allow transcription initiation. Transcription was limited to a single round by adding heparin, which binds and inactivates free but not initiated RNAP, along with the remaining nucleotides. Reactions were incubated further and stopped by addition of urea. The products of transcription were analyzed by denaturing PAGE. A phosphorimage of the gel was used to quantify the major ^{32}P-labelled transcript by densitometry using Imagequant.

The inhibition of transcription from four different promoters by Soj was investigated. P*spoIIG* was selected because it is known to be repressed *in vivo* in a Δ*spo0J* mutant and therefore is a presumed target for Soj transcription inhibition, and transcription initiation at this promoter *in vitro* has been well studied. I constructed a mutant of the P*spoIIG* (P*spoIIG18)* by removing 4 bp between the -10 and -35 consensus sequences (Fig. 19A). This change was predicted, and I showed experimentally (Fig. 19B) to change the promoter from being dependent on Spo0A~P for activity to being Spo0A~P independent. The basis of the Spo0A~P dependence is that the separation between the -10 and -35 sequences is 5 bp greater than the optimal distance. Thus this promoter is identical in sequence to P*spoIIG*, except for the internal deletion. Two other promoters P*abrB*, and P*A2* were used as controls because transcription of these genes has not been shown to be negatively regulated by Soj *in vivo*; moreover, they are amenable for use in the single round transcription assay. The product of *abrB* is a transition state regulator which controls the expression of multiple genes in late log phase and early stationary phase. The *A2* promoter from bacteriophage φ29 drives expression of several genes during the early stages of the lytic cycle in *B. subtilis*.

Fig. 19. Inhibition of transcription initiation *in vitro* by Soj. (A) Sequence of P*spoIIG* and shortened *spoIIG* promoters. The region between +1 and –60 is indicated. The –10 and –35 sequences are in boldface letters. Underlined bases indicate 0A boxes. Dashes indicate bases deleted from BglII-treated pUCIIGBglII*trpA* by incubation with mung bean nuclease followed by ligation (described in Materials and Methods (section 2.7)). Italicized letters in P*spoIIG*BglII indicate a BglII site that was introduced into pUCIIG*trpA*. (B) Spo0A dependence of transcription from P*spoIIG*, and independence of transcription from P*spoIIG18*. Transcription from P*spoIIG* and P*spoIIG18* in the presence and absence of Spo0AC was assayed. Transcription assays were composed and performed as indicated in the Materials and Methods (section 11). Products from transcription assays were separated by electrophoresis through an 8% denaturing polyacrylamide gel. The major transcript was detected and quantified by exposure of the gel to a phosphor screen followed by analysis with Imagequant v5.2. Error bars represent the standard deviation from the average of four independent assays. (C) Soj-mediated transcription inhibition from different promoter templates. Four promoter templates were used: P*spoIIG* (i); P*A2* (ii); P*abrB* (iii); P*spoIIG18* (iv). The indicated concentrations of Soj were incubated with P*spoIIG* (the insert indicates transcription at lower Soj concentrations), or P*A2* and ATP plus GTP (and Spo0AC at 1 μM when P*spoIIG* was used) for 2 min in transcription buffer with BSA (0.1 mg ml-1) at 37°C before the addition of RNAP. After another 2 min, heparin plus GTP and UTP were added, and the reaction was stopped after 5 min of elongation. Relative transcription was measured as the percentage of transcription in the absence of Soj. To maintain a consistent ionic strength among samples, Soj was diluted into elution buffer and a constant volume was added to each reaction. The same volume of storage buffer alone was added to the control reactions. Assays of Soj-mediated transcription inhibition at P*abrB* were performed as described for P*A2*, except the initiation nucleotides used were ATP plus GTP plus UTP, and the transcripts were separated by electrophoresis on a 12% denaturing polyacrylamide gel. Soj-mediated transcription inhibition at P*spoIIG18* in the presence (■) or absence (♦) of 1 μM Spo0AC was assayed and analyzed as described for P*spoIIG*. Error bars represent the standard deviation from the average percentage of at least three independent transcription assays.

A

```
PspoIIG          5'-TTTTCCTCTCAACATTAATTGACAGACTTTCCCACAGAGCTTGCTTTATACTTATGAAGCA-3'
PspoIIG18        5'-TTTTCCTCTCAACATTAATTGACAGACTTTCCCACA----TTGCTTTATACTTATGAAGCA-3'
PspoIIGBglII     5'-TTTTCCTCTCAACATTAATTGACAGACTTTCCCACAGATCTTGCTTTATACTTATGAAGCA-3'
                                |        |        |        |        |        |        |
                               -60      -50      -40      -30      -20      -10      +1
```

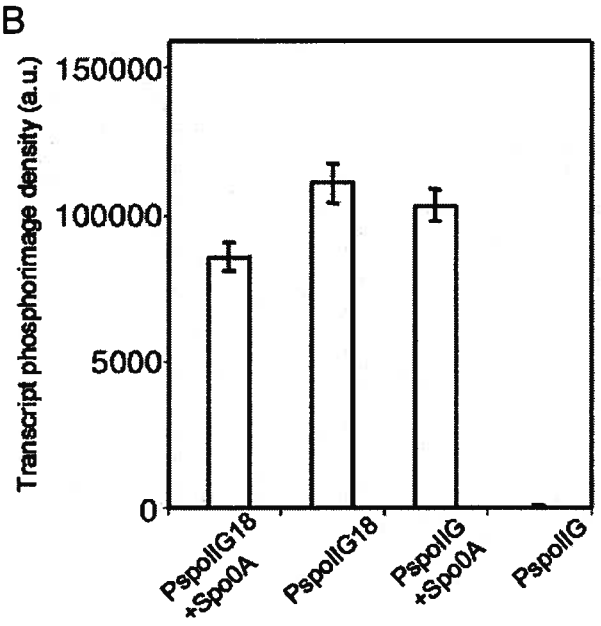

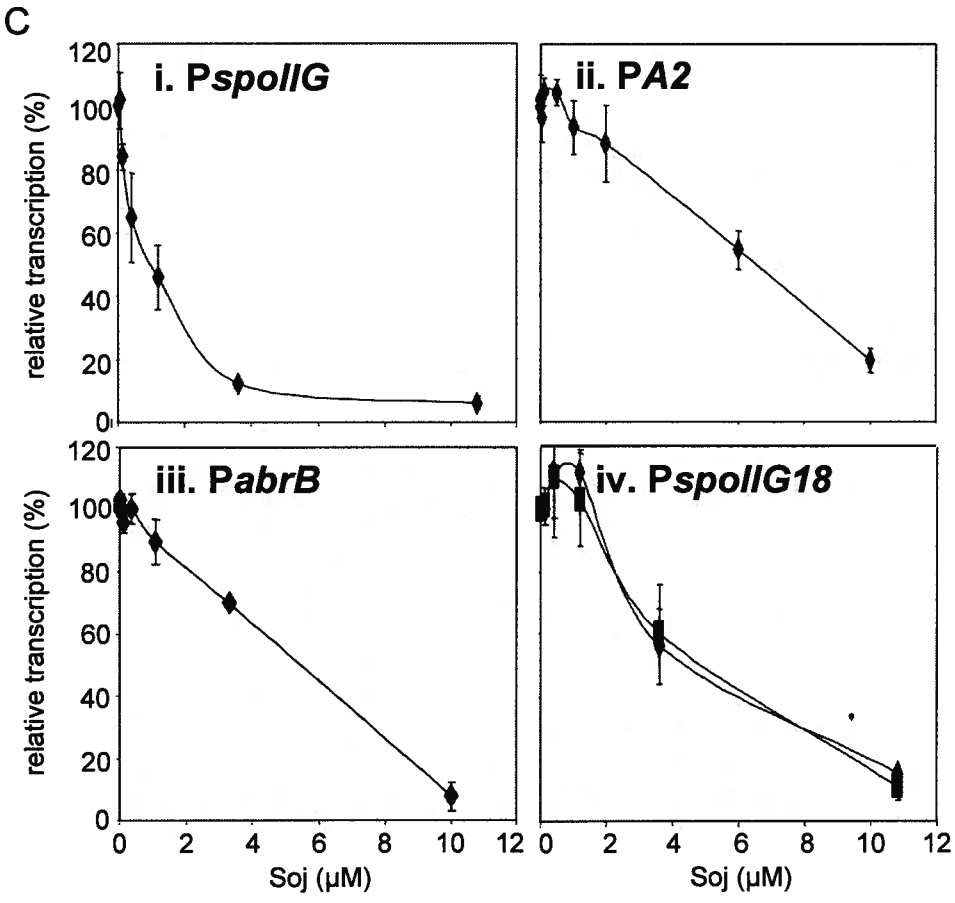

As seen in Fig. 19C the addition of increasing concentrations of Soj resulted in a decrease in the amount of transcript from all promoters used in the transcription assays. In all cases the inclusion of 10 μM Soj resulted in >85% reduction of the primary transcript compared to conditions where Soj elution buffer alone was added. The effect of increasing Soj concentrations differed when P*spoIIG* was used as the template compared to other promoter templates. A 50% reduction in relative transcription from P*spoIIG* was observed when Soj was included at 1 μM. Approximately 5-fold higher Soj concentrations were required for the same reduction in relative transcription from the other 3 promoters. The higher concentrations of Soj required for a 50% reduction in relative transcription from P*spoIIG18* compared to P*spoIIG* indicated that Soj-mediated transcription inhibition at P*spoIIG* was likely not due to Soj binding to a specific sequence because only 4 bp differed between the two. The data support a model where Soj preferentially antagonizes Spo0A-dependent transcription activation.

8 Detection of Soj-DNA Complexes by Light Scattering.

Size exclusion chromatography indicated that the majority of Soj is dimeric (Fig. 13). Soj binding to DNA characterized by EMSAs and DNase protection assays, indicated that multiple Soj dimers bound to DNA cooperatively as indicated by Hill plots of the data. Data from DNase protection assays indicated that the binding of Soj dimers along the length of the DNA could completely cover the fragment. Sedimentation assays in Fig. 16 indicated that Soj-DNA structures were of sufficient size to be cleared from solution by low speed centrifugation, and EMSAs indicated that they were too large to enter 0.5% agarose or 4.5% acrylamide gels (Fig. 15). Furthermore, I noticed that reactions containing Soj, ATP and DNA in conditions which resulted in DNA sedimentation, were visibly turbid. I was interested in characterizing the formation of the complexes with a method that would allow a more continuous assay rather than the discontinuous assays of EMSA and sedimentation.

I chose to use 90° light scattering for this assay because of the availability of suitable instruments. To monitor light scattering Soj-DNA structures I used 90° light scattering using a Cary Eclipse fluorescence spectrophotometer. The instrument has a lamp which emits 350 nm wavelength light, a detector at 90° from the incident light, and a photomultiplier tube with adjustable voltage to change the detector sensitivity. The instrument also has the capability to record multiple data points over time. To measure the light scattering, Soj was added to reactions with ATP or ADP in a cuvette (1 cm light path) with moderate stirring, at 30°C. After

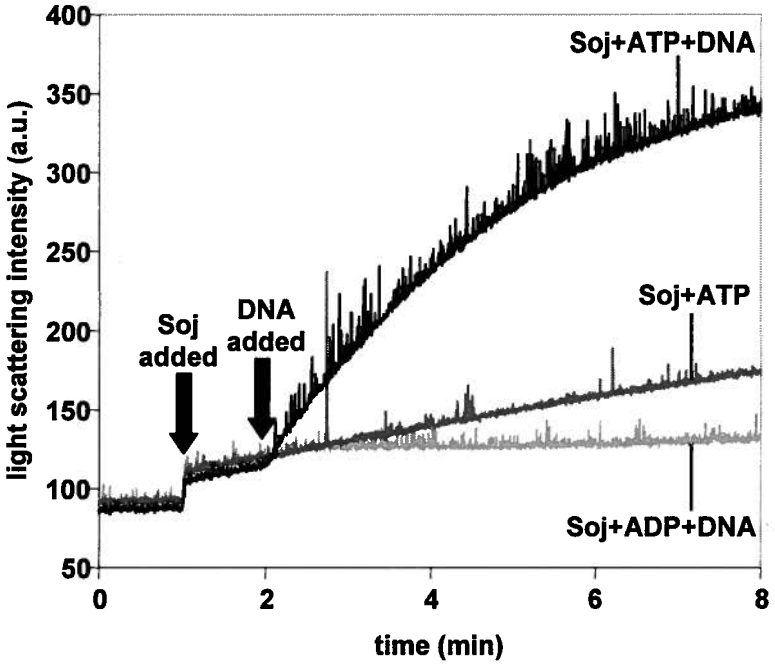

Fig. 20. Light scattering by DNA and Soj-ATP. Soj (1 μM) was incubated with 1 mM of the indicated adenosine nucleotide in a UV/vis plastic cuvette (10 mm light path) in 1.5 ml of ATPase buffer with 100 mM NaCl. After 1 min, pUC19 DNA (0.5 ng μl^{-1}, 0.78 μM bp concentration final) was added where indicated and light scattering in arbitrary units (a.u.) was monitored. Fluorescence spectrophotometer PMT voltage in this assay was 600 V.

1 minute, DNA was added and the extent of light scattering (350 nm) was followed over approximately 8 min. Some differences among the light scattering profiles from different light scattering experiments with similar conditions were noted, however the overall trends in the extent, rates and requirements for light scattering were observed in a large number of experiments, and typical examples are shown.

Fig. 20 shows results from experiments where pUC19, Soj and either ATP or ADP were mixed and light scattering was monitored over 6-8 min. When 1 μM Soj was added to a reaction with ATP, a small immediate increase in light scattering was observed (Fig. 20) and light scattering slowly increased over the following 10 min. The same trend was observed when Soj was added to a reaction with ADP (data not shown). When pUC19 DNA (0.5 ng μl^{-1},0.78 μM final bp concentration) was added to Soj plus ATP, a second large increase in light scattering was observed. This DNA-dependent increase was not observed when ADP was substituted for ATP. The DNA-dependent light scattering was unaffected by whether the DNA was circular, or linearized by restriction endonuclease treatment (data not shown). Whatever the molecular mechanism that is responsible for the increase in light scattering in the presence of DNA, it was dependent on the presence of ATP. The similarity between the charge, counter ions, *et cetera* associated with adding the ATP versus ADP makes it unlikely the trinucelotide dependence is due to some ionic interaction. Thus it seemed likely that the observed changes in light scattering when DNA was added to Soj and ATP depended on an effect of ATP on Soj.

Mixtures of Soj, ADP, and DNA consistently scattered less light than Soj incubated with ATP in the absence of DNA. In fact Soj, ADP, and DNA scattered less light than any other condition including Soj and ADP without DNA (not shown). At present it is not known why this result was observed, but it could indicate that Soj-ADP might transiently interact with DNA to stabilize a Soj species which scatter less light than Soj bound to either ATP or ADP in the absence of DNA.

SojG12V did not alter the electrophoretic mobility of DNA (Fig. 15A), although it was capable of ATP hydrolysis (Fig. 9). SojG12V was added to light scattering assays to investigate whether SojG12V differed from wild type Soj with respect to light scattering. Mixtures containing SojG12V, DNA, and ATP were monitored over time only small changes in light scattering were observed when SojG12V (Fig. 21). The presence of ADP instead of ATP did not change the light scattering profile for SojG12V plus DNA (data not shown). Thus conditions required for the light scattering by Soj and SojG12V paralleled the conditions required for DNA binding as observed in other assays (Fig. 15), which indicated that light

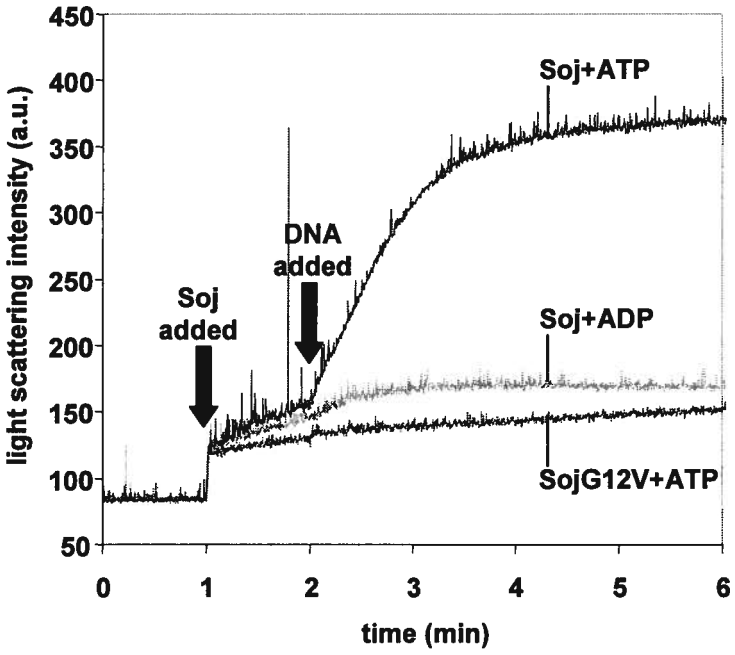

Fig. 21. Light Scattering by SojG12V. Soj, or SojG12V (1 μM), was added to a light scattering assay, as described in Materials and Methods (section 12) containing the indicated nucleotide (1 mM). Following 1 min of incubation pUC19 DNA (0.5 ng μl^{-1}, 0.78 μM bp concentration final) was added to each mixture. PMT voltage in these assays was 600 V.

scattering monitored the formation of Soj-DNA structures. In addition the data suggested that ATP but not ADP was a co-factor for forming these structures. Light scattering by wild type Soj + ATP + DNA in Fig. 21 had a faster rate of formation compared to the same conditions in Fig. 20, and reached a plateau within two minutes after DNA addition whereas a plateau was not observed in Fig 20. I considered these minor variations in protein activity between different preparations of purified Soj. For example, the wild type Soj used in Fig. 20 could have been less active than that used in Fig. 21. The difference could also result from differences in the purity of the ATP used in each assay. Older solutions of ATP may have contained more ADP from spontaneous breakdown of ATP duringstorage (and therefore a lower concentration of ATP) resulting in lower rates of light scattering observed in Fig. 20. As a result of these minor variations I did not attempt to measure "specific activities" of complex formation and I used comparative experiments done on a single day to examine properties such as the effect of DNA length (see below).

Monitoring formation of SojD40A-DNA complexes as measured by light scattering presented a technical hurdle that turned out to insurmountable. SojD40A alone resulted in high levels of light scattering independent of nucleotide and/or DNA (data not shown) and no additional effects of adding DNA could be determined. EMSA results which indicated that the DNA binding activity of SojD40A was ATP-dependent (Fig. 15A), suggested that SojD40A light scattering in the absence of DNA binding (no DNA, or DNA in the presence of ADP) was due to some characteristic of SojD40A that promotes aggregation of the protein itself. This effect could be related to a larger fraction of ~105 kDa species observed in size exclusion chromatography of SojD40A-ATP compared to wild type Soj-ATP or a high MW band observed in BN-PAGE of SojD40A in the absence of nucleotides (Figs. 13, 14A). However, the basis of SojD40A light scattering effect is not known at this time, and the discrepancies between the light scattering of SojD40A and size exclusion chromatography and BN-PAGE assays remain unresolved.

I next investigated the effect of Soj concentration on rates and levels of light scattering changes. Varying concentrations of Soj were pre-incubated with ATP for 1 min and then pUC19 DNA was added (0.5 ng μl^{-1}, 0.78 μM final bp concentration) and the light scattering monitored. The light scattering intensities, from the time of DNA addition, for 1, 2, and 4 μM Soj are shown in Fig. 22A. Because of the high scattering intensity observed with 4 μM Soj, it was necessary to decrease the PMT voltage in this experiment compared to the setting used in Figs. 20-21. The low PMT voltage resulted in a small increase in light scattering at 1 μM Soj

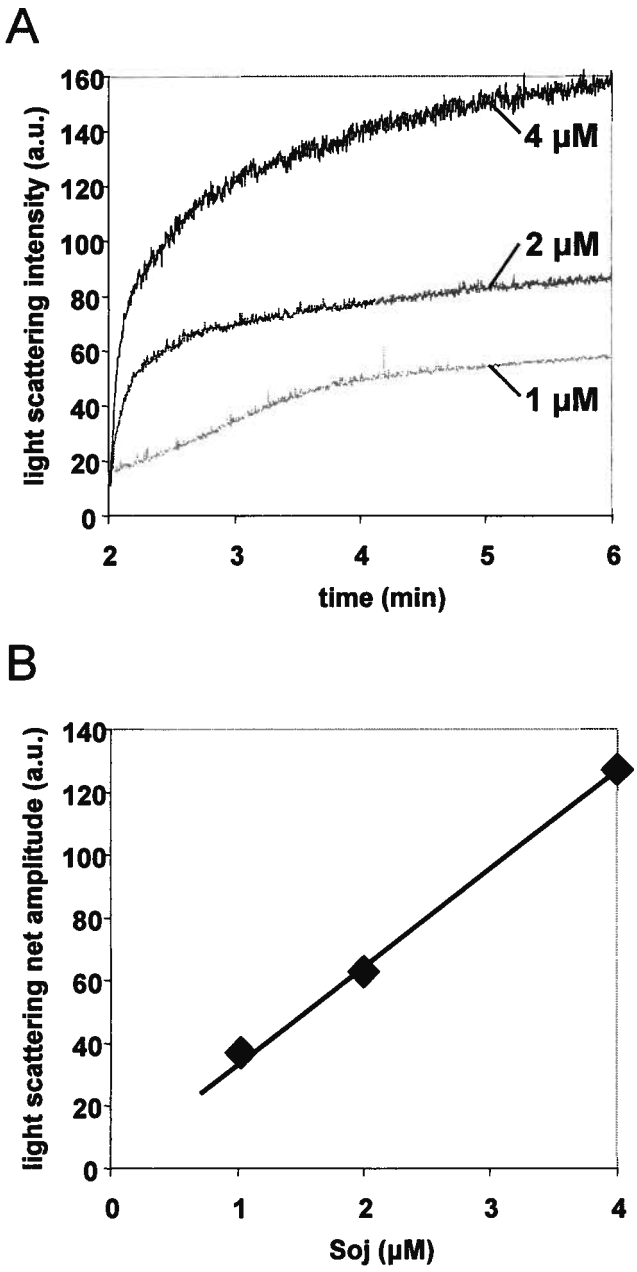

Fig. 22. Light scattering as a function of Soj concentrations. (A) Light scattering at 3 Soj concentrations. DNA (pUC19, 0.5 ng μl^{-1}, 0.78 µM bp concentration final) was added at 2 min to mixture containing the indicated concentration of Soj preincubated with 1 mM ATP as described in Materials and Methods (section 12). Fluorescence spectrophotometer PMT voltage was 500 V in this assay. (B) Maximum net light scattering as a function of Soj concentration. The net change in light scattering between 2 min (DNA addition) and 4.5 min time points in panel A is plotted as a function of the Soj concentration in the reaction.

Table 8. Initial Rates of Increase of Light Scattering for Different Soj Concentrations.

Soj (μM)	Rate of Light Scattering Increase (a.u. min^{-1})[a]
1	25
2	432
4	858

a. Light scattering rates for each Soj concentration are the average of two replicate light scattering experiments.

compared to experiments in Fig. 20-21. Increased Soj concentrations increased both the levels and rates of light scattering upon DNA addition. The initial rate of increase in light scattering, calculated from the slope of the linear portion of light scattering curves from two replicate experiments, for each Soj concentration is indicated in Table 8. The rate increased almost 20-fold between 1 μM and 2 μM Soj, but increased only ~2 fold between 2 μM and 4 μM Soj. These rates indicated that Soj-ATP DNA structure formation might be cooperative but saturates between 2 μM and 4 μM Soj. The net increase in light scattering was calculated by subtracting the light scattering value at the time of DNA addition from the light scattering value at 6 min. While the initial rate of increase in light scattering was not a linear function of Soj, the overall amount of light scattering was roughly a linear function of Soj concentration (Fig. 22B).

The effect of Soj concentration in EMSAs, and DNase protection assays showed similar trends, where small increases in Soj concentration led to a large increase in Soj interaction with DNA. In EMSAs no DNA binding was observed at 1 μM Soj, while at 2 μM Soj ~50% of the DNA was bound by Soj (Fig. 15). In DNase I protection assays no full length DNA was observed at 2 μM Soj, whereas 4 μM Soj led to appearance of full length DNA (Fig. 17B). One significant difference between light scattering assays and other assays described above was the detection of light scattering at 1 μM Soj (in the presence of ATP and DNA). Other assays did not detect Soj interaction with DNA at 1 μM final Soj concentration so possibly the light scattering assay is one of the most sensitive measures of Soj-DNA interaction.

The effect of ATP concentration on the formation of Soj-DNA structures was investigated. DNA was added to reactions of Soj preincubated with various ATP concentrations and light scattering was observed (Fig. 23A). A change in light scattering in reactions containing Soj and DNA was observed in the presence of ATP compared to light scattering by Soj and DNA without ATP, as previously observed. The change in light scattering level 6 min after DNA addition was calculated for each ATP concentration, and then the observed change in an identical reaction without ATP was subtracted. The rate of light scattering over the first 6 min increased as the ATP concentration was increased (Fig. 23B). Comparing the effect of ATP concentrations on light scattering, with the effect on the initial velocity of Soj ATPase (Fig. 11B), indicated that the concentration of ATP required for 50% activity for each assay differed by a factor of two. The K_m for ATP in enzymatic hydrolysis of ATP was determined to be 180 μM, while the concentration of ATP which gave 50% of the light scattering rate observed at 1 mM ATP occurred at approximately 360 μM, indicating similar levels of ATP binding are required for both ATPase activity and formation of light scattering complexes.

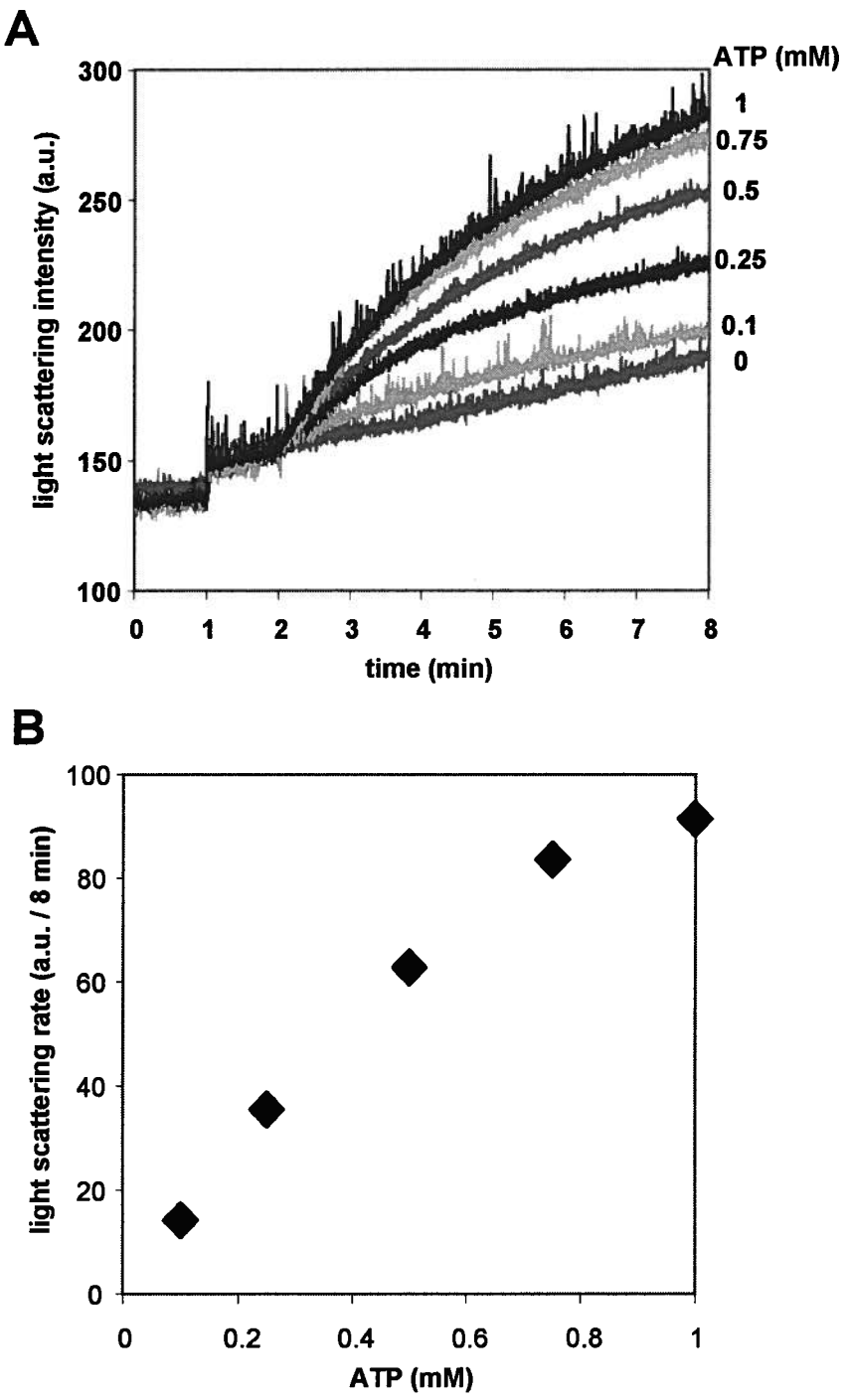

Fig. 23. ATP dependence of Soj light scattering. (A) Effect of ATP concentration on Soj-DNA light scattering. Soj (1 μM) was incubated with the indicated concentration of ATP for 1 min as described in Materials and Methods (section 12). After 1 min pUC19 DNA was added (0.5 ng μl^{-1}, 0.78 μM bp concentration) and light scattering was monitored for another 6 min. PMT voltage was 600V in this assay. (B) The net change in light scattering of Soj and DNA reactions between 2 min (DNA addition) and 8 min for each ATP concentration condition was corrected by subtraction of the net light scattering amplitude from light scattering reactions of Soj and DNA without ATP in the same time interval from panel A. The net change in light scattering was plotted as a function of ATP concentration.

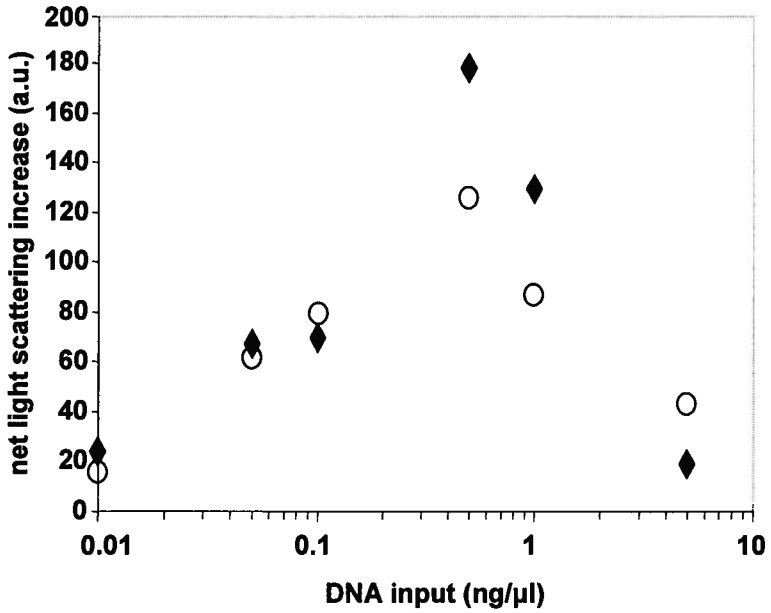

Fig. 24. DNA concentration dependence of Soj-ATP DNA light scattering. The net change in light scattering was determined 2.5 min (○), and 5 min (♦) after addition of pUC19 DNA to 1 µM Soj preincubated with 1 mM ATP as described in Materials and Methods (Section 12). PMT voltage in these assays was 600 V.

The characterization of light scattering dependence on DNA was monitored by addition of pUC19 DNA at various concentrations to reactions containing 1 μM Soj preincubated with 1 mM ATP. The observed net increase in light scattering at 2.5 and 5 min after DNA addition is plotted versus DNA concentration in Fig. 24. At both time points the maximum increase in light scattering occurred at ~0.5 ng μl^{-1} (0.78 μM final bp concentration) DNA. Lower DNA concentration (0.01 - 0.1 ng μl^{-1}) resulted in lower levels of light scattering. A ten-fold increase in DNA concentration input (to 5 ng μl^{-1}, 7.8 μM final bp concentration) also led to a decrease in light scattering. At low concentration DNA may be limiting in the formation of Soj-DNA light scattering structures. Since high DNA concentration resulted in levels of light scattering below the maximum, possibly at high DNA input Soj dimers are too dispersed on the DNAs to form structures that scatter light. If this were the case it would have implications for the structure of the light scattering complex.

The formation of Soj DNA structures that scattered light was also investigated by varying the length of DNA added to reactions of Soj-ATP. DNA molecules ranging from 0.1 to 2.6 kb were created using primers and templates indicated in Table 3. Primers, templates, and unincorporated dNTPs were separated from PCR products using a Qiagen PCR cleanup kit. Plasmid DNA (2.6 kb) was linearized by digestion of CsCl gradient-purified pUC19 with HindIII with no further cleanup. The concentration of the DNAs were calculated from the OD_{260} of a small PCR sample, and checked by comparing band intensities of small samples with the band intensities of known DNA concentrations from a DNA ladder following agarose gel electrophoresis. The determination of DNA concentrations by two independent methods was used to increase the possibility that any differences in light scattering profiles were due to changes in DNA length, and concentration.

The effect of DNA length on the formation of light scattering structures is shown by the data in Fig. 25A. In this experiment all DNA concentrations were 0.5 ng μl^{-1} (0.78 μM bp concentration); however, the molar concentration of the DNA fragments will vary. All of the DNAs supported light scattering with Soj-ATP. The increase in light scattering was characterized by a lag before the curves increased linearly for a few minutes and then approached an apparent saturation. There was a longer lag when smaller DNA lengths were added to the reactions (see enlarged scale in Fig. 25B). The lag time is plotted versus DNA length (Fig. 25C). The lag time decreased as the DNA length increased, and was essentially absent with a 2.6 kb DNA. The slope of the linear portion of the light scattering time course

Fig. 25. Effect of DNA size on light scattering by Soj. (A) Formation of light scattering complexes over time using DNA of different length. Soj (1 μM) was incubated with ATP (1mM) as described in Materials and Methods (section 12). DNA fragments of indicated lengths were added at 2 min to a final concentration of 0.5 ng μl^{-1} (0.78 μM bp concentration) and light scattering was monitored. PMT voltage in this assay was 600V. (B) The portions of light scattering profiles from panel A between 2 min and 4.5 min are shown. (C) Changes in apparent lag time for formation of light scattering complexes after addition of DNAs of different lengths. The lag time, measured as the time between DNA addition and when the rate of light scattering increase became linear as a function of time, was plotted as a function of the DNA length added to light scattering reactions in panel A. (D) Changes in the rate of increase in light scattering for different DNA lengths. The rate of increase in light scattering was calculated from the average slope of the linear portion of the light scattering curves from panel A. These values were plotted as a function of the DNA length added to light scattering reactions. (E) The net change in light scattering observed after addition of different DNA lengths. The net change in light scattering from 2 min (DNA addition) to 8 min was plotted as a function of the DNA length added to light scattering reactions.

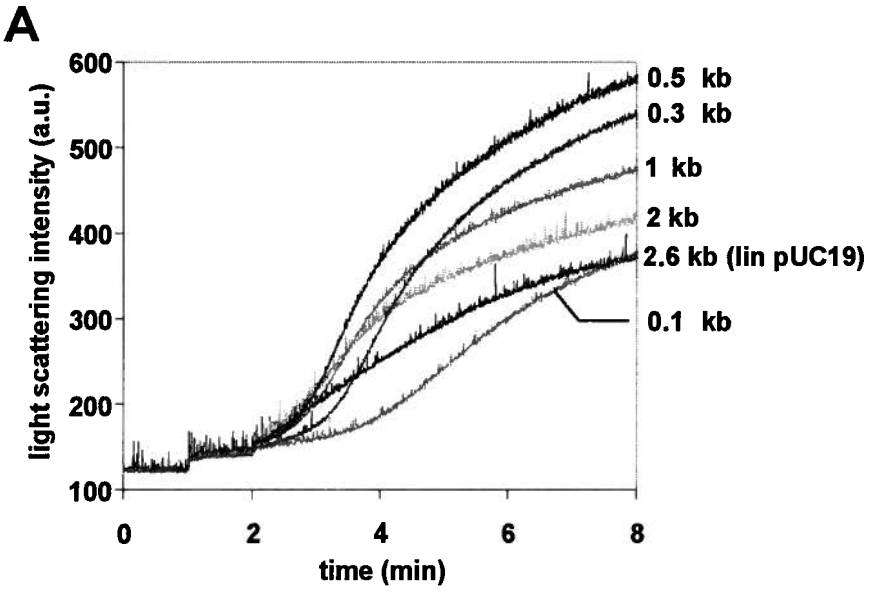
A
light scattering intensity (a.u.)
600
500
400
300
200
100
0
2
4
6
8
time (min)
0.5 kb
0.3 kb
1 kb
2 kb
2.6 kb (lin pUC19)
0.1 kb

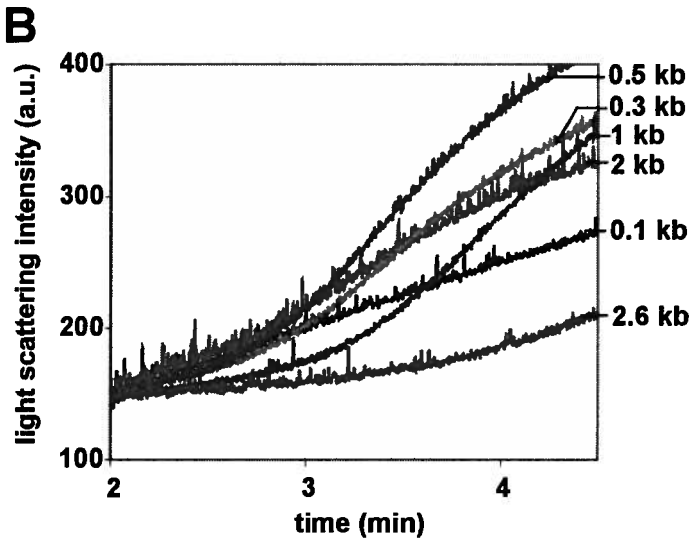
B
light scattering intensity (a.u.)
400
300
200
100
2
3
4
time (min)
0.5 kb
0.3 kb
1 kb
2 kb
0.1 kb
2.6 kb

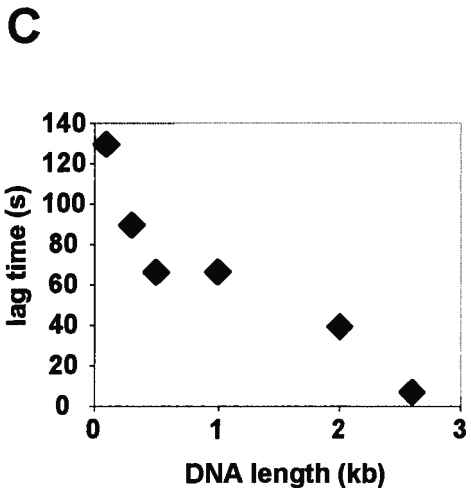
C
lag time (s)
140
120
100
80
60
40
20
0
0
1
2
3
DNA length (kb)

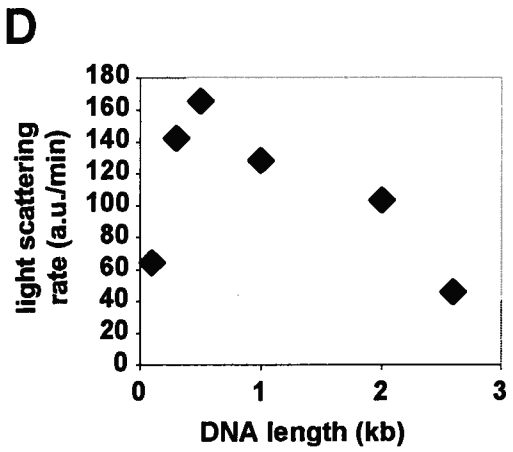
D
light scattering rate (a.u./min)
180
160
140
120
100
80
60
40
20
0
0
1
2
3
DNA length (kb)

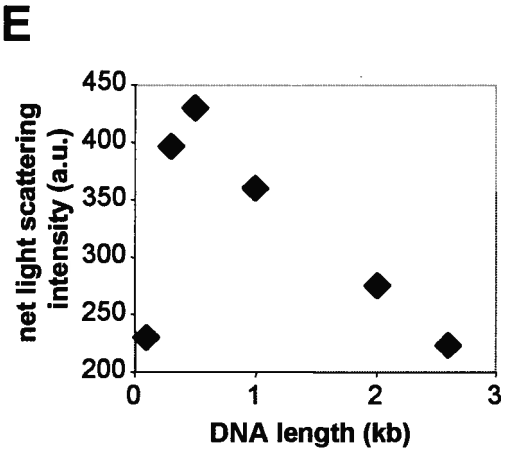
E
net light scattering intensity (a.u.)
450
400
350
300
250
200
0
1
2
3
DNA length (kb)

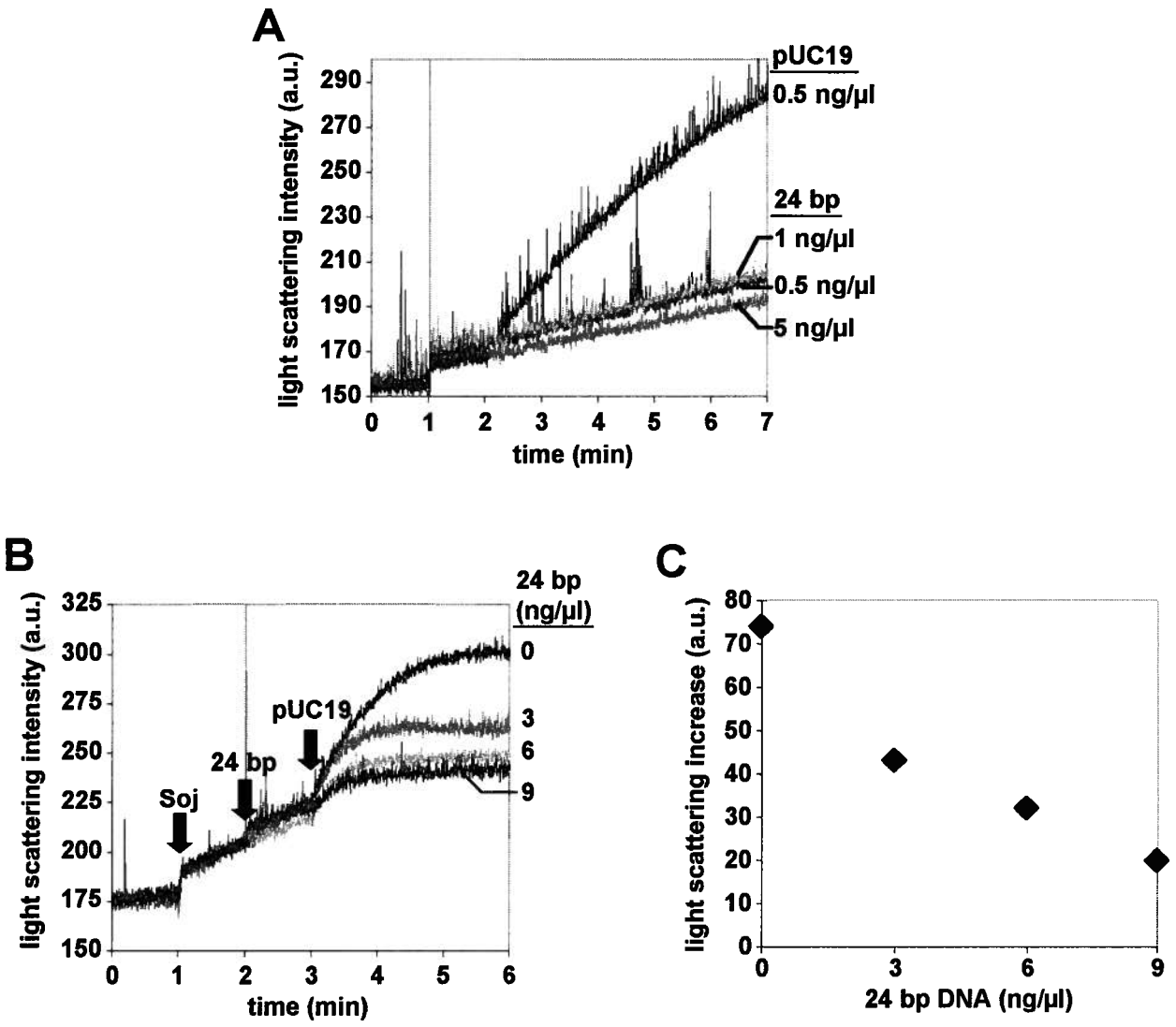

Fig. 26. A 24 bp DNA does not stimulate formation of light scattering complexes. (A) Soj (1 µM) was incubated with 1 mM ATP for 1 min as described in Materials and Methods (section 12), before either a 24 bp duplex DNA (final concentration indicated) or pUC19 DNA (0.5 ng μl^{-1}) was added and light scattering was monitored. (B) The final concentrations of 24 bp DNA indicated on the right were added to Soj+ATP as described in Materials and Methods (section 12). After a 1 min incubation, pUC19 DNA was added (3 min, 0.5 ng μl^{-1} final) and light scattering was monitored. (C) The net change in light scattering determined from the curves in panel B 3 min after addition of pUC19 DNA is plotted as a function of 24 bp DNA concentration added (at 2 min).

also differed with DNA length. The slope was greatest with the 500 bp DNA addition and was lower with both shorter and longer molecules (Fig. 25D). The net changes in light scattering levels, measured at 6 minutes after DNA addition, also differed with DNA length (Fig. 25E). The light scattering levels were observed to peak at about 500 bp in three independent light scattering assays with different Soj protein preparations. In control experiments with the shorter DNA molecules the formation of Soj and DNA light scattering complexes did not occur in solution containing ADP or no nucleotide (data not shown), and so appeared to require ATP. As detected by EMSA (Fig. 15), Soj-ATP was capable of binding to a 24 bp duplex oligonucleotide. However, addition of a 24 bp double stranded DNA to Soj and ATP did notcause an increase in light scattering over a range of DNA concentrations (Fig. 26A). Furthermore, preincubation of Soj-ATP with the 24 bp double stranded DNA prior to addition of pUC19 DNA inhibited light scattering observed when plasmid DNA alone was added to Soj-ATP (Fig. 26B). The inhibition of plasmid DNA-mediated light scattering by the 24 bp DNA increased with the concentration of the 24 bp double stranded DNA (Fig. 26C). These data indicated that 24 bp DNA did not allow formation of structures that scatter light. Since the 100 bp DNA did support formation of complexes that scattered light, the minimum length of DNA required to form light scattering structures was apparently between 24 bp and 100 bp.

The effect of DNA lengths on Soj-ATP light scattering lag times was unexpected. Identical masses of DNA should represent the addition of identical amounts of Soj binding sites. A simple model where Soj bound DNA cooperatively due to a preference for binding sites adjacent to a Soj dimer already bound to DNA does not predict the different lags observed upon addition of different length DNA. The data could be explained by a model where multiple Soj dimers bound to adjacent DNA sites form 'tracts' of Soj multimers on DNA which are able to interact with other Soj 'tracts' either on the same or different DNA molecules, and this possibility will be further addressed in the Discussion.

9 Soj-DNA Complexes Resolved by Transmission Electron Microscopy.

Direct visualization of Soj bound to DNA by negative stain transmission electron microscopy was attempted to examine the ultrastructure of a Soj-DNA complex. Soj-ATP was incubated with pUC19 DNA and the complexes were collected by centrifugation. The pellet fraction was resuspended in buffer without ATP, and quickly applied to a carbon coated grid The grids were stained with uranyl acetate (Fig. 27). Micrographs of the linearized pUC19

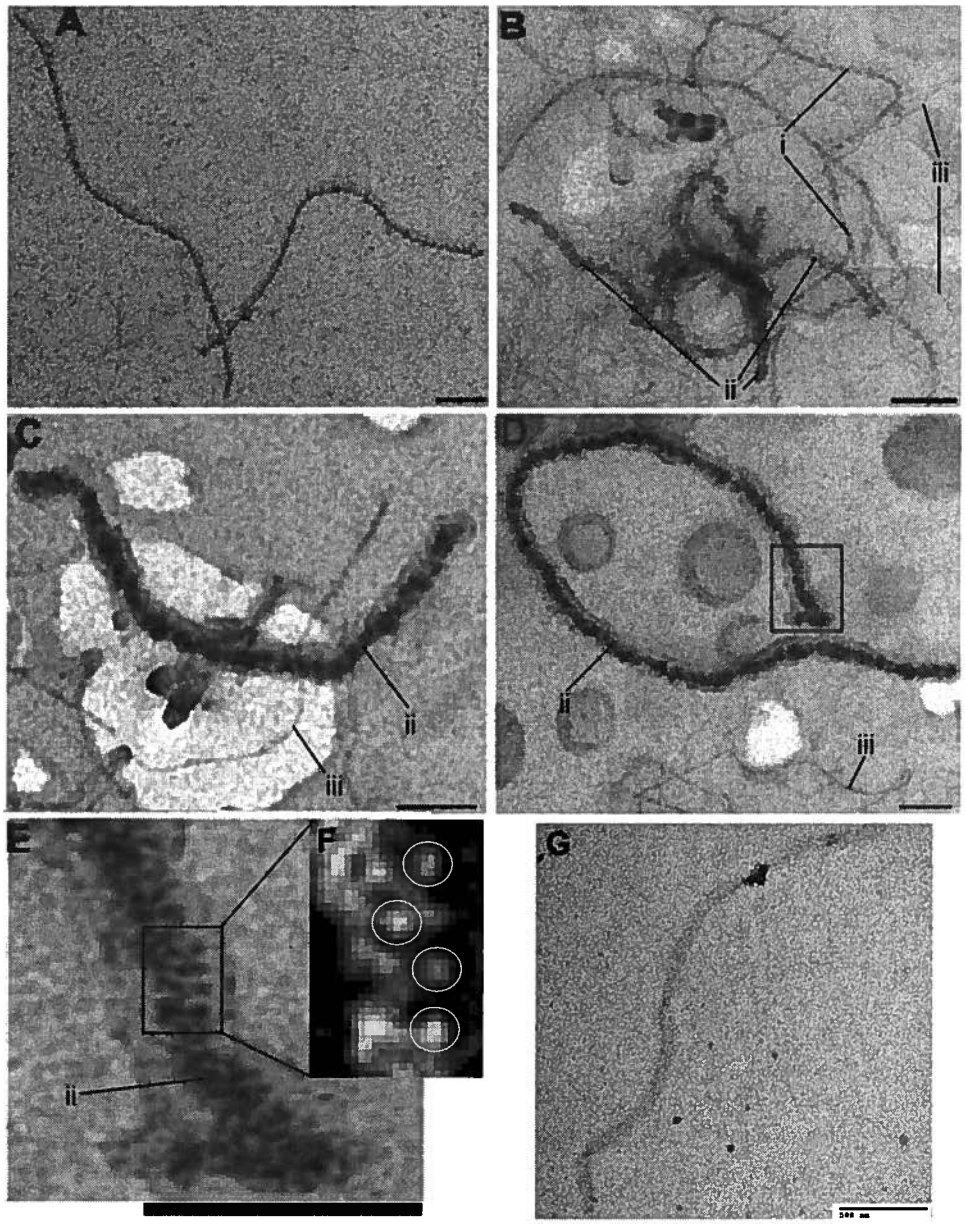

Fig. 27. Transmission electron micrographs of negatively stained sedimented Soj-ATP DNA structures. Soj (4 μM) was incubated with nucleotide (1 mM) and DNA (2 ng μl^{-1}) in ATPase buffer with 100 mM NaCl and treated as sedimentation assays described in Materials and Methods (section 9). Pellet fractions were resuspended in buffer and placed on the glow discharged carbon coated TEM grids and stained with uranyl acetate as described in the Materials and Methods. (A) Micrograph of linear plasmid DNA used in assays without Soj. (B-D) Micrographs of resuspended sedimented complexes from reactions containing Soj, ATP, and plasmid DNA. (E) Digitally magnified inset of boxed area from D. Bars in panels A-E are 100 nm. (F) Boxed area of panel E where the greyscale is inverted and the brightness and contrast have been adjusted by Photoshop v6.0 to highlight points of electron densities (white circles). (G) Representative field of view from a grid prepared without Soj or DNA (an embedded carbon coat impurity shows a focal reference, scale bar 500 nm). Roman numerals i-iii in panels A-E indicate structures of varying diameter described in the text.

DNA template alone used in sedimentation assays (Fig. 27A) showed linear molecules of uniform diameter. When Soj-ATP and DNA were incubated, sedimented and applied to the grids, a variety of structures were observed. After many attempts no higher quality pictures were obtained. The widths of these structure, where it was possible to determine them, were approximately 6-12 nm or 17-22 nm (labeled i and ii, respectively, in Fig. 27B-D). I selected one area that is boxed in Fig.27D and used digital magnification to look for areas of greater electron density that might represent the position of the Soj proteins.(Fig. 27E). The points of electron density were further highlighted by inverting the greyscale and adjusting the brightness and contrast of Fig. 27E. Points of electron density with dimensions approximately 5-6 nm in width appear to be visible (Fig. 27F). The dimension of these dots would be consistent with the previously published dimensions of a Soj dimer from *T. thermophilus* (Leonard *et al.*, 2005). The 5-6 nm wide electron dense structures are potentially in a higher order repeating structure. All of the micrographs also showed DNA not bound by Soj-ATP (labeled iii in Fig. 27). This was expected given that at 4 μM Soj DNA sedimentation was incomplete in sedimentation assays and at 4 μM Soj, protection of DNA from DNase I digestion was incomplete (Figs. 16 and 17B). DNA unbound by Soj could also represent decay of complexes during grid preparation as the dehydration requires wicking away the buffer that contains the ATP. Structures seen in Fig. 27B-E were not observed in conditions without ATP or DNA (Fig. 27F) The structures with widths equal to or larger than 17 nm in Fig. 27B might represent Soj-Soj interactions between complexes bound to different DNA molecules, indicating the possibility that Soj can form higher order structures and bridge DNA molecules (addressed in the Discussion).

10 Soj Interaction with Spo0J

Spo0J is required *in vivo* to antagonize the negative regulation of sporulation by Soj. A simple model by which Spo0J affects Soj is by a direct interaction. Several lines of experimental evidence support such a direct interaction between Soj and Spo0J. Plasmids with a *parS* sequence are stabilized in *B. subtilis* and *E. coli* in the absence of antibiotic selection only when both Soj and Spo0J are expressed (Hester and Lutkenhaus, 2007; Lin and Grossman, 1998; Yamaichi and Niki, 2000). Chemical cross-linking treatment of *B. subtilis* followed by resolution of Soj-Spo0J conjugates by Western blots using αSoj and αSpo0J antibodies, also support a direct Soj interaction with Spo0J (Ogura *et al.*, 2003). The interaction of Soj and

Spo0J *in vitro* was assayed by multiple techniques with the expectation that these interactions would affect the *in vitro* activities and characteristics of Soj) or Spo0J.

10.1 Soj ATP hydrolysis is stimulated by Spo0J.

The ATPase activity of some members of the ParA/MinD family of proteins has been shown to be stimulated *in vitro* by the cognate ParB (or the protein encoded by the second ORF of the operon). The MinE stimulation of the ATPase of MinD is required for the proper function of MinD *in vivo*. A point mutation in MinE that cannot stimulate MinD ATPase *in vitro* leads to the production of minicells when expressed in *E. coli* (Hu and Lutkenhaus, 2001).

If Soj and Spo0J followed the MinD/MinE pattern, Spo0J would stimulate Soj ATPase activity, and this stimulation could be detected in ATPase assays. Purified recombinant Spo0J was added to Soj and α^{32}P-ATP, in the presence or absence of DNA. The production of ADP was assayed as described in the Results Section 3, and the Materials and Methods. ATPase values were corrected for the presence of radioactive ADP in the ATP preparations. Soj ATPase values were also corrected by subtracting the values of ADP produced by the indicated concentration Spo0J or DNA alone for each time point. This ensured that the calculated stimulation were observations of Soj ATPase activity stimulation by Spo0J. In a typical experiment the background without Soj was ~5% of total ADP produced when Soj was added, and Spo0J reactions without Soj were ~15 % of total ADP produced when Soj was added.

Fig. 28 shows the data from a representative experiment to monitor the effect of Spo0J on ATPase activity, with or without DNA. In the absence of DNA, Spo0J stimulated a 1.7 +/- 0.4 fold increase in ADP production by Soj compared to ADP production by Soj alone (measured as nmol ADP produced / nmol Soj, n=14 independent ATPase assay reactions, P value ~0.019 as calculated by a two tailed Student's T test). The inclusion of plasmid DNA along with Spo0J and Soj led to a further increase in the ATP hydrolysis activity of Soj. In the presence of Spo0J and DNA, ATP hydrolysis by Soj (measured as nmol ADP/nmol Soj) increased by a factor of 2.5 +/-0.7 compared to the levels of ATP hydrolysis by Soj alone (n=17 independent ATPase assay reactions, P value ~1.3×10^{-4} as calculated by a two tailed Student's T test). No stimulation of Soj ATPase activity was observed by the addition of DNA alone in any condition. The stimulation of Soj-dependent ATPase activity by Spo0J was further characterized by monitoring ATP hydrolysis by Soj over a range of Spo0J concentrations in the presence of DNA (Fig. 29). As the concentration of Spo0J increased, so too did the production

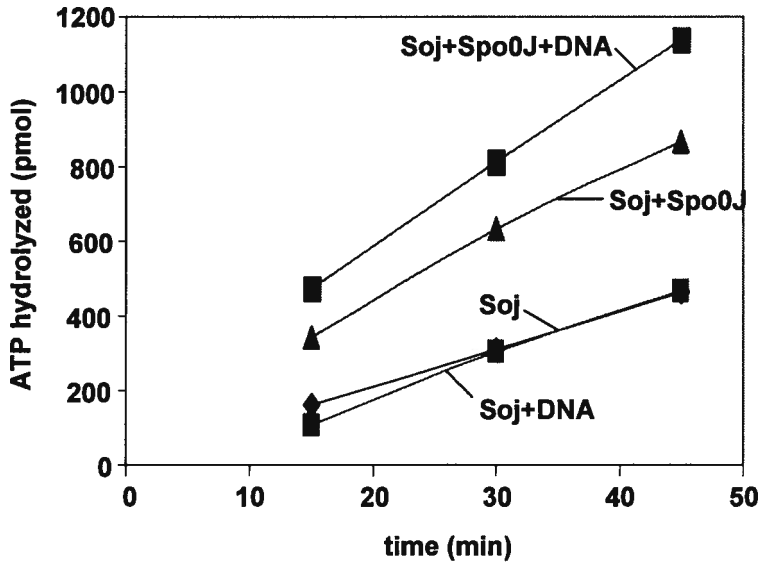

Fig. 28. Stimulation of Soj ATPase by Spo0J. Soj (3 μM) and α^{32}P-ATP (250 μM, 1.33 Ci mmol^{-1}), were incubated with Spo0J (3 μM) where indicated, with or without pUC19 DNA (6 ng μl^{-1}), in 30 μl of ATPase buffer with 100 mM NaCl at 37°C. At the indicated time aliquots were removed, ATPase stopped, and ADP was detected and quantified as described in Materials and Methods (section 5). The amount of ADP produced was plotted as a function of time. ADP produced from parallel reactions containing no protein, Spo0J, and/or DNA was assayed at the indicated time points. These values were subtracted from ATPase reactions containing Soj, Spo0J, and/or DNA where appropriate.

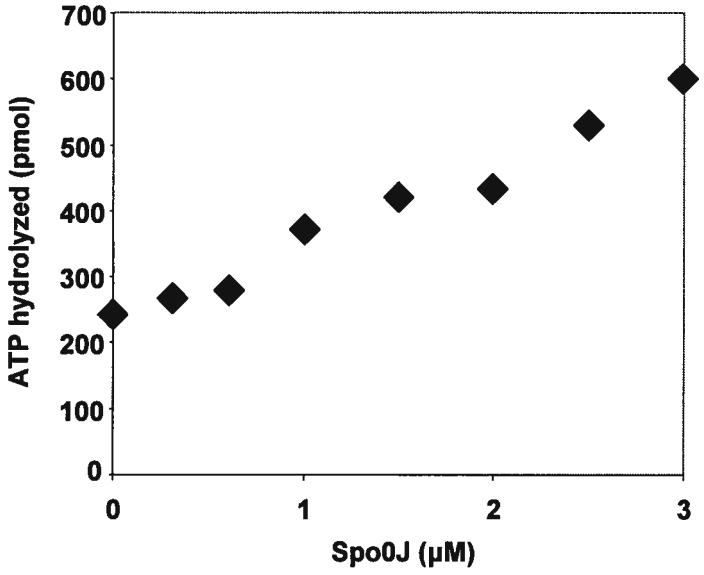

Fig. 29. Stimulation of Soj ATPase by Spo0J. Soj (3 μM), α^{32}P-ATP (250 μM, 1.33 Ci mmol^{-1}), and pUC19 DNA (6 ng μl^{-1}) were incubated with the indicated concentration of Spo0J in 20 μl of ATPase buffer with 100 mM NaCl at 37°C. After 15 min reactions were stopped and ADP was detected and quantified as described in Materials and Methods (section 5). The amount of ATP hydrolyzed was plotted as a function of Spo0J concentration. For each point, ATPase reactions containing the indicated concentration of Spo0J without Soj were assayed. These values were subtracted from the ATPase values from reactions of Soj with the appropriate Spo0J concentration to give corrected Soj ATPase values.

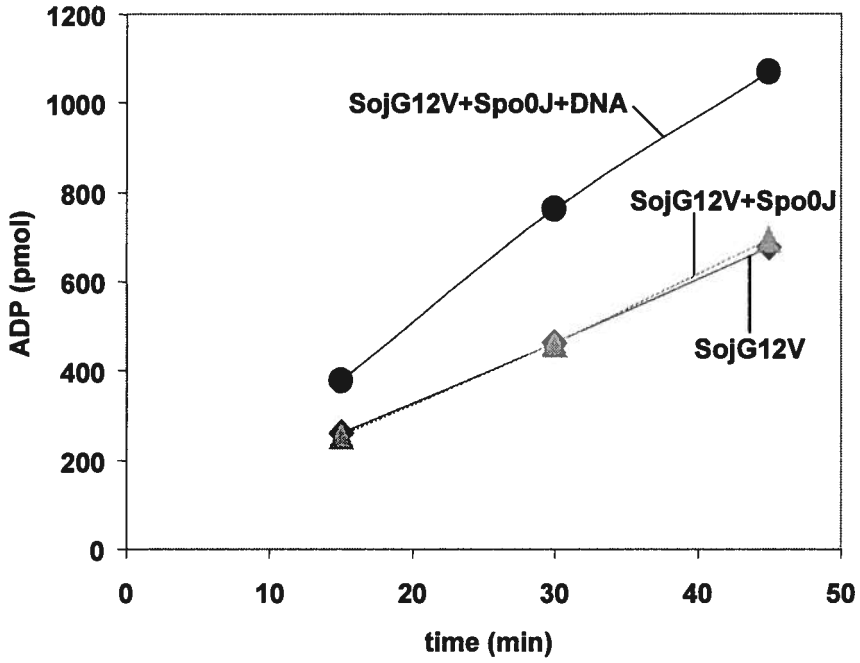

Fig. 30. Stimulation of SojG12V ATPase by Spo0J. SojG12V (3 μM) and α^{32}P-ATP (250 μM, 1.33 Ci mmol^{-1}), were incubated with Spo0J (3 μM) where indicated, with or without pUC19 DNA (6 ng μl^{-1}), in 30 μl of ATPase buffer with 100 mM NaCl, at 37°C. At the indicated time aliquots were removed, ATPase stopped, and ADP was detected and quantified as described in Materials and Methods (section 5). The amount of ADP produced was plotted as a function of time. ADP produced from parallel ATPase reactions containing no protein, Spo0J, and/or DNA was assayed at the indicated time points. These values were subtracted from SojG12V ATPase reactions containing Spo0J and/or DNA where appropriate to give Soj ATPase values.

of ADP. The increase in ATP hydrolysis by Soj as a function of Spo0J concentration was roughly linear over the range tested.

The stimulation of SojG12V ATPase by Spo0J was also investigated. The ATPase activity of SojG12V was stimulated by Spo0J in the presence, but not the absence, of DNA. Results from a representative experiment are shown in Fig. 30. Inclusion of both DNA and Spo0J in SojG12V ATPase reactions resulted in a 1.7 +/- 0.1 fold stimulation (n=6 independent ATPase assay reactions, P value ~2.3 x 10^{-6} as calculated by a two tailed Student's T test). Unlike wild type Soj, no stimulation of SojG12V ATPase by Spo0J alone was observed. As with wild type Soj, SojG12V ATPase activity was not stimulated by DNA alone (not shown).

The stimulation of Soj ATPase activity by Spo0J could be caused in two ways. First, the interaction of Spo0J with Soj could stimulate an increase in the catalysis of ATP hydrolysis by Soj. Alternatively, Spo0J could act as a Soj nucleotide exchange factor. Stimulation of ATP hydrolysis, and stimulation of ATP exchange which leads to increased ATPase levels have both been demonstrated in different ParA/MinD ATPases by the cognate partner protein. The possibility that Spo0J is a nucleotide exchange factor was investigated by monitoring ATP binding by Soj in the presence of Spo0J by UV crosslinking assays. Results from these experiments were inconclusive, so this question remains unanswered.

10.2 Soj and Spo0J interact to Form High Molecular Weight Protein Complexes.

Other members of the ParA and ParB family of proteins have been demonstrated to form large protein complexes or 'fibres' that consist of ordered protein multimers. The possibility that the interaction of Soj and Spo0J could result in the formation of larger protein complexes was assessed.

It was reasoned that if Soj and Spo0J interacted to form large protein complexes these complexes could be sufficiently large to be pelleted by low speed centrifugation. Sedimentation assays were performed by mixing Soj (3 μM) and Spo0J (3 μM) in the presence or absence of bacteriophage φ29 genomic DNA, with either ATP or ADP (described in the Materials and Methods). Bacteriophage φ29 genomic DNA has several Spo0J binding sites (*parS*). Following centrifugation of the reactions in a microfuge (~16k x g, 20 min), the proteins were identified by SDS-PAGE of aliquots of the supernatants and resuspended pellets from the centrifuged mixtures. The amount of protein corresponding to Soj and Spo0J was estimated by densitometry of digital images of Coomassie brilliant blue stained gels using Imagequant, and

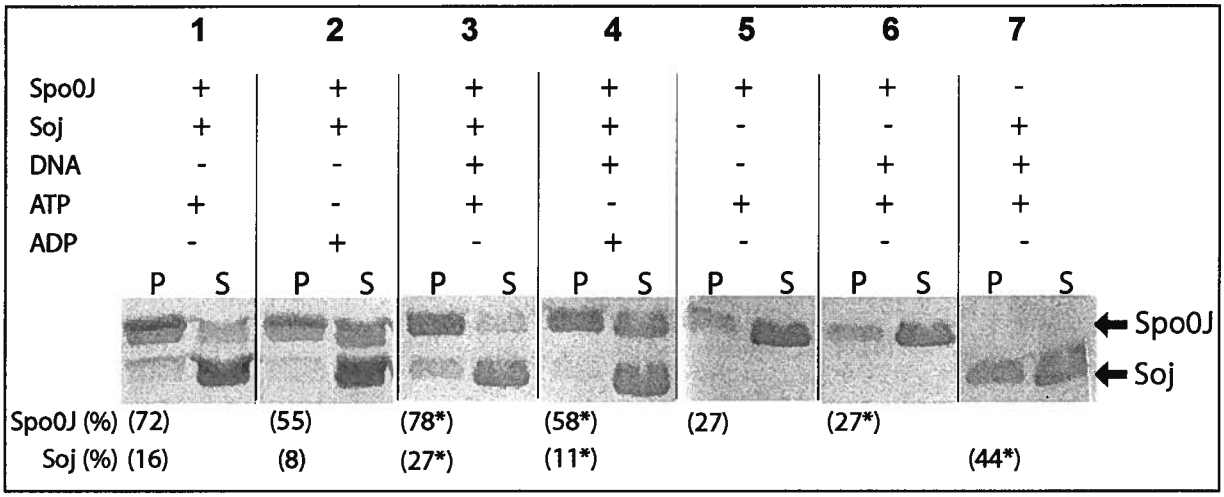

Fig. 31. Sedimentation assays of Soj and SpoOJ. The indicated components (Soj and SpoOJ, 3 μM; nucleotide, 1 mM; bacteriophage ϕ29 genomic DNA, 6 ng μl^{-1} (0.5 nM)) were incubated in 40 μl of ATPase buffer with 100 mM NaCl, for 5 min at 37°C. Supernatant (S) and pellet (P) fractions were separated by centrifugation for 20 min at 16k x g at room temperature. Fractions were treated as described in Materials and Methods (section 9), separated by SDS-PAGE and stained with Coomassie Brilliant Blue. An image of the gel was generated using an AlphaImager Gel documentation system. Numbers in parentheses indicate the band density of the pellet fraction over the sum of supernatant and pellet fraction band densities (given as percent values) for the indicated protein as determined by Imagequant v5.2. Values in parentheses with asterisks represent the average of two independent sedimentation reactions.

these values were used to calculate the fraction of each protein recovered in the pellet and supernatant fractions from the sedimentation assay.

As seen in Fig. 31 when Spo0J was incubated with Soj in the presence or absence of DNA or either nucleotide, then subjected to centrifugation, a large fraction of Spo0J was recovered in the pellet (Fig. 31, lanes 1-4). The pellets contained only a small fraction of Soj. Relatively low levels of Spo0J were recovered in the pellets following centrifugation of reactions containing only Spo0J, with or without DNA in the presence of ATP (Fig. 31, lanes 5 and 6). Comparing the effect of ATP versus ADP (Fig. 31, compare lanes 1 and 2, and lanes 3 and 4) indicated the presence of ATP resulted in a small increase in the fraction of sedimented Spo0J compared to the same reaction conditions where ADP was present. In reactions where Soj was incubated with Spo0J, ATP, and DNA the fraction of Soj that sedimented was reduced compared to the fraction seen with ATP and DNA without Spo0J (Fig. 31, compare lanes 3 and 7). This suggested that Spo0J may reduce the formation of sedimentable Soj DNA complexes. The sedimentation of a large fraction of total Spo0J but a relatively low fraction of Soj from mixtures containing Spo0J incubated with Soj, indicated that the protein complexes were composed mostly of Spo0J.

Formation of complexes between Spo0J and Soj was monitored by light scattering. Light scattering was assessed as described in Materials and Methods Section 12. Soj (1 μM) was incubated in the presence of either ATP or ADP at 30°C. After one min, an equimolar amount of Spo0J was added and light scattering was monitored for another 3 min. Upon addition of Spo0J to Soj incubated with either ATP or ADP, a large increase in light scattering was consistently observed (Fig. 32; duplicate experiments for each nucleotide condition are indicated). This large increase in light scattering was not observed when Soj or Spo0J were incubated alone in the same reaction conditions (Figs. 20-21, and data not shown, respectively), although Soj did form much less intense light scattering signals. The slopes of the linear portion of the light scattering curves were steep and slightly increased when ATP was included compared to ADP. A slightly higher level of light scattering was observed in the presence of ATP compared to ADP which was compatible with the slightly increased sedimentation of Spo0J from mixtures of Soj and Spo0J in the presence of ATP compared to ADP from Fig. 31. The ability of SojG12V to interact with Spo0J in the presence of ATP was investigated by light scattering assays in a similar manner as wild type Soj. SojG12V (0.5 μM) was incubated with ATP for one min, an equimolar amount of Spo0J was added and light scattering was monitored for 3 minutes (Fig. 33). A sharp increase in light scattering upon addition of Spo0J (at 2 min)

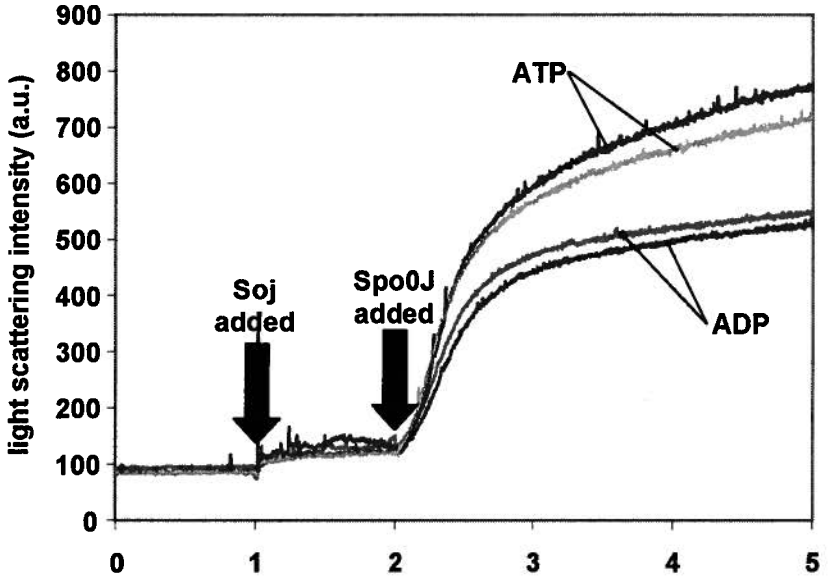

Fig. 32. Light scattering by Soj and SpoOJ. Soj (1 μM) was incubated with 1 mM of the indicated adenosine nucleotide in1.5 ml of ATPase buffer with 100 mM NaCl as described in the Materials and Methods (section12). After 1 min, SpoOJ (1μM) was added and light scattering was monitored. Fluorescence spectrophotometer PMT voltage in this assay was 600 V.

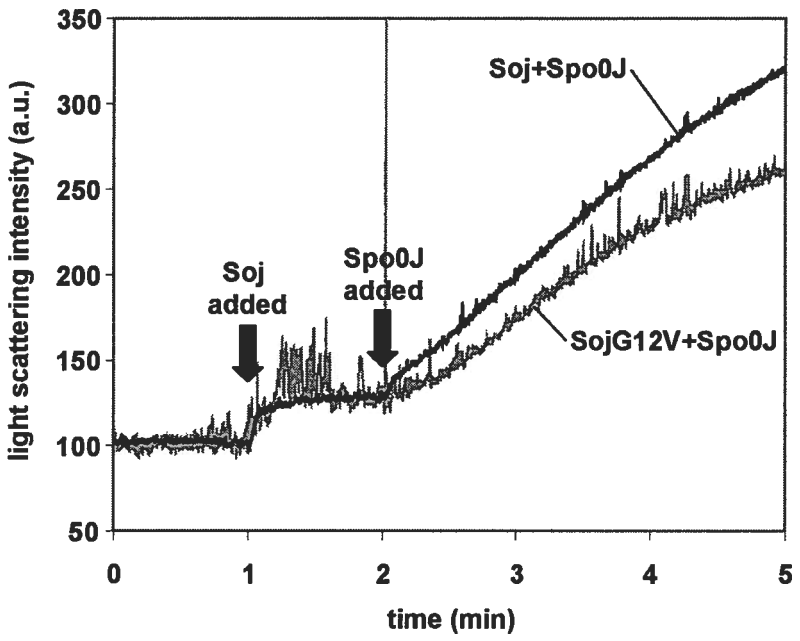

Fig. 33. Light scattering by Soj or SojG12V, and Spo0J. Where indicated Soj, or SojG12V (0.5 μM) was incubated with 1 mM of the indicated adenosine nucleotide in 1.5 ml of ATPase buffer with 100 mM NaCl as described in Materials and Methods (section 12). After 1 min, Spo0J (0.5 μM) was added and light scattering was monitored. Fluorescence spectrophotometer PMT voltage in this assay was 600 V.

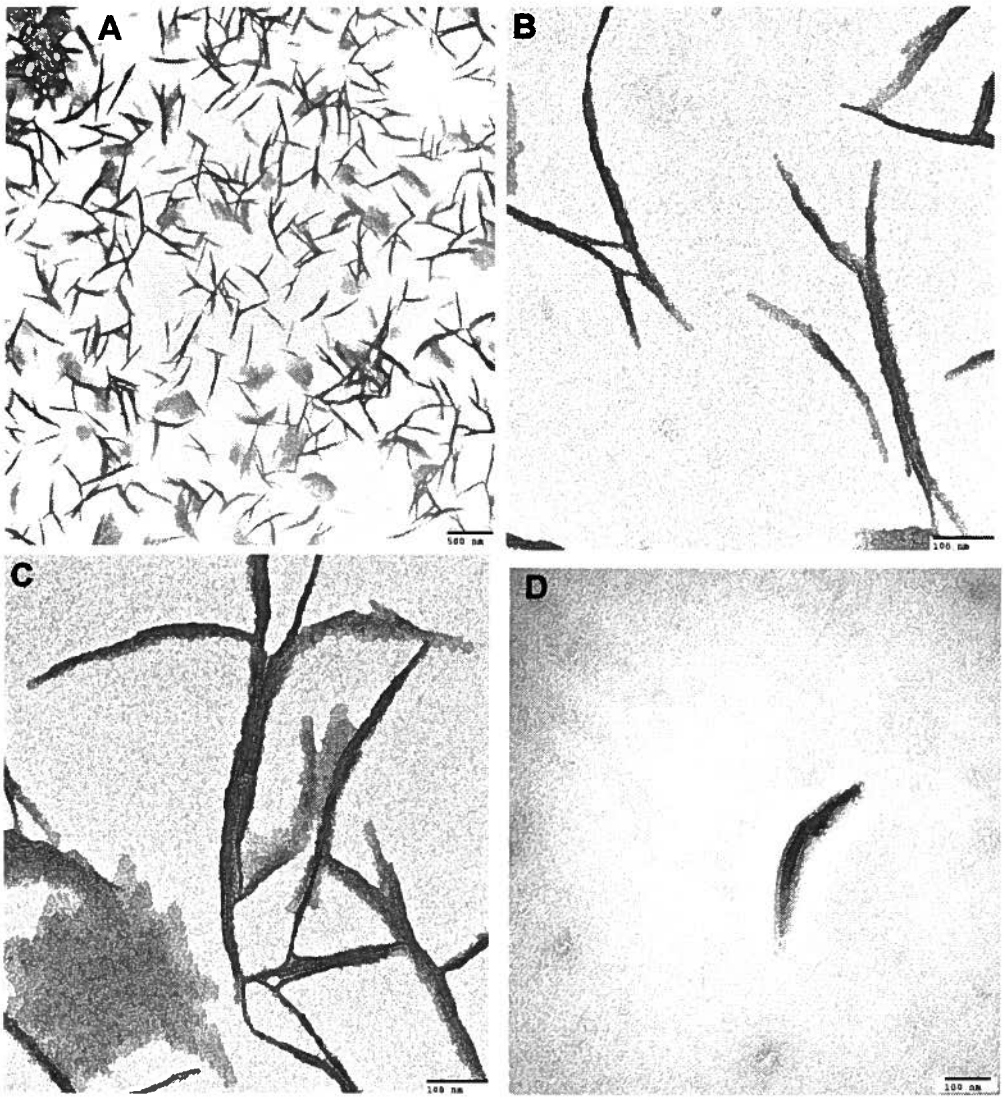

Fig. 34. Transmission electron micrographs of negatively stained Soj-Spo0J structures. Soj and Spo0J (1 μM) were incubated with ATP (1 mM) in 20 μl of ATPase buffer with 100 mM NaCl. A small sample of the reaction was applied to a carbon coated grid and stained with 1 % uranyl acetate as described in the Materials and Methods (section 13.2). Grids were examined by transmission electron microscopy and micrograph images were captured as described in Materials and Methods (section 13.2). (A) 30 000 times magnification from a grid prepared with Soj and Spo0J. Scale bar 500 nm. (B-C) 200 000 times magnification from a grid prepared with Soj and Spo0J. Scale bars 100 nm. (D) 30 000 times magnification of a grid prepared with Spo0J and nucleotide. Scale bar 100 nm.

was observed with both SojG12V and wild type Soj. The rates of increase of light scattering during the linear portions of the curves were similar for Soj and SojG12V. These results indicated that like wild type Soj, SojG12V was able to stimulate formation of light scattering protein complexes in the presence of Spo0J.

The protein complexes which resulted from incubation of Soj and Spo0J were examined by staining with uranyl acetate and transmission electron microscopy using the same methodology as used for Soj. Electron micrographs of structures resulting from incubating Soj and Spo0J are presented in Fig. 34A-C. The overall dimensions of these structures were approximately 400-700 nm in length and approximately 25-45 nm in width. These filamentous structures appeared to be composed of stacked striations that are approximately 4 nm to 7 nm across. These ends of the filamentous structures appeared to be frayed and in several examples filaments might be joined to other stacked striated structures. Filaments were observed only in conditions where Soj and Spo0J were incubated together prior to application to the EM grid. The filaments were absent if either Soj or Spo0J were omitted from the incubation prior to application to the grid. A representative field of view of Spo0J alone is shown in Fig. 34D where a carbon coat imperfection is used as a focal reference.

The crystal structure of the N-terminal domain of Spo0J from *T. thermophilus* has been solved (Leonard *et al.*, 2004). BlastP protein sequence alignment of the *T. thermophilus* protein fragment used to solve the crystal structure showed it to be 47% identical to the Spo0J protein from *B. subtilis.* Using the analysis of the truncated *T. thermophilus* Spo0J crystal structure with DeepView/ Swiss-pdb viewer (Guex and Peitsch, 1997), I estimated that an approximate dimensions of 62Å x 47Å x 42Å for the truncated Spo0J dimer. Since the sedimentation assays of Soj and Spo0J (Fig. 31) indicated that the structures from Fig. 34 should consist primarily of Spo0J. The width of the striations in the structures in Fig. 34, would be similar to the dimensions of a Spo0J dimer.

DISCUSSION

Experiments in this thesis addressed the properties of Soj, a protein that negatively regulates sporulation. The characterization of Soj addressed how it interacts with adenosine nucleotides, and how interaction with nucleotides affects the DNA binding activity of Soj *in vitro*. A characterization of the interaction between Soj and Spo0J was also presented. A better understanding of these interactions *in vitro* is important to understand how these ParA and ParB family proteins affect sporulation. In the Discussion I will first outline the technical advances that were important for these experiments. Second, the *in vitro* properties of Soj will be related to its function *in vivo*, and compared to the properties of Par proteins in other organisms. A model of how Soj interacts with DNA in an ATP-dependent manner will be presented, as well as an outline of how Soj interacts with Spo0J and DNA. Models for the role of Soj and Spo0J in *B. subtilis* and the impacts of these models on sporulation will be presented.

1 Technical Modifications.

1.1 Soj purification.

Previous to this work, the recombinant hexahistidine tagged Soj purified from *E. coli* could not hydrolyze ATP, or bind double-stranded DNA (Cervin *et al.*, 1998). I used information from studies of the *C. crescentus* ParA protein to modify the purification scheme incorporating adenosine nucleotides in the purification buffers (Easter and Gober, 2002). The inclusion of ATP or ADP in the purification protocol resulted in Soj preparations that consistently bound and hydrolyzed ATP. I also included very high salt washes of the protein while it was on the Ni-NTA agarose resin (Fig. 7). The inclusion of high salt in the buffers for purification of Soj prevented DNA contamination which interfered with the characterization of Soj DNA binding. The exclusion of a dialysis or buffer exchange step to remove either imidazole or nucleotides improved the yield of active, soluble Soj, as did the immediate freezing of Soj on dry ice following elution from the Ni-NTA agarose column.

Even with the purification modifications, Soj tends to form precipitates in liquid solution in 1-2 hours. This was the rationale behind eliminating the step which removed imidazole or nucleotide by dialysis. This lack of solubility was likely not a result of a lack of charge as at pH 8 (the pH of buffers used for purification and all the activity assays). Soj had a net negative

charge and therefore was predicted to remain in solution. Other researchers have noted poor solubility of ParA proteins (Barilla *et al.*, 2005; Leonard *et al.*, 2005). It is possible that in general ParA proteins tend to multimerize which results in reduced solubility *in vitro*.

1.2 Light Scattering Assays.

The possibility that Soj could form multimeric structures on DNA was indicated by work that characterized Soj from *T. thermophilus* (Leonard *et al.*, 2005). I reasoned that these structures would have distinctive optical properties. Light scattering was found to be a sensitive assay which could detect Soj DNA interactions at low concentrations of Soj and DNA. The effectiveness of this assay allowed me to generate a refined model for the interaction of Soj on DNA that is discussed further in this section.

2 Soj ATP Binding and Hydrolysis.

The specificity of Soj binding to ATP was demonstrated by UV-crosslinking assays. Soj was shown to possess some dATP binding activity although the yield was low compared to the binding of ATP (Fig. 4A). Soj binding to ATP reached a maximum quickly (~1 min). Both Soj mutants (SojG12V and SojD40A) also bound ATP (Fig. 8D).

Using thin layer chromatography, Soj was demonstrated to possess a low level ATPase activity. The initial rate of ATPase as a function of ATP concentration indicated Michaelis Menton kinetics. The V_{max} of ~180 pmol ATP $nmol^{-1}$ min^{-1} corresponded to a turnover number (k_{cat}) of 3 $x10^{-3}$ s^{-1} at saturating ATP concentrations, and a K_m of 175 μM (Fig 7B). The low k_{cat}/K_m values for Soj indicated that it was not an efficient ATP hydrolyzing enzyme. The low ATPase is consistent with the idea that Soj is not likely to provide energy to drive biological processes such as chromosome segregation.

Soj ATP binding and hydrolysis activities were similar to those of MinD from *E. coli*, which is the most extensively characterized MinD/Mrp family ATPase (Lutkenhaus, 2007). MinD can bind ATP, ADP and dATP, and it hydrolyzes ATP with a V_{max} of 62 pmol ATP $nmol^{-1}$ min^{-1} corresponding to a turnover number of 1 $x10^{-3}$ s^{-1} and a K_m of 40 μM (de Boer *et al.*, 1991). Although their ATPase activities are 3-fold different, Soj and MinD are similar and distinct from other WalkerAB ATPases that exhibit ATPase specific activities several orders of magnitude higher (Leipe *et al.*, 2002). To date no other ParA/Soj protein has been subject to a

detailed enzymatic analysis of its ATPase activity that would allow a comparison to the parameters calculated here.

The ATPase activity of SojG12V is similar to wild type Soj (Fig. 9). This result was unexpected and not predicted by the characterization of an equivalent mutant MinD/Mrp protein (Barilla *et al.*, 2005). This indicated that the loss of function phenotype observed for *B. subtilis* strains expressing SojG12V instead of wild type Soj was not due to loss of the ATPase activity of Soj. Protein sequence data indicate that the G12 residue of Soj is conserved in the MinD/Mrp family (Leipe *et al.*, 2002; Lutkenhaus and Sundaramoorthy, 2003). Structural data indicate that MinD/Mrp family proteins form sandwich dimers, where the ATP molecules bound by the Walker A motifs (P-loops) are in close proximity. The structures of dimers of NifH (Chiu *et al.*, 2001; Jang *et al.*, 2000; Jang *et al.*, 2004; Sarma *et al.*, 2007; Schmid *et al.*, 2002; Sen *et al.*, 2004; Sen *et al.*, 2006; Strop *et al.*, 2001), ArsA (Zhou *et al.*, 2000), δ protein (Pratto *et al.*, 2008), and *T. thermophilus* Soj (Leonard *et al.*, 2005) have been solved. In all these structures the residues equivalent to G12 of *B. subtilis* Soj are buried in the dimer interface and are at the closest points of contact between the two ATP binding motifs of the monomers.

The SojG12V mutant was constructed by another research group in the hope that it would be an equivalent mutation to a Ha-*ras* p21 mutant, because the valine residue is conserved in the Walker A motif in that protein (Quisel *et al.*, 1999). However Ha-ras p21 is a monomeric GTPase protein with a Walker A motif that is different from the motif in the Mrp/MinD family (Bhattacharya *et al.*, 2004; Leipe *et al.*, 2002). The equivalent G12V mutation in Ha-ras p21 does not abrogate GTP hydrolysis; rather, it renders the mutant protein insensitive to activation by GTPase activating proteins (Maegley *et al.*, 1996; Vogel *et al.*, 1988). However, it was assumed that the mutant was not able to hydrolyze ATP. The altered localization of SojG12V-GFP in *B. subtilis* was attributed to loss of this function (Quisel *et al.*, 1999). The equivalent *T. thermophilus* Soj mutant (SojG16V) has been briefly described, but no data were presented regarding its ATPase activity (Leonard *et al.*, 2005). The ATPase activity of ParF (a type Ib plasmid ParA) and a mutant of ParF (G11A, equivalent to G12V) indicated that the G11A mutation reduced ATPase activity (Barilla *et al.*, 2005). It is unclear why a decrease in ATPase activity was reported for this mutant, but the report also indicates that a mutation at an invariant lysine (K15Q) was ATPase proficient (Barilla *et al.*, 2005). The invariant lysine is required for proper binding of ATP to coordinate ATP hydrolysis in numerous Walker AB ATPases, so the ATPase activity of ParF K15Q contradicts a large body of data in the literature regarding WalkerAB ATPase proteins (Leipe *et al.*, 2002; Saraste *et al.*,

1990). This discrepancy has not been resolved. Data presented here indicate that SojG12V hydrolyzes ATP, so its altered characteristics *in vivo* are due to some other property of this mutant.

That SojD40A could bind, but not hydrolyze, ATP was expected (Fig. 8D, 9) (Leonard *et al.*, 2005). Protein sequence and structural data indicate that the aspartic acid residue in the equivalent position in the larger superfamily of GTPases is situated at the catalytic core of the protein and coordinates the Mg^{2+} cofactor required for hydrolysis (Leipe *et al.*, 2002).

The presence of ADP in Soj ATPase reactions had a small, negative impact on Soj ATPase, suggesting that Soj could bind ADP but that it had a higher affinity for ATP than ADP. A striking increase in ATPase activity resulting from the addition of either ATP or ADP during the purification of Soj was noted, although why ATP or ADP inclusion during the purification protocol impacted its ATPase activity is not well understood. This requirement has been noted in the purification of at least one other ParA/Soj protein (Easter and Gober, 2002).

3 Soj Dimerization and Multimerization.

Members of the MinD/Mrp superfamily of proteins, including Soj are usually reported to form nucleotide-dependent dimers (Leipe *et al.*, 2002). In my work size exclusion chromatography indicated that Soj forms dimers in the presence of either ATP or ADP (Fig. 13). There was no indication that either ADP or ATP differentially affected dimerization, and the majority of the protein in preparations used in this thesis was in the dimeric form (~75-80%). The monomer-dimer profiles obtained by size exclusion chromatography in the presence of ADP for SojG12V, and SojD40A were similar to those of wild type Soj (Fig. 13). Nucleotide exchange by Soj likely requires that the protein dissociate into monomers, as the nucleotide binding pocket of other Mrp/MinD family members is buried in the dimer interface. The structure of δ, a ParA protein from pSM19035, bound to Mg-ATPγS indicates that this protein could exchange nucleotide while the protein is a dimer as the nucleotide binding pockets are solvent exposed (Pratto *et al.*, 2008). Soj from *B. subtilis* has 25% sequence identity and 49% sequence similarity to the δ protein (compared to 50% sequence identity and 65% sequence similarity to Soj from *T. thermophilus*). More data are required to ascertain whether the nucleotide binding pockets of *B. subtilis* Soj are solvent exposed or not, and therefore if it can exchange bound nucleotide as a dimer or a monomer.

In the presence of ATP, the size exclusion chromatograms of wild type Soj, and SojD40A showed a peak eluting at lower volumes than the dimer form. For wild type Soj this larger species was observed as a shoulder on the dimer (Fig. 13). For SojD40A this larger species was the majority of the protein (76%). Estimation of the molecular weight from the elution of molecular weight standards indicated an approximate size of ~100 kDa for the larger Soj species. In both cases, these data suggest formation of species approximately the size of a Soj tetramer.

The apparent quaternary structure of Soj was not different in the presence of ATP versus ADP. This result is similar to those found with P1 ParA and δ from pSM19035 where the formation of dimers is equal in the presence of either ATP or ADP binding. However, this result contrasts to those found with Soj from *T. thermophilus*, and MinD from *E. coli,* where dimerization was observed to be ATP-dependent (Hu and Lutkenhaus, 2003; Leonard *et al.*, 2005). The recent publication by Hester and Lutkenhaus (2007) indicated that *B. subtilis* Soj dimerization was also ATP-dependent. Multiple experimental approaches throughout the course of my research (size exclusion chromatography shown here, and additional data not shown) showed that Soj preparations were a mixture of monomers and dimers. It is unclear why Hester and Lutkenhaus (2007) observed Soj dimers only in the presence of ATP. A possible explanation is that the ATP-dependent dimerization reported for Soj from *T. thermophilus* and *B. subtilis* was carried out with proteins that were not purified in the presence of nucleotides and this may have affected the behaviour of Soj in both cases.

Stabilization of a Soj dimers by ADP would be compatible with structural data from MinD/Mrp superfamily proteins. An important feature of the Mrp/MinD family is a universally conserved lysine (K11 in *B. subtilis* Soj), 5 residues N-terminal to the universal lysine responsible for ATP binding by all P-loop NTPases (Leipe *et al.*, 2002; Lutkenhaus and Sundaramoorthy, 2003). In the crystal structure of a NifH dimer (one of the family members) bound to ADP, the equivalent lysine makes intermonomer contacts to the β phosphate of ADP bound by the other monomer (Chiu *et al.*, 2001; Jang *et al.*, 2000; Jang *et al.*, 2004; Sarma *et al.*, 2007; Schmid *et al.*, 2002; Sen *et al.*, 2004; Sen *et al.*, 2006; Strop *et al.*, 2001). So it is possible that the K11 in Soj can stabilize a dimeric conformation while bound to ADP, as the β phosphate is still present as a ligand. The dimerization of NifH bound to ADP could also be a result of other determinants elsewhere on the dimer interface, which may also have parallels in *B. subtilis* Soj. What these determinants might be is difficult to identify as sequence alignment does not indicate any known dimerization motifs. The dimer of pSM19035 δ protein is

stabilized by interaction of a hydrophobic surface at the dimer interface that would be otherwise solvent exposed, and reciprocal inter-monomer salt bridges (Pratto *et al.*, 2008). The distribution of hydrophobic residues in the dimer interface of the *T. thermophilus* structure is similar to that of δ protein structure, and charged residues are absent throughout most of this interface. The sequence similarity between Soj from *T. thermophilus* and *B. subtilis* is high, especially for residues situated at the dimer interface. The dimerization of *B. subtilis* Soj-ADP could be stabilized by either hydrophobic interactions or inter monomer salt bridges.

4 DNA Binding by Soj.

DNA binding by Soj was demonstrated by EMSAs, sedimentation assays, and DNase protection assays. In all of the assays a strict ATP dependence was observed for the interaction of Soj with DNA. In EMSAs Soj was able to bind 24 bp, 100 bp, and 2.6 kb DNA (Fig. 15). The binding of Soj to DNA equal to or larger than 100 bp was cooperative. A model based on the structure of Soj from *T. thermophilus,* and protein residues involved in the DNA binding activity of *B. subtilis* Soj, predicts an approximate Soj DNA footprint of 20 bp based on the length of DNA that would be in close contact with the protein (Hester and Lutkenhaus, 2007). In this model the DNA-binding surface is formed only in the context of a Soj dimer, as the Soj monomer is not predicted to have structural motifs compatible with DNA binding.

Binding of Soj to 24 bp DNA was tested by EMSAs and gave rise to multiple species with different electrophoretic mobilities. The simplest explanation of the patterns is that one species corresponds to one Soj dimer bound to a 24 bp DNA, and the second species corresponds to two Soj dimers binding to each other, with either one or both dimers binding a separate DNA molecule.

EMSAs with 100 bp DNA fragments showed an unusual pattern; for each Soj input a single species of a specific electrophoretic mobility was resolved. The electrophoretic mobility of the single observed species changed as Soj input increased. If Soj dimers bound independently to DNA and multiple Soj dimers could bind to a single 100 bp DNA, the expected EMSA would show multiple electrophoretic species corresponding to the binding of 1-5 Soj dimers seen gradually shifting over increasing Soj inputs (100 bp DNA is expected to bind 3-5 Soj dimers given a 20-25 bp footprint). One explanation of these results is that in this assay, the different Soj-DNA species do not resolve due to similar electrophoretic mobilities (for example DNAs with 3, 4 and 5 Soj might have the same mobility for some reason) . Another

explanation is that binding of Soj dimers may not be independent. Soj binding could be highly cooperative, so that when a single Soj dimer binds to DNA another binds almost instantaneously so that Soj-DNA intermediates expected at a given Soj concentration are not observed. Another possibility is that Soj forms multiple higher order complexes in solution in a concentration dependent manner which can then bind DNA. At 2 μM Soj dimers might predominate in solution, therefore the DNA would be bound by Soj dimers. The doubling of Soj concentration could favour the formation of the next highest order Soj multimer. If that Soj multimer binds DNA with higher affinity than a Soj dimer, it out compete the dimer for DNA binding even though there are still dimers in solution. Eight μM Soj could favour the formation of the next higher order form, such as two interacting tetramers or a hexamer which could bind to DNA, which could out compete lower order Soj multimers by binding with a higher affinity resulting in the detection of only one electrophoretic species. Further tests of this hypothesis could be done by examining the DNA binding patterns at varying protein to DNA ratios.

Evidence supporting the binding of multiple Soj dimers (up to several hundred) to a single DNA molecule was obtained by low speed sedimentation of both Soj and DNA in the presence of ATP (Fig. 16). It is not likely that the binding of a single Soj dimer to DNA would result in plasmid DNA sedimentation at low centrifugal force. The finding that Soj and DNA could be sedimented from mixtures of Soj and DNA supported the binding of multiple Soj dimers to a single DNA molecule. DNA sedimentation was not a linear function of Soj input. Calculation of the amount of DNA bound (done by measuring loss of free DNA) versus Soj concentration indicated cooperativity in Soj binding by a Hill plot,

DNA binding by Soj was also followed using a DNase I protection assay (Fig. 17), and evidence for stepwise additions of Soj was obtained from DNase I cutting pattern. The size differences between adjacent DNA sizes indicated an approximate "footprint" of ~45 bp (Fig. 18). Given the structural prediction that 20 bp of DNA is closely associated with a Soj dimer (Hester and Lutkenhaus, 2007) this footprint could result from the binding of two Soj dimers to the DNA, either both at one end or one to each end of a cluster of Soj dimers. Evidence for tetramers was found in size exclusion chromatography (Fig. 13). Thus the possibly that Soj tetramers form in solution and bind to DNA directly should be further investigated.

Solutions containing Soj-ATP and DNA were found to scatter light. This technique appeared to be the most sensitive assay to detect Soj-DNA interactions. As light scattering was observed with a concentration of Soj as low as 1 μM; a DNA binding by Soj was not detected by other assays at this level of Soj input. SojG12V was not able to form light scattering

complexes with (Fig. 21). The other biochemical analyses indicated that SojG12V was specifically deficient in DNA binding, supporting the notion that the observed light scattering required ATP-dependent DNA binding.

The Soj-DNA complexes were examined by transmission electron microscopy. The resulting structures supported data which indicated Soj spreading on DNA. The varying diameters of Soj DNA structures suggested that areas covered by Soj might interact to form a "bridge". This bridging would form larger complexes, possibly those which scatter light as well as the complexes that can be pelleted at moderate g force.

5 A Model of Soj DNA Binding Leading to Light Scattering.

Binding of Soj to 24 bp DNA was observed in EMSAs (Fig. 15), but did not lead to light scattering in any condition assayed (Fig. 26). A 24 bp duplex DNA could accommodate the binding of one Soj dimer according to a structural model based on the structure of a *T. thermophilus* Soj dimer (Hester and Lutkenhaus, 2007). These data indicate that a population of Soj dimers bound to 24 bp DNA complexes cannot adopt a conformation required for light scattering. The approximate 45 bp Soj DNA "footprint" detected by DNase I assays (Figs. 17-18) would be consistent with two Soj dimers binding to a DNA either independently or as a tetramer that forms before DNA binding. Soj association with DNA, assayed by DNase I protection was interpreted to reflect Soj spreading (an initial random binding with additional Soj dimers bound to adjacent sites on the same DNA molecule). Since Soj bound to a 24 bp DNA did not scatter light, while Soj bound to the 100 bp DNA (that can bind multiple Soj dimers) did scatter light, it appears that multiple Soj dimers bound to the same DNA molecule are required for the formation of light scattering complexes. Logically, the formation of the complexes that scatter light might involve multiple sequential steps beginning with binding of a single Soj dimer to make an initial complex I (cI). In subsequent steps, additional Soj dimers bind the same DNA molecule cooperatively, resulting a higher order complex II (cII) on the same DNA molecule which would scatter light. The formation of cI and cII from Soj-ATP dimers and DNA equal to or larger than 100 bp is represented by reaction 1 and 2:

(Reaction 1) $Soj + DNA \rightleftharpoons cI$

(Reaction 2) $cI + (Soj)_n \rightleftharpoons cII$

The comparison between the light scattering patterns seen with the 24 bp and 100 bp DNA leads to the interpretation that for light scattering to occur Soj multimers must be bound to the same DNA molecule. A useful future experiment would be to assay DNA fragments between 24 bp and 100 bp in length for their ability to generate light scattering complexes when combined with Soj-ATP.

The idea that cII, which contains multiple Soj dimers is required for light scattering is consistent with results from experiments reported here. For example light scattering dependence on DNA concentration showed that both high and low concentrations of DNA decreased light scattering compared to the levels of light scattering at moderate DNA concentrations of 0.5 ng μl^{-1} (Fig. 24). As well, the presence of 24 bp DNA inhibited formation of light scattering structures on plasmid DNA. This suggests that at high concentrations, 24 bp DNA could compete for Soj dimers with complexes formed on larger molecules reducing formation of cII.

A model where cII itself caused light scattering may not entirely explain the results of the light scattering experiments where DNA of different lengths were tested (Fig. 25). The key observation was that the lag time (defined as the time before the light scattering increase began to be linear) decreased as the length of DNA added increased. There is no obvious reason for the lag if light scattering were measuring only the binding of Soj dimers onto individual DNAs to create a population of independent cII complexes.

The lag in light scattering could be explained by a model where cI and cII form as described by reaction 1 and 2 (see above), but an additional step, the interactions of cIIs is responsible for light scattering. These cII interactions could take place between cII formed on different DNA molecules (in the case of smaller DNA) or between cIIs formed on the same DNA molecule (in the case of longer DNAs). The absence of the lag when 2.6 kb DNA was used could result if cIIs formed on the same DNA molecule can fold back to interact. This

would be predicted to be a faster reaction than when the cIIs are on different DNAs since cII interactions are uni-molecular (therefore zero order and basically at infinite concentration) In essence the diffusion contribution to the rate of cII interaction has been eliminated.

These cII interactions are consistent with electron micrograph images of Soj and DNA where there appear to be structures of varying diameters. The cII interactions may bridge multiple Soj-DNA nucleoprotein resulting in larger diameter structures. Despite extensive searches of the literature, and requests for technical specifications from the manufacturer of the spectrophotometer used in these studies, I was unable to find the necessary specifications to provide an estimate for the minimum size of particle that would scatter light in my experiments. Such information would greatly improve our ability to interpret the light scattering results. At present the light scattering experiments presented here cannot separate changes in the structure of Soj bound to DNA in solution from an increase in the total number of Soj-DNA particles in solution. In spite of this deficiency, the technique was useful to probe the nucleotide requirements of Soj DNA interaction. More detailed electron micrographs and/or a more detailed optical characterization (i.e. dynamic light scattering, particle sizing) of Soj-DNA nucleoprotein will be needed to give a clearer indication of the interactions of Soj spread on DNA.

5.1 Insights from SojG12V and SojD40A for the Soj DNA Binding Model.

SojD40 and SojG12V both behave as partial loss of function mutants *in vivo*; however, *in vitro* each mutant exhibits a different defect compared to wild type Soj. SojD40A bound ATP, but was ATPase negative. Like wild type Soj, SojD40A formed dimers and multimers, and had ATP-dependent DNA binding activity. SojG12V ATPase was catalytically similar to wild type Soj, and was able to dimerize. However SojG12V, unlike Soj and SojD40A, did not show evidence of a tetrameric species in size exclusion chromatography, and was not able to bind DNA under any condition.

Since SojG12V and SojD40A mutants both bound ATP and formed dimers it appeared that dimerization was not sufficient for DNA binding. SojD40A, an ATPase deficient mutant, bound DNA; therefore, ATP hydrolysis was not required for the DNA binding activity of Soj. However, the effect of ATP on DNA binding showed that it was required for association with DNA. SojG12V was an active ATPase, was able to dimerize, but like Soj-ADP, SojG12V-ATP could not bind DNA. One way to interpret these results is that like a Soj-ADP dimer, a

SojG12V-ATP dimer was not able to adopt a conformation required for DNA binding. In this model ATP is an allosteric effector that modifies the shape of the Soj dimer to drive DNA binding.

The hypothesis of ATP as an allosteric effector of Soj is supported by structural evidence of such a shift in NifH, another member of the MinD/Mrp superfamily. When NifH is crystallized bound to ADP-tetrafluoroaluminate (AlF_4^-), which mimics the ATP bound state or the transition state of ATP hydrolysis, the Walker A motif (P-loop) of each subunit is ~4 Å apart. In contrast a ~10 Å distance separates the P-loops observed in the structure of the ADP-bound NifH dimer (Schindelin *et al.*, 1997). It is possible that such a conformational change could occur in Soj. The *B. subtilis* Soj G12 equivalent residue in *T. thermophilus* Soj and other Mrp/MinD structures is situated at the middle of the P-loop (Leipe *et al.*, 2002). It is possible that a valine at this position modifies the ATP-dependent conformation by causing a steric clash, so that SojG12V-ATP cannot bind DNA. Recent experiments that described ParA-ATP binding non-specifically to DNA were presented during the proceedings of the Canadian Society for Microbiology annual general meeting (B. Funnell *et al.*; Calgary, 2008). Data presented suggested that ParA-ATP adopts a conformation required for non-specific DNA binding not achieved by a ParA-ADP dimer. ParA-ADP binds specifically to the *parOP* site as a dimer through its N-terminal DNA binding motif (absent from Soj) and regulates *par* operon expression (Davey and Funnell, 1994).

6 Soj Interaction with Spo0J.

The ATPase activity of Soj was stimulated 1.7 fold by Spo0J, and 2.5 fold by Spo0J in combination with DNA. The ATPase stimulation in both conditions was determined to be statistically significant. Stimulation of Soj ATPase by Spo0J was increased by the presence of DNA. This result could be interpreted to indicate that either Soj bound to DNA is more sensitive to stimulation by Spo0J, or that Spo0J which is itself a DNA binding protein is a better ATPase stimulator of Soj when it is bound to DNA. Investigation of SojG12V ATPase stimulation by Spo0J indicated that Spo0J alone was not able to stimulate SojG12V ATPase activity. The addition of DNA to reactions containing SojG12V and Spo0J resulted in a 1.7 fold increase in Soj ATPase, which was also determined to be statistically significant. Since SojG12V cannot bind DNA but is otherwise unaffected in ATPase activity compared to Soj, it is

more likely that the effect of DNA is on the ability of Spo0J to stimulate the ATPase activity of Soj, rather than Soj bound to DNA being more sensitive to ATPase stimulation.

A feature of many MinD/Mrp family proteins is the modulation of their ATPase activity. Several cases have been studied where ATPase activity is stimulated by their cognate partner protein. For example, ATPase stimulation of plasmid encoded ParAs vary: plasmid P1 ParA ATPase is stimulated 9-10-fold by interaction with ParB-*parS* (Davis *et al.*, 1992); plasmid TP228 ParF ATPase is stimulated 13-fold by ParG (Barilla *et al.*, 2005); and plasmid pSM19035 δ protein ATPase is stimulated 3.4-fold by interaction with ω protein bound to *parS* (Pratto *et al.*, 2008). *E. coli* MinD bound to phospholipids vesicles ATPase is stimulated 9-fold upon interaction with MinE (Hu and Lutkenhaus, 2001; Lackner *et al.*, 2003). *H. pylori* Soj ATPase is stimulated 2-fold by interaction with Spo0J-*parS* (Lee *et al.*, 2006). *C. crescentus* ParA ATPase is stimulated 5-fold by ParB (Easter and Gober, 2002). However *C. crescentus* ParA and ParB are unusual in that stimulation of ParA is due to nucleotide exchange catalyzed by ParB (Easter and Gober, 2002).

The stimulation of the ATPase activity of plasmid ParA proteins is thought to be required for the segregation of replicated sister plasmids; however, the mechanism by which ParA ATPase promotes separation of plasmid DNA is unclear, and may differ among plasmids. In *E. coli* the ATPase stimulation of MinD by MinE is required to release MinD from the membrane so that it can oscillate between poles (Lutkenhaus, 2007). Stimulation of ParA in *C. crescentus* (which is by nucleotide exchange) is required to balance the intracellular levels of ParA-ATP and ParA-ADP, which are important for cell cycle progression, as high levels of ParA-ADP in cells depleted of ParB correlate with decreased growth and cell division (Easter and Gober, 2002; Figge *et al.*, 2003).

Mixing Soj and Spo0J led to formation of protein complexes that could be sedimented by low speed centrifugation. SDS-PAGE analysis of the supernatant and pellet fractions indicated that the sedimented protein was mostly Spo0J. The presence of ATP instead of ADP slightly increased the sedimentation of Spo0J, indicating that Soj-ATP interacted better with Spo0J to stimulate formation of Spo0J complexes. The presence of DNA did not affect the sedimentation of Spo0J complexes. A striking feature of the Soj-Spo0J interaction was the relative absence of Soj in the sedimented protein. The level of Soj in these pellet fractions was not above background observed with Soj alone or with Soj plus DNA and ADP (when Soj does not bind DNA). This indicates that Soj acted either as a nucleus for Spo0J complexes or that Soj was catalytic in formation of sedimentable Spo0J complexes.

The sedimentation of Soj-ATP after incubation with Spo0J and DNA was reduced by almost two fold compared to its sedimentation when incubated with DNA alone. One explanation of these results is that the interaction of Soj with Spo0J inhibits the binding of Soj to DNA, and the formation of Soj-DNA. Spo0J is also a DNA binding protein so it could compete with Soj for DNA binding. This possibility was not investigated as the sedimentation of DNA in these assays was not measured.

The formation of large structures containing Spo0J was also measured using light scattering mixtures containing Soj and Spo0J with either ATP or ADP. The formation of complexes that scattered light was immediate upon addition of Spo0J to Soj, and did not depend on whether ATP or ADP was present. However, the level of the increase in light scattering was higher in the presence of ATP compared to ADP. This agreed with the increased sedimentation of Spo0J in Soj-Spo0J experiments with ATP versus ADP, and indicates the stimulation of Spo0J multimer formation by Soj was favoured by the presence of ATP. SojG12V was able to interact with Spo0J and to stimulate the formation of light scattering structures to a similar extent as Soj. This result indicates that the block to DNA binding was not a block to interaction with Spo0J, and that the proposed ATP-induced conformational shift in Soj was not required for interaction of Soj and Spo0J.

Structures resulting from the interaction of Soj and Spo0J were examined by transmission electron microscopy. These structures were long and filamentous, composed of stacked layers or striations. These striations were similar in width to the estimated dimensions of a Spo0J dimer (Leonard *et al.*, 2004). Stacked layers were observed to branch from some of the larger filaments and rejoin other larger filamentous structures making bridges between the filaments. These filamentous structures were unique to reactions where Soj and Spo0J were incubated together before application to the EM grid, and were qualitatively different from Soj-DNA structures. The filamentous structures resulting from Soj-Spo0J interactions likely contained only small amounts of Soj, because Soj sedimentation was minimal after incubation with Spo0J.

7 Soj Interactions with Nucleotide, DNA, and Spo0J.

A diagram of Soj interactions with adenosine nucleotides, DNA and Spo0J shown in this thesis is presented in Fig. 35. Size exclusion chromatography indicates that Soj exists as both

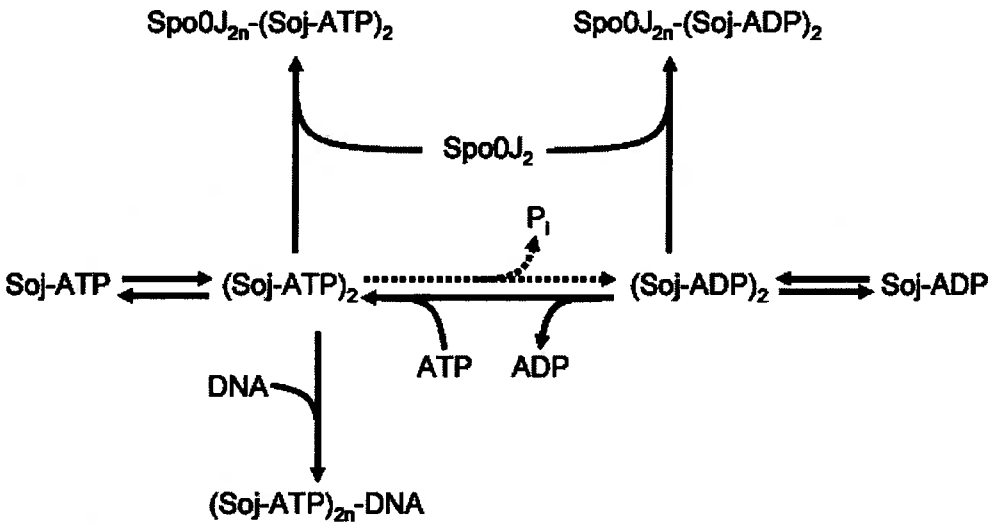

Fig. 35. Interaction of Soj with nucleotides, DNA, and Spo0J. Soj bound to either ATP or ADP exists as monomers (e.g. Soj-ATP) and dimers (e.g. $(Soj\text{-}ATP)_2$). Soj can exchange bound ADP for ATP. Multiple Soj-ATP dimers can bind to DNA to create Soj-DNA nucleoprotein complexes. Soj bound has a weak ATPase activity that can be stimulated by interaction with Spo0J (hatched line). Interaction of Soj with Spo0J results in the formation of multimeric Spo0J structures that likely contain small amounts of Soj (e.g. $Spo0J_{2n}\text{-}(Soj\text{-}ATP)_2$, where n are whole numbers to indicate Spo0J dimer multimers).

monomers and dimers bound to either ATP or ADP, but the majority of Soj are dimers. Soj has a weak ATPase activity similar to other MinD and ParA proteins. Soj-ATP dimers bind DNA and form multimeric structures on DNA. Spo0J stimulates the ATPase activity of Soj-ATP dimers (Fig. 35, dotted arrows). The interaction of Soj and Spo0J resulted in the formation of Spo0J multimers, but it is not known if the multimers of Spo0J stimulated by the presence of Soj were able to bind DNA because DNA sedimentation in those assays was not measured. The interaction of Soj-ADP with Spo0J also resulted in the formation of multimeric Spo0J filaments.

8 Relevance of Results to *In Vivo* Soj and Spo0J Data.

In wild type cells, Soj-GFP fusions are observed distributed at cell poles, division septa, or as foci of Soj in the cytosol (Murray and Errington, 2008; Quisel *et al.*, 1999). Only a small fraction of Soj-GFP in the wild type cell is associated with the chromosome. In Δ*spo0J* cells (spo$^-$), Soj is distributed on the chromosome indicating that when Soj is bound to the chromosome sporulation is inhibited. These results also indicate that the role of Spo0J in the antagonism of Soj could be to prevent association of Soj with chromosomal DNA either directly or indirectly. Spo0J could antagonize such association by stimulation of the ATPase activity of Soj (results presented here). Soj-ADP that would be released from the chromosome could exchange nucleotide to rebind ATP and either rebind the chromosome (only to be dissociated from DNA again by Spo0J) or associate with the cell poles. Association with the poles requires the cell contain the MinD protein but the mechanism for this requirement is not known. A polar distribution is observed for SojG12V but not SojK16A (cytosolic distribution) (Murray and Errington, 2008; Quisel *et al.*, 1999). Data in my thesis indicate that SojG12V is capable of binding ATP, and data in the literature indicate that SojK16A is likely unable to bind ATP. Therefore, it seems likely that polar distributed Soj is bound to ATP. Interactions of Soj-ATP with proteins (MinD) at the pole likely keep Soj-ATP from interacting with Spo0J or from binding the chromosome. Expression of SojG12V in a Δ*spo0J* background does not inhibit sporulation, which correlates to its failure to associate with the chromosome (Murray and Errington, 2008; Quisel *et al.*, 1999). Data presented here demonstrate that the failure of SojG12V to associate with the chromosome as observed *in vivo* could be due to a loss of DNA-binding activity that I propose requires a conformational change in Soj. Presumably localization of Soj at the poles of the cells *in vivo* does not require the conformational change induced by ATP.

Examination of cells which express SojD40A-GFP reveals fluorescent foci which co-localize with Spo0J when it is present, but are distributed on chromosomal DNA in a Δ*spo0J* background (Murray and Errington, 2008). These results are consistent with SojD40A being able to interact with both Spo0J and DNA as seen in the work reported here. Given the highly cooperative nature of Soj-ATP binding to DNA, the inability of SojD40A to hydrolyze ATP (demonstrated here) might result in SojD40A-ATP being trapped on the chromosome *in vivo*. This view is consistent with observations that SojD40A inhibits sporulation both in the presence and absence of Spo0J, and is distributed on the chromosome in a Δ*spo0J* background or colocalized with Spo0J-*parS* foci when Spo0J is present.

Finally I present a general model for Soj and Spo0J function in *B. subtilis*. This is based on the assumption that the primary role of Soj/Spo0J in *B. subtilis* is to negatively regulate initiation of sporulation rather than to carry out specific functions associated with vegetative DNA replication, segregation or cell division. One key finding from analysis of Soj-GFP distribution in various genetic backgrounds is that the inhibition of sporulation correlates with the distribution of Soj more or less evenly along the chromosome (Marston and Errington, 1999a; Quisel *et al.*, 1999). I have demonstrated in this work that Soj DNA-binding activity is modulated by its nucleotide-bound state. In order for Soj to bind the chromosome it must be in an ATP-bound state. The stimulation of Soj ATPase activity by Spo0J would shift the Soj nucleotide-bound state to be ADP-bound and loss of Spo0J *in vivo* would promote Soj association with DNA because the ATPase activity of Soj would be lower.

The association of Soj with DNA in a Δ*spo0J* background is associated with a decrease in the expression of stage II sporulation genes (Ireton *et al.*, 1994; Quisel *et al.*, 1999; Quisel and Grossman, 2000). Two possibilities exist for how this could happen. The first is that Soj could bind DNA at the stage II genes and directly repress transcription. Data which support this idea include the finding that Soj was found specifically associated with stage II sporulation gene promoters by chromosomal Soj immunoprecipitation experiments, and that this promoter-specific association was increased in a Δ*spo0J* background (Quisel *et al.*, 1999; Quisel and Grossman, 2000).

Data that support Soj acting directly as a repressor was presented here. I found that *in vitro,* Spo0A dependent transcription was more sensitive to Soj than Spo0A independent transcription (Fig. 19). In particular P*spoIIG18,* (a mutant of *PspoIIG*) was less sensitive to inhibition of transcription initiation compared to P*spoIIG* (Fig. 15). Sensitivity of *PspoIIG* to Soj was not likely due to Soj binding a specific P*spoIIG* sequence because P*spoIIG18* was so

similar to P*spoIIG*. The increased sensitivity of P*spoIIG* could be explained if Soj DNA binding interfered with Spo0A~P DNA binding. Soj could also interact with Spo0A~P on or off DNA to inhibit Spo0A~P- RNAP. Sequence-specific binding of Soj to DNA was not observed in any of my experiments so that although Soj inhibited P*spoIIG* transcription at a lower concentration than from the control promoters, a more detailed analysis of why this was observed is still required.

The second possibility for how Soj inhibits sporulation is that Soj acts indirectly to affect Spo0A~P levels and therefore sporulation-specific transcription. Support for this possibility comes from recent observations which indicate that in Δ*spo0J* strains, an additional mutation in *sda* rescues sporulation (spo+) (Murray and Errington, 2008). This finding implies Soj and Sda are part of the same regulatory pathway. Sda has been shown to inhibit KinA and likely KinB autophosphorylation directly (Rowland *et al.*, 2004; Whitten *et al.*, 2007). Sda therefore would reduce the concentrations of Spo0A~P in the cell and decrease expression of stage II sporulation genes that depend on Spo0A~P.

Sporulation is transiently blocked during artificial replicative stress (UV irradiation, elongation inhibition, mutations in replication initiation proteins) and this blockage requires Sda (Burkholder *et al.*, 2001; Ruvolo *et al.*, 2006). In wild type cells under these stress conditions, *sda* transcription increases and Sda protein levels in the cell increase transiently, later decreasing due to proteolysis. *Sda* gene expression is positively regulated by DnaA (Ishikawa *et al.*, 2007). DnaA-ATP binds to specific DNA sequences termed DnaA boxes and promotes initiation of replication (Moriya *et al.*, 1988). A DnaA box is found in the promoter region of *sda* and co-immunoprecipitation experiments have detected DnaA-ATP binding to the *sda* promoter. Several studies have suggested that transcription from *sda* changes when DnaA levels in the cell are altered. In the report describing that a *sda* deletion rescues the spo$^-$ phenotype of a Δ*spo0J* strain, the authors also presented data which suggested a direct interaction between DnaA and Soj (Murray and Errington, 2008). The authors also suggested that this interaction could alter DnaA-dependent replication initiation at *oriC*. These interesting results leave unanswered how Soj could impact DnaA function at *oriC* and how this interaction influences expression of *sda*.

In a Δ*spo0J* strain (spo$^-$), Soj-GFP is found spread along the chromosome and replication increases as measured by an increase in the ratio of origins to termini (Lee and Grossman, 2006; Murray and Errington, 2008; Ogura *et al.*, 2003). *In vivo* SojD40A-GFP is primarily associated with Spo0J (which is itself associated with the chromosome), and to a lesser extent with the chromosome. In a Δ*spo0J* background SojD40A-GFP associates evenly

with the chromosome, sporulation is inhibited, and the cell contains an increase in the number of origins relative to the wild type. These data would be consistent with Soj acting as a positive regulator of replication initiation when bound to the chromosome. However increased replication initiation is also observed in Δ*soj* and Δ*(soj-spo0J)* mutants, arguing against Soj acting as a positive regulator of replication initiation. One way to explain these conflicting data is that Soj negatively regulates DnaA, but when Soj is spread along the chromosome, the negative effects are prevented. Obviously in a Δ*soj* strain negative regulation of DnaA by Soj would be lost. Both Δ*soj* and Δ*(soj-spo0J)* lead to increased initiation of DNA replication (Lee and Grossman, 2006; Murray and Errington, 2008; Ogura *et al.*, 2003). The increased replication initiation in a Δ*spo0J* background, and in cells expressing SojD40A is accompanied by inhibition of sporulation that depends on Sda. In contrast, in Δ*soj* or Δ(*soj-spo0J*) strains the increase in replication initiation happens without inhibiting sporulation, indicating that Sda is not activated. This could indicate that Soj is required for expression of Sda, possibly in cooperation with DnaA.

Despite the logic of the argument above, there are data in the literature that are not consistent with Soj acting to alter sporulation gene expression through Sda. One study indicated that the deletion of *spo0J* does not affect the phosphorylation of Spo0A based on analysis of *abrB* repression and *spo0A* induction during stationary phase and sporulation (Cervin *et al.*, 1998). Both *abrB* repression and *spo0A* activation require Spo0A~P; however, there was little difference in *abrB* repression or *spo0A* induction during stationary phase between *Δspo0J* and wild type cultures. If Sda were activated, then the phosphate flow to Spo0A should be reduced which should be reflected in *abrB* and *spo0A* expression. Further investigation of this discrepancy is required.

The two possibilities for how Soj inhibits sporulation in the absence of Spo0J need not be exclusive. Soj could both affect Spo0A~P levels through the phosphorelay by activation of Sda, and independently repress the transcription of stage II genes. If the role of Soj is to inhibit sporulation quickly, this could happen more efficiently if Soj both repressed gene transcription and prevented Spo0A phosphorylation. Both possibilities for how Soj inhibits expression of stage II genes and inhibit sporulation merit further investigation to uncover specific mechanisms.

The number of Soj molecules per cell has not been experimentally determined. It is not clear how many Soj dimers bound to chromosomal DNA *in vivo* would create nucleoprotein structures that could affect the initiation of sporulation. The cooperative nature of DNA binding

and formation of Soj nucleoprotein presented herein indicate that even several hundred copies of Soj bound to the chromosome might impact chromosome structure by the formation of Soj nucleoprotein.

DNA replication in a Δ*soj* or Δ(*soj-spo0J*) mutants is not altered to the point where sporulation cannot proceed, which indicates that control over replication initiation is not the primary role of Soj and Spo0J. When *B. subtilis* exits vegetative growth it must ensure that replication is coordinated so that both the forespore and mother cell receive a full chromosome upon sporulation. More than 35 years ago it was proposed that the replication status of the chromosome affects sporulation (Mandelstam *et al.*, 1971; Mandelstam and Higgs, 1974). Researchers postulated a window of time following replication initiation in which initiation of sporulation is negatively regulated so that *B. subtilis* does not sporulate with the improper genetic content. After that window of time, the status of chromosome replication is compatible with sporulation until a new round of DNA replication is initiated and sporulation is again inhibited. Upon replication initiation (controlled by DnaA) the signal that transmits inhibition of sporulation must be transient so that the cell can resume its capacity to sporulate as its genetic content reaches the requirement of two full chromosomes. Sda could provide such a signal.

The negative regulation of sporulation by Soj requires Sda, and current data suggest that Soj could affect Sda through its interaction with DnaA. It is not clear what state of Soj associates with DnaA but it likely depends on the nucleotide bound to Soj. Given the possibility that Soj-ATP binds the chromosome and does not inhibit DnaA activity, it is tempting to propose that Soj-ADP interacts with DnaA to inhibit replication. The level of Soj-ADP in the cell is critically regulated by the activity of Spo0J which can stimulate the ATPase of Soj. Signals which control Spo0J activity are unclear, but identification of such a signal would be an important contribution to understanding the complex mechanism of how chromosome replication and sporulation initiation are properly timed.

9 The Role of Chromosomal Par Proteins in Bacteria.

A striking feature of ParA and ParB systems is the diversity in function and contribution to cell physiology among bacterial species. The Par system of *C. crescentus* is unique among bacteria because both Par proteins are essential (Easter and Gober, 2002; Figge *et al.*, 2003; Mohl and Gober, 1997; Mohl *et al.*, 2001). Depletion of either causes a division defect which results in filamentation. This indicates that in *C. crescentus* both Par proteins are required for

productive cell division. It is worth noting that cell division is a developmental process in this organism and like sporulation in *B. subtilis* results in the production of two cell types (Laub *et al.*, 2007). In *S. coelicolor* ParA and ParB are not essential genes, but do affect an aspect of coordinating spore compartment septation and chromosome segregation (Jakimowicz *et al.*, 2007b). Unlike *B. subtilis* and *C. crescentus,* development of *S. coelicolor* can proceed when the Par system is mutated.

The only other bacterial species aside from *C. crescentus* where a Par protein has been suggested to be essential is *V. cholerae*. The *parB* gene encoded on the large chromosome has not been successfully deleted despite reported attempts (Saint-Dic *et al.*, 2006). This indicates that the role of ParB in this organism is indispensable for vegetative growth. *V. cholerae* reproduces by binary fission and does not engage in a developmental process, so Par function in this species is unlike that of *C. crescentus* and *B. subtilis*.

The literature indicates that chromosomal Par protein systems have been adapted to perform different functions associated with the chromosome in different cells. Further research will be needed to illuminate how these common systems are used in individual bacterial species to suit the particular niche in which a bacterial species survives.

REFERENCES

Abramoff, M., Magelhaes, P., and Ram, S. (2004) Image Processing with ImageJ. *Biophotonics International* **11**: 36-42.

Allen, R.M., Homer, M.J., Chatterjee, R., Ludden, P.W., Roberts, G.P., and Shah, V.K. (1993) Dinitrogenase reductase- and MgATP-dependent maturation of apodinitrogenase from *Azotobacter vinelandii*. *J Biol Chem* **268**: 23670-23674.

Arigoni, F., Duncan, L., Alper, S., Losick, R., and Stragier, P. (1996) SpoIIE governs the phosphorylation state of a protein regulating transcription factor sigma F during sporulation in *Bacillus subtilis*. *Proc Natl Acad Sci U S A* **93**: 3238-3242.

Austin, S., and Abeles, A. (1983) Partition of unit-copy miniplasmids to daughter cells. II. The partition region of miniplasmid P1 encodes an essential protein and a centromere-like site at which it acts. *J Mol Biol* **169**: 373-387.

Austin, S., and Wierzbicki, A. (1983) Two mini-F-encoded proteins are essential for equipartition. *Plasmid* **10**: 73-81.

Autret, S., Nair, R., and Errington, J. (2001) Genetic analysis of the chromosome segregation protein Spo0J of *Bacillus subtilis*: evidence for separate domains involved in DNA binding and interactions with Soj protein. *Mol Microbiol* **41**: 743-755.

Autret, S., and Errington, J. (2003) A role for division-site-selection protein MinD in regulation of internucleoid jumping of Soj (ParA) protein in *Bacillus subtilis*. *Mol Microbiol* **47**: 159-169.

Barilla, D., Rosenberg, M.F., Nobbmann, U., and Hayes, F. (2005) Bacterial DNA segregation dynamics mediated by the polymerizing protein ParF. *EMBO J* **24**: 1453-1464.

Bartosik, A.A., Lasocki, K., Mierzejewska, J., Thomas, C.M., and Jagura-Burdzy, G. (2004) ParB of *Pseudomonas aeruginosa*: interactions with its partner ParA and its target parS and specific effects on bacterial growth. *J Bacteriol* **186**: 6983-6998.

Bhattacharya, M., Babwah, A.V., and Ferguson, S.S. (2004) Small GTP-binding protein-coupled receptors. *Biochem Soc Trans* **32**: 1040-1044.

Bignell, C., and Thomas, C.M. (2001) The bacterial ParA-ParB partitioning proteins. *J Biotechnol* **91**: 1-34.

Bork, P., Sander, C., and Valencia, A. (1992) An ATPase domain common to prokaryotic cell cycle proteins, sugar kinases, actin, and hsp70 heat shock proteins. *Proc Natl Acad Sci U S A* **89**: 7290-7294.

Bouet, J.Y., and Funnell, B.E. (1999) P1 ParA interacts with the P1 partition complex at parS and an ATP-ADP switch controls ParA activities. *EMBO J* **18**: 1415-1424.

Bouet, J.Y., Ah-Seng, Y., Benmeradi, N., and Lane, D. (2007) Polymerization of SopA partition ATPase: regulation by DNA binding and SopB. *Mol Microbiol* **63**: 468-481.

Britton, R.A., Lin, D.C., and Grossman, A.D. (1998) Characterization of a prokaryotic SMC protein involved in chromosome partitioning. *Genes Dev* **12**: 1254-1259.

Broder, D.H., and Pogliano, K. (2006) Forespore engulfment mediated by a ratchet-like mechanism. *Cell* **126**: 917-928.

Burgess, B.K., and Lowe, D.J. (1996) Mechanism of Molybdenum Nitrogenase. *Chem Rev* **96**: 2983-3012.

Burkholder, W.F., Kurtser, I., and Grossman, A.D. (2001) Replication initiation proteins regulate a developmental checkpoint in *Bacillus subtilis*. *Cell* **104**: 269-279.

Burton, B.M., Marquis, K.A., Sullivan, N.L., Rapoport, T.A., and Rudner, D.Z. (2007) The ATPase SpoIIIE transports DNA across fused septal membranes during sporulation in *Bacillus subtilis*. *Cell* **131**: 1301-1312.

Cervin, M.A., Spiegelman, G.B., Raether, B., Ohlsen, K., Perego, M., and Hoch, J.A. (1998) A negative regulator linking chromosome segregation to developmental transcription in *Bacillus subtilis*. *Mol Microbiol* **29**: 85-95.

Chater, K.F. (2001) Regulation of sporulation in *Streptomyces coelicolor* A3(2): a checkpoint multiplex? *Curr Opin Microbiol* **4**: 667-673.

Chiu, H., Peters, J.W., Lanzilotta, W.N., Ryle, M.J., Seefeldt, L.C., Howard, J.B., and Rees, D.C. (2001) MgATP-Bound and nucleotide-free structures of a nitrogenase protein complex between the Leu 127 Delta-Fe-protein and the MoFe-protein. *Biochemistry* **40**: 641-650.

Claessen, D., de Jong, W., Dijkhuizen, L., and Wosten, H.A. (2006) Regulation of *Streptomyces* development: reach for the sky! *Trends Microbiol* **14**: 313-319.

Clarke, S., and Mandelstam, J. (1987) Regulation of stage II of sporulation in *Bacillus subtilis*. *J Gen Microbiol* **133**: 2371-2380.

Claverys, J.P., Prudhomme, M., and Martin, B. (2006) Induction of competence regulons as a general response to stress in gram-positive bacteria. *Annu Rev Microbiol* **60**: 451-475.

Cordell, S.C., and Lowe, J. (2001) Crystal structure of the bacterial cell division regulator MinD. *FEBS Lett* **492**: 160-165.

Daniel, R.A., Noirot-Gros, M.F., Noirot, P., and Errington, J. (2006) Multiple interactions between the transmembrane division proteins of *Bacillus subtilis* and the role of FtsL instability in divisome assembly. *J Bacteriol* **188**: 7396-7404.

Davey, M.J., and Funnell, B.E. (1994) The P1 plasmid partition protein ParA. A role for ATP in site-specific DNA binding. *J Biol Chem* **269**: 29908-29913.

Davis, M.A., Martin, K.A., and Austin, S.J. (1992) Biochemical activities of the parA partition protein of the P1 plasmid. *Mol Microbiol* **6**: 1141-1147.

de Boer, P.A., Crossley, R.E., and Rothfield, L.I. (1989) A division inhibitor and a topological specificity factor coded for by the minicell locus determine proper placement of the division septum in *E. coli*. *Cell* **56**: 641-649.

de Boer, P.A., Crossley, R.E., Hand, A.R., and Rothfield, L.I. (1991) The MinD protein is a membrane ATPase required for the correct placement of the *Escherichia coli* division site. *Embo J* **10**: 4371-4380.

Dmowski, M., Sitkiewicz, I., and Ceglowski, P. (2006) Characterization of a novel partition system encoded by the delta and omega genes from the streptococcal plasmid pSM19035. *J Bacteriol* **188**: 4362-4372.

Easter, J., Jr., and Gober, J.W. (2002) ParB-stimulated nucleotide exchange regulates a switch in functionally distinct ParA activities. *Mol Cell* **10**: 427-434.

Ebersbach, G., and Gerdes, K. (2005) Plasmid segregation mechanisms. *Annu Rev Genet* **39**: 453-479.

Edgar, R., Biek, D., and Yarmolinsky, M. (2006) P1 plasmid partition: in vivo evidence for the ParA- and ParB-mediated formation of an anchored parS complex in the absence of a partner parS. *Mol Microbiol* **59**: 276-287.

Edwards, D.H., and Errington, J. (1997) The *Bacillus subtilis* DivIVA protein targets to the division septum and controls the site specificity of cell division. *Mol Microbiol* **24**: 905-915.

Erdmann, N., Petroff, T., and Funnell, B.E. (1999) Intracellular localization of P1 ParB protein depends on ParA and parS. *Proc Natl Acad Sci U S A* **96**: 14905-14910.

Errington, J. (1993) *Bacillus subtilis* sporulation: regulation of gene expression and control of morphogenesis. *Microbiol Rev* **57**: 1-33.

Errington, J. (2003) Regulation of endospore formation in *Bacillus subtilis*. *Nat Rev Microbiol* **1**: 117-126.

Figge, R.M., Easter, J., and Gober, J.W. (2003) Productive interaction between the chromosome partitioning proteins, ParA and ParB, is required for the progression of the cell cycle in *Caulobacter crescentus*. *Mol Microbiol* **47**: 1225-1237.

Funnell, B.E. (1988) Mini-P1 plasmid partitioning: excess ParB protein destabilizes plasmids containing the centromere parS. *J Bacteriol* **170**: 954-960.

Garner, E.C., Campbell, C.S., Weibel, D.B., and Mullins, R.D. (2007) Reconstitution of DNA segregation driven by assembly of a prokaryotic actin homolog. *Science* **315**: 1270-1274.

Gerdes, K., Moller-Jensen, J., and Bugge Jensen, R. (2000) Plasmid and chromosome partitioning: surprises from phylogeny. *Mol Microbiol* **37**: 455-466.

Glaser, P., Sharpe, M.E., Raether, B., Perego, M., Ohlsen, K., and Errington, J. (1997) Dynamic, mitotic-like behavior of a bacterial protein required for accurate chromosome partitioning. *Genes Dev* **11**: 1160-1168.

Godfrin-Estevenon, A.M., Pasta, F., and Lane, D. (2002) The parAB gene products of *Pseudomonas putida* exhibit partition activity in both *P. putida* and *Escherichia coli*. *Mol Microbiol* **43**: 39-49.

Greene, E.A., and Spiegelman, G.B. (1996) The Spo0A protein of *Bacillus subtilis* inhibits transcription of the abrB gene without preventing binding of the polymerase to the promoter. *J Biol Chem* **271**: 11455-11461.

Guex, N., and Peitsch, M.C. (1997) SWISS-MODEL and the Swiss-PdbViewer: an environment for comparative protein modeling. *Electrophoresis* **18**: 2714-2723.

Hamoen, L.W., Venema, G., and Kuipers, O.P. (2003) Controlling competence in *Bacillus subtilis*: shared use of regulators. *Microbiology* **149**: 9-17.

Handke, L.D., Shivers, R.P., and Sonenshein, A.L. (2008) Interaction of *Bacillus subtilis* CodY with GTP. *J Bacteriol* **190**: 798-806.

Hatano, T., Yamaichi, Y., and Niki, H. (2007) Oscillating focus of SopA associated with filamentous structure guides partitioning of F plasmid. *Mol Microbiol* **64**: 1198-1213.

Hayashi, I., Oyama, T., and Morikawa, K. (2001) Structural and functional studies of MinD ATPase: implications for the molecular recognition of the bacterial cell division apparatus. *EMBO J* **20**: 1819-1828.

Henriques, A.O., and Moran, C.P., Jr. (2007) Structure, assembly, and function of the spore surface layers. *Annu Rev Microbiol* **61**: 555-588.

Hester, C.M., and Lutkenhaus, J. (2007) Soj (ParA) DNA binding is mediated by conserved arginines and is essential for plasmid segregation. *Proc Natl Acad Sci U S A* **104**: 20326-20331.

Hilbert, D.W., and Piggot, P.J. (2004) Compartmentalization of gene expression during *Bacillus subtilis* spore formation. *Microbiol Mol Biol Rev* **68**: 234-262.

Hirano, M., Mori, H., Onogi, T., Yamazoe, M., Niki, H., Ogura, T., and Hiraga, S. (1998) Autoregulation of the partition genes of the mini-F plasmid and the intracellular localization of their products in *Escherichia coli*. *Mol Gen Genet* **257**: 392-403.

Howard, K.S., McLean, P.A., Hansen, F.B., Lemley, P.V., Koblan, K.S., and Orme-Johnson, W.H. (1986) Klebsiella pneumoniae nifM gene product is required for stabilization and activation of nitrogenase iron protein in *Escherichia coli*. *J Biol Chem* **261**: 772-778.

Hu, Z., and Lutkenhaus, J. (2001) Topological regulation of cell division in *E. coli*. spatiotemporal oscillation of MinD requires stimulation of its ATPase by MinE and phospholipid. *Mol Cell* **7**: 1337-1343.

Hu, Z., Gogol, E.P., and Lutkenhaus, J. (2002) Dynamic assembly of MinD on phospholipid vesicles regulated by ATP and MinE. *Proc Natl Acad Sci U S A* **99**: 6761-6766.

Hu, Z., and Lutkenhaus, J. (2003) A conserved sequence at the C-terminus of MinD is required for binding to the membrane and targeting MinC to the septum. *Mol Microbiol* **47**: 345-355.

Ireton, K., Gunther, N.W.t., and Grossman, A.D. (1994) spo0J is required for normal chromosome segregation as well as the initiation of sporulation in *Bacillus subtilis*. *J Bacteriol* **176**: 5320-5329.

Ishikawa, S., Core, L., and Perego, M. (2002) Biochemical characterization of aspartyl phosphate phosphatase interaction with a phosphorylated response regulator and its inhibition by a pentapeptide. *J Biol Chem* **277**: 20483-20489.

Ishikawa, S., Ogura, Y., Yoshimura, M., Okumura, H., Cho, E., Kawai, Y., Kurokawa, K., Oshima, T., and Ogasawara, N. (2007) Distribution of stable DnaA-binding sites on the *Bacillus subtilis* genome detected using a modified ChIP-chip method. *DNA Res* **14**: 155-168.

Jakimowicz, D., Chater, K., and Zakrzewska-Czerwinska, J. (2002) The ParB protein of *Streptomyces coelicolor* A3(2) recognizes a cluster of parS sequences within the origin-proximal region of the linear chromosome. *Mol Microbiol* **45**: 1365-1377.

Jakimowicz, D., Gust, B., Zakrzewska-Czerwinska, J., and Chater, K.F. (2005) Developmental-stage-specific assembly of ParB complexes in *Streptomyces coelicolor* hyphae. *J Bacteriol* **187**: 3572-3580.

Jakimowicz, D., Mouz, S., Zakrzewska-Czerwinska, J., and Chater, K.F. (2006) Developmental control of a parAB promoter leads to formation of sporulation-associated ParB complexes in *Streptomyces coelicolor*. *J Bacteriol* **188**: 1710-1720.

Jakimowicz, D., Brzostek, A., Rumijowska-Galewicz, A., Zydek, P., Dolzblasz, A., Smulczyk-Krawczyszyn, A., Zimniak, T., Wojtasz, L., Zawilak-Pawlik, A., Kois, A., Dziadek, J., and Zakrzewska-Czerwinska, J. (2007a) Characterization of the mycobacterial chromosome segregation protein ParB and identification of its target in *Mycobacterium smegmatis*. *Microbiology* **153**: 4050-4060.

Jakimowicz, D., Zydek, P., Kois, A., Zakrzewska-Czerwinska, J., and Chater, K.F. (2007b) Alignment of multiple chromosomes along helical ParA scaffolding in sporulating *Streptomyces* hyphae. *Mol Microbiol* **65**: 625-641.

Jang, S.B., Seefeldt, L.C., and Peters, J.W. (2000) Insights into nucleotide signal transduction in nitrogenase: structure of an iron protein with MgADP bound. *Biochemistry* **39**: 14745-14752.

Jang, S.B., Jeong, M.S., Seefeldt, L.C., and Peters, J.W. (2004) Structural and biochemical implications of single amino acid substitutions in the nucleotide-dependent switch regions of the nitrogenase Fe protein from *Azotobacter vinelandii*. *J Biol Inorg Chem* **9**: 1028-1033.

Jiang, M., Shao, W., Perego, M., and Hoch, J.A. (2000) Multiple histidine kinases regulate entry into stationary phase and sporulation in *Bacillus subtilis*. *Mol Microbiol* **38**: 535-542.

Kim, H.J., Calcutt, M.J., Schmidt, F.J., and Chater, K.F. (2000) Partitioning of the linear chromosome during sporulation of *Streptomyces coelicolor* A3(2) involves an oriC-linked parAB locus. *J Bacteriol* **182**: 1313-1320.

Koonin, E.V. (1993) A superfamily of ATPases with diverse functions containing either classical or deviant ATP-binding motif. *J Mol Biol* **229**: 1165-1174.

Koonin, E.V., Wolf, Y.I., and Aravind, L. (2000) Protein fold recognition using sequence profiles and its application in structural genomics. *Adv Protein Chem* **54**: 245-275.

Kroos, L., Zhang, B., Ichikawa, H., and Yu, Y.T. (1999) Control of sigma factor activity during *Bacillus subtilis* sporulation. *Mol Microbiol* **31**: 1285-1294.

Lackner, L.L., Raskin, D.M., and de Boer, P.A. (2003) ATP-dependent interactions between *Escherichia coli* Min proteins and the phospholipid membrane in vitro. *J Bacteriol* **185**: 735-749.

Lasocki, K., Bartosik, A.A., Mierzejewska, J., Thomas, C.M., and Jagura-Burdzy, G. (2007) Deletion of the parA (soj) homologue in *Pseudomonas aeruginosa* causes ParB instability and affects growth rate, chromosome segregation, and motility. *J Bacteriol* **189**: 5762-5772.

Laub, M.T., Shapiro, L., and McAdams, H.H. (2007) Systems biology of *Caulobacter*. *Annu Rev Genet* **41**: 429-441.

Lee, M.J., Liu, C.H., Wang, S.Y., Huang, C.T., and Huang, H. (2006) Characterization of the Soj/Spo0J chromosome segregation proteins and identification of putative parS sequences in *Helicobacter pylori*. *Biochem Biophys Res Commun* **342**: 744-750.

Lee, P.S., Lin, D.C., Moriya, S., and Grossman, A.D. (2003) Effects of the chromosome partitioning protein Spo0J (ParB) on oriC positioning and replication initiation in *Bacillus subtilis*. *J Bacteriol* **185**: 1326-1337.

Lee, P.S., and Grossman, A.D. (2006) The chromosome partitioning proteins Soj (ParA) and Spo0J (ParB) contribute to accurate chromosome partitioning, separation of replicated sister origins, and regulation of replication initiation in *Bacillus subtilis*. *Mol Microbiol* **60**: 853-869.

Lee, S., and Price, C.W. (1993) The minCD locus of *Bacillus subtilis* lacks the minE determinant that provides topological specificity to cell division. *Mol Microbiol* **7**: 601-610.

Leipe, D.D., Wolf, Y.I., Koonin, E.V., and Aravind, L. (2002) Classification and evolution of P-loop GTPases and related ATPases. *J Mol Biol* **317**: 41-72.

Leonard, T.A., Butler, P.J., and Lowe, J. (2004) Structural analysis of the chromosome segregation protein Spo0J from *Thermus thermophilus*. *Mol Microbiol* **53**: 419-432.

Leonard, T.A., Butler, P.J., and Lowe, J. (2005) Bacterial chromosome segregation: structure and DNA binding of the Soj dimer--a conserved biological switch. *EMBO J* **24**: 270-282.

Lewis, K. (2000) Programmed death in bacteria. *Microbiol Mol Biol Rev* **64**: 503-514.

Lewis, R.A., Bignell, C.R., Zeng, W., Jones, A.C., and Thomas, C.M. (2002) Chromosome loss from par mutants of *Pseudomonas putida* depends on growth medium and phase of growth. *Microbiology* **148**: 537-548.

Li, Y., Dabrazhynetskaya, A., Youngren, B., and Austin, S. (2004) The role of Par proteins in the active segregation of the P1 plasmid. *Mol Microbiol* **53**: 93-102.

Lin, D.C., Levin, P.A., and Grossman, A.D. (1997) Bipolar localization of a chromosome partition protein in *Bacillus subtilis*. *Proc Natl Acad Sci U S A* **94**: 4721-4726.

Lin, D.C., and Grossman, A.D. (1998) Identification and characterization of a bacterial chromosome partitioning site. *Cell* **92**: 675-685.

Lutkenhaus, J., and Sundaramoorthy, M. (2003) MinD and role of the deviant Walker A motif, dimerization and membrane binding in oscillation. *Mol Microbiol* **48**: 295-303.

Lutkenhaus, J. (2007) Assembly dynamics of the bacterial MinCDE system and spatial regulation of the Z ring. *Annu Rev Biochem* **76**: 539-562.

Maegley, K.A., Admiraal, S.J., and Herschlag, D. (1996) Ras-catalyzed hydrolysis of GTP: a new perspective from model studies. *Proc Natl Acad Sci U S A* **93**: 8160-8166.

Mandelstam, J., Sterlini, J.M., and Kay, D. (1971) Sporulation in *Bacillus subtilis*. Effect of medium on the form of chromosome replication and on initiation to sporulation in *Bacillus subtilis*. *Biochem J* **125**: 635-641.

Mandelstam, J., and Higgs, S.A. (1974) Induction of sporulation during synchronized chromosome replication in *Bacillus subtilis*. *J Bacteriol* **120**: 38-42.
Margolin, W. (2005) FtsZ and the division of prokaryotic cells and organelles. *Nat Rev Mol Cell Biol* **6**: 862-871.
Marston, A.L., Thomaides, H.B., Edwards, D.H., Sharpe, M.E., and Errington, J. (1998) Polar localization of the MinD protein of *Bacillus subtilis* and its role in selection of the mid-cell division site. *Genes Dev* **12**: 3419-3430.
Marston, A.L., and Errington, J. (1999a) Dynamic movement of the ParA-like Soj protein of B. subtilis and its dual role in nucleoid organization and developmental regulation. *Mol Cell* **4**: 673-682.
Marston, A.L., and Errington, J. (1999b) Selection of the midcell division site in *Bacillus subtilis* through MinD-dependent polar localization and activation of MinC. *Mol Microbiol* **33**: 84-96.
Milner-White, E.J., Coggins, J.R., and Anton, I.A. (1991) Evidence for an ancestral core structure in nucleotide-binding proteins with the type A motif. *J Mol Biol* **221**: 751-754.
Mohl, D.A., and Gober, J.W. (1997) Cell cycle-dependent polar localization of chromosome partitioning proteins in *Caulobacter crescentus*. *Cell* **88**: 675-684.
Mohl, D.A., Easter, J., Jr., and Gober, J.W. (2001) The chromosome partitioning protein, ParB, is required for cytokinesis in *Caulobacter crescentus*. *Mol Microbiol* **42**: 741-755.
Moir, A. (2006) How do spores germinate? *J Appl Microbiol* **101**: 526-530.
Molle, V., Fujita, M., Jensen, S.T., Eichenberger, P., Gonzalez-Pastor, J.E., Liu, J.S., and Losick, R. (2003a) The Spo0A regulon of *Bacillus subtilis*. *Mol Microbiol* **50**: 1683-1701.
Molle, V., Nakaura, Y., Shivers, R.P., Yamaguchi, H., Losick, R., Fujita, Y., and Sonenshein, A.L. (2003b) Additional targets of the *Bacillus subtilis* global regulator CodY identified by chromatin immunoprecipitation and genome-wide transcript analysis. *J Bacteriol* **185**: 1911-1922.
Moller-Jensen, J., Jensen, R.B., and Gerdes, K. (2000) Plasmid and chromosome segregation in prokaryotes. *Trends Microbiol* **8**: 313-320.
Moller-Jensen, J., Jensen, R.B., Lowe, J., and Gerdes, K. (2002) Prokaryotic DNA segregation by an actin-like filament. *EMBO J* **21**: 3119-3127.
Moller-Jensen, J., Borch, J., Dam, M., Jensen, R.B., Roepstorff, P., and Gerdes, K. (2003) Bacterial mitosis: ParM of plasmid R1 moves plasmid DNA by an actin-like insertional polymerization mechanism. *Mol Cell* **12**: 1477-1487.
Moriya, S., Fukuoka, T., Ogasawara, N., and Yoshikawa, H. (1988) Regulation of initiation of the chromosomal replication by DnaA-boxes in the origin region of the *Bacillus subtilis* chromosome. *EMBO J* **7**: 2911-2917.
Murray, H., Ferreira, H., and Errington, J. (2006) The bacterial chromosome segregation protein Spo0J spreads along DNA from parS nucleation sites. *Mol Microbiol* **61**: 1352-1361.
Murray, H., and Errington, J. (2008) Dynamic control of the DNA replication initiation protein DnaA by Soj/ParA. *Cell* (in press).
Mysliwiec, T.H., Errington, J., Vaidya, A.B., and Bramucci, M.G. (1991) The *Bacillus subtilis* spo0J gene: evidence for involvement in catabolite repression of sporulation. *J Bacteriol* **173**: 1911-1919.
Nicholson, M.L. (2003) Using thermal inactivation kinetics to calculate the probability of extreme spore longevity: implications for paleomicrobiology and lithopanspermia. *Orig Life Evol Biosph.* **33**:621-631
Ogura, T., and Hiraga, S. (1983) Partition mechanism of F plasmid: two plasmid gene-encoded products and a cis-acting region are involved in partition. *Cell* **32**: 351-360.

Ogura, Y., Ogasawara, N., Harry, E.J., and Moriya, S. (2003) Increasing the ratio of Soj to Spo0J promotes replication initiation in *Bacillus subtilis*. *J Bacteriol* **185**: 6316-6324.

Ohlsen, K.L., Grimsley, J.K., and Hoch, J.A. (1994) Deactivation of the sporulation transcription factor Spo0A by the Spo0E protein phosphatase. *Proc Natl Acad Sci U S A* **91**: 1756-1760.

Orlova, A., Garner, E.C., Galkin, V.E., Heuser, J., Mullins, R.D., and Egelman, E.H. (2007) The structure of bacterial ParM filaments. *Nat Struct Mol Biol* **14**: 921-926.

Perego, M., Hanstein, C., Welsh, K.M., Djavakhishvili, T., Glaser, P., and Hoch, J.A. (1994) Multiple protein-aspartate phosphatases provide a mechanism for the integration of diverse signals in the control of development in *B. subtilis*. *Cell* **79**: 1047-1055.

Perego, M. (1997) A peptide export-import control circuit modulating bacterial development regulates protein phosphatases of the phosphorelay. *Proc Natl Acad Sci U S A* **94**: 8612-8617.

Perego, M. (2001) A new family of aspartyl phosphate phosphatases targeting the sporulation transcription factor Spo0A of *Bacillus subtilis*. *Mol Microbiol* **42**: 133-143.

Phillips, Z.E., and Strauch, M.A. (2002) *Bacillus subtilis* sporulation and stationary phase gene expression. *Cell Mol Life Sci* **59**: 392-402.

Pichoff, S., and Lutkenhaus, J. (2001) Escherichia coli division inhibitor MinCD blocks septation by preventing Z-ring formation. *J Bacteriol* **183**: 6630-6635.

Piggot, P.J., and Hilbert, D.W. (2004) Sporulation of *Bacillus subtilis*. *Curr Opin Microbiol* **7**: 579-586.

Popp, D., Narita, A., Oda, T., Fujisawa, T., Matsuo, H., Nitanai, Y., Iwasa, M., Maeda, K., Onishi, H., and Maeda, Y. (2008) Molecular structure of the ParM polymer and the mechanism leading to its nucleotide-driven dynamic instability. *EMBO J* **27**: 570-579.

Pratto, F., Cicek, A., Weihofen, W.A., Lurz, R., Saenger, W., and Alonso, J.C. (2008) *Streptococcus pyogenes* pSM19035 requires dynamic assembly of ATP-bound ParA and ParB on parS DNA during plasmid segregation. *Nucleic Acids Res* **36**: 3676-3689

Prentki, P., Chandler, M., and Caro, L. (1977) Replication of prophage P1 during the cell cycle of *Escherichia coli*. *Mol Gen Genet* **152**: 71-76.

Ptacin, J.L., Nollmann, M., Becker, E.C., Cozzarelli, N.R., Pogliano, K., and Bustamante, C. (2008) Sequence-directed DNA export guides chromosome translocation during sporulation in *Bacillus subtilis*. *Nat Struct Mol Biol* **15**: 485-493.

Quisel, J.D., Lin, D.C., and Grossman, A.D. (1999) Control of development by altered localization of a transcription factor in *B. subtilis*. *Mol Cell* **4**: 665-672.

Quisel, J.D., and Grossman, A.D. (2000) Control of sporulation gene expression in *Bacillus subtilis* by the chromosome partitioning proteins Soj (ParA) and Spo0J (ParB). *J Bacteriol* **182**: 3446-3451.

Rangaraj, P., Shah, V.K., and Ludden, P.W. (1997) ApoNifH functions in iron-molybdenum cofactor synthesis and apodinitrogenase maturation. *Proc Natl Acad Sci U S A* **94**: 11250-11255.

Raskin, D.M., and de Boer, P.A. (1999a) Rapid pole-to-pole oscillation of a protein required for directing division to the middle of *Escherichia coli*. *Proc Natl Acad Sci U S A* **96**: 4971-4976.

Raskin, D.M., and de Boer, P.A. (1999b) MinDE-dependent pole-to-pole oscillation of division inhibitor MinC in *Escherichia coli*. *J Bacteriol* **181**: 6419-6424.

Real, G., Autret, S., Harry, E.J., Errington, J., and Henriques, A.O. (2005) Cell division protein DivIB influences the Spo0J/Soj system of chromosome segregation in *Bacillus subtilis*. *Mol Microbiol* **55**: 349-367.

Rosen, B.P. (1990) The plasmid-encoded arsenical resistance pump: an anion-translocating ATPase. *Res Microbiol* **141**: 336-341.

Rowland, S.L., Burkholder, W.F., Cunningham, K.A., Maciejewski, M.W., Grossman, A.D., and King, G.F. (2004) Structure and mechanism of action of Sda, an inhibitor of the histidine kinases that regulate initiation of sporulation in *Bacillus subtilis*. *Mol Cell* **13**: 689-701.

Ruvolo, M.V., Mach, K.E., and Burkholder, W.F. (2006) Proteolysis of the replication checkpoint protein Sda is necessary for the efficient initiation of sporulation after transient replication stress in *Bacillus subtilis*. *Mol Microbiol* **60**: 1490-1508.

Saint-Dic, D., Frushour, B.P., Kehrl, J.H., and Kahng, L.S. (2006) A parA homolog selectively influences positioning of the large chromosome origin in *Vibrio cholerae*. *J Bacteriol* **188**: 5626-5631.

Sakai, N., Yao, M., Itou, H., Watanabe, N., Yumoto, F., Tanokura, M., and Tanaka, I. (2001) The three-dimensional structure of septum site-determining protein MinD from *Pyrococcus horikoshii* OT3 in complex with Mg-ADP. *Structure* **9**: 817-826.

Sambrook, J., Fritsch, E.F., and Maniatis, T. (1989) *Molecular Cloning: A Laboratory Manual*: Cold Spring Harbor, NY.

Saraste, M., Sibbald, P.R., and Wittinghofer, A. (1990) The P-loop--a common motif in ATP- and GTP-binding proteins. *Trends Biochem Sci* **15**: 430-434.

Sarma, R., Mulder, D.W., Brecht, E., Szilagyi, R.K., Seefeldt, L.C., Tsuruta, H., and Peters, J.W. (2007) Probing the MgATP-bound conformation of the nitrogenase Fe protein by solution small-angle X-ray scattering. *Biochemistry* **46**: 14058-14066.

Satola, S.W., Baldus, J.M., and Moran, C.P., Jr. (1992) Binding of Spo0A stimulates *spoIIG* promoter activity in *Bacillus subtilis*. *J Bacteriol* **174**: 1448-1453.

Schindelin, H., Kisker, C., Schlessman, J.L., Howard, J.B., and Rees, D.C. (1997) Structure of ADP x AlF4(-)-stabilized nitrogenase complex and its implications for signal transduction. *Nature* **387**: 370-376.

Schmid, B., Einsle, O., Chiu, H.J., Willing, A., Yoshida, M., Howard, J.B., and Rees, D.C. (2002) Biochemical and structural characterization of the cross-linked complex of nitrogenase: comparison to the ADP-AlF4(-)-stabilized structure. *Biochemistry* **41**: 15557-15565.

Schumacher, M.A. (2008) Structural biology of plasmid partition: uncovering the molecular mechanisms of DNA segregation. *Biochem J* **412**: 1-18.

Sen, S., Igarashi, R., Smith, A., Johnson, M.K., Seefeldt, L.C., and Peters, J.W. (2004) A conformational mimic of the MgATP-bound "on state" of the nitrogenase iron protein. *Biochemistry* **43**: 1787-1797.

Sen, S., Krishnakumar, A., McClead, J., Johnson, M.K., Seefeldt, L.C., Szilagyi, R.K., and Peters, J.W. (2006) Insights into the role of nucleotide-dependent conformational change in nitrogenase catalysis: Structural characterization of the nitrogenase Fe protein Leu127 deletion variant with bound MgATP. *J Inorg Biochem* **100**: 1041-1052.

Seredick, S. (2006) Spo0A Stimulated Transcription Initiation at the *Bacillus subtilis spoIIG* Promoter. In PhD Thesis department of Microbiology and Immunology Vancouver: University of British Columbia, pp. 148.

Setlow, P. (2003) Spore germination. *Curr Opin Microbiol* **6**: 550-556.

Setlow, P. (2007) I will survive: DNA protection in bacterial spores. *Trends Microbiol* **15**: 172-180.

Shivers, R.P., and Sonenshein, A.L. (2004) Activation of the *Bacillus subtilis* global regulator CodY by direct interaction with branched-chain amino acids. *Mol Microbiol* **53**: 599-611.

Strop, P., Takahara, P.M., Chiu, H., Angove, H.C., Burgess, B.K., and Rees, D.C. (2001) Crystal structure of the all-ferrous [4Fe-4S]0 form of the nitrogenase iron protein from *Azotobacter vinelandii*. *Biochemistry* **40**: 651-656.

Surtees, J.A., and Funnell, B.E. (2003) Plasmid and chromosome traffic control: how ParA and ParB drive partition. *Curr Top Dev Biol* **56**: 145-180.

Switzer, R.C., 3rd, Merril, C.R., and Shifrin, S. (1979) A highly sensitive silver stain for detecting proteins and peptides in polyacrylamide gels. *Anal Biochem* **98**: 231-237.

Takamatsu, H., and Watabe, K. (2002) Assembly and genetics of spore protective structures. *Cell Mol Life Sci* **59**: 434-444.

Trempy, J.E., Bonamy, C., Szulmajster, J., and Haldenwang, W.G. (1985) *Bacillus subtilis* sigma factor sigma 29 is the product of the sporulation-essential gene *spoIIG*. *Proc Natl Acad Sci U S A* **82**: 4189-4192.

van den Ent, F., Moller-Jensen, J., Amos, L.A., Gerdes, K., and Lowe, J. (2002) F-actin-like filaments formed by plasmid segregation protein ParM. *EMBO J* **21**: 6935-6943.

Varughese, K.I. (2002) Molecular recognition of bacterial phosphorelay proteins. *Curr Opin Microbiol* **5**: 142-148.

Vogel, U.S., Dixon, R.A., Schaber, M.D., Diehl, R.E., Marshall, M.S., Scolnick, E.M., Sigal, I.S., and Gibbs, J.B. (1988) Cloning of bovine GAP and its interaction with oncogenic ras p21. *Nature* **335**: 90-93.

Walker, J.E., Saraste, M., Runswick, M.J., and Gay, N.J. (1982) Distantly related sequences in the alpha- and beta-subunits of ATP synthase, myosin, kinases and other ATP-requiring enzymes and a common nucleotide binding fold. *EMBO J* **1**: 945-951.

Wang, L., Grau, R., Perego, M., and Hoch, J.A. (1997) A novel histidine kinase inhibitor regulating development in *Bacillus subtilis*. *Genes Dev* **11**: 2569-2579.

Webb, C.D., Graumann, P.L., Kahana, J.A., Teleman, A.A., Silver, P.A., and Losick, R. (1998) Use of time-lapse microscopy to visualize rapid movement of the replication origin region of the chromosome during the cell cycle in *Bacillus subtilis*. *Mol Microbiol* **28**: 883-892.

Whitten, A.E., Jacques, D.A., Hammouda, B., Hanley, T., King, G.F., Guss, J.M., Trewhella, J., and Langley, D.B. (2007) The structure of the KinA-Sda complex suggests an allosteric mechanism of histidine kinase inhibition. *J Mol Biol* **368**: 407-420.

Wittig, I., Braun, H.P., and Schagger, H. (2006) Blue native PAGE. *Nat Protoc* **1**: 418-428.

Yamaichi, Y., and Niki, H. (2000) Active segregation by the *Bacillus subtilis* partitioning system in *Escherichia coli*. *Proc Natl Acad Sci U S A* **97**: 14656-14661.

Yamaichi, Y., Fogel, M.A., McLeod, S.M., Hui, M.P., and Waldor, M.K. (2007) Distinct centromere-like parS sites on the two chromosomes of *Vibrio* spp. *J Bacteriol* **189**: 5314-5324.

Zhou, T., Radaev, S., Rosen, B.P., and Gatti, D.L. (2000) Structure of the ArsA ATPase: the catalytic subunit of a heavy metal resistance pump. *EMBO J* **19**: 4838-4845.

Zhou, T., Radaev, S., Rosen, B.P., and Gatti, D.L. (2001) Conformational changes in four regions of the *Escherichia coli* ArsA ATPase link ATP hydrolysis to ion translocation. *J Biol Chem* **276**: 30414-30422.